University of Massachusetts Medical School

eScholarship@UMMS

Energy Metabolism and the Induction of the Unfolded Protein Response: A Dissertation

Alison M. Burkart
University of Massachusetts Medical School Worcester

Let us know how access to this document benefits you.

ENERGY METABOLISM AND THE INDUCTION OF THE UNFOLDED PROTEIN RESPONSE

A Dissertation Presented

By

Alison Marie Burkart

Submitted to the Faculty of the
University of Massachusetts Graduate School of Biomedical Sciences, Worcester
In partial fulfillment of the requirements for the degree of

DOCTOR OF PHILOSOPHY

September 10, 2010

Interdisciplinary Graduate Program

COPYRIGHT NOTICE

ENERGY METABOLISM AND THE INDUCTION OF THE UNFOLDED PROTEIN RESPONSE

A Dissertation Presented By

Alison Marie Burkart

The signatures of the Dissertation Defense Committee signifies completion and approval as to style and content of the Dissertation

_____

Silvia Corvera, M.D., Thesis Advisor

_____

Marcus Cooper, M.D., Member of Committee

_____

Vamsi Mootha, M.D., Member of Committee

_____

Fumihiko Urano, M.D., Ph.D., Member of Committee

_____

Yong-Xu Wang, Ph.D., Member of Committee

The signature of the Chair of the Committee signifies that the written dissertation meets the requirements of the Dissertation Committee

_____

Michael Czech, Ph.D., Chair of Committee

The signature of the Dean of the Graduate School of Biomedical Sciences signifies that the student has met all graduation requirements of the School

_____

Anthony Carruthers, Ph.D.
Dean of the Graduate School of Biomedical Sciences

Interdisciplinary Graduate Program

September 10, 2010

ACKNOWLEDGEMENTS

I would first like to thank my mentor, Dr. Silvia Corvera. She has trained me to be a thoughtful and rigorous scientist in my pursuit of knowledge. She has always offered her assistance but also taught me to work independently. She has helped me develop skills that will be with me throughout the rest of my career.

I wish to thank my thesis committee members, Drs. Michael Czech, Heidi Tissenbaum, Fumihiko Urano, and Yong-Xu Wang for all their advice and support during my graduate career.

I would like to acknowledge my dissertation examination committee members, Drs. Marcus Cooper, Michael Czech, Vamsi Mootha, Fumihiko Urano, and Yong-Xu Wang, for taking the time to help me complete this last stage in obtaining my doctoral degree.

Research is a team effort. To that end I would like to thank all the members of the Corvera and Czech laboratories, both past and present. They have assisted me throughout my studies with guidance, reagents, helping hands, support, and friendship. My Chouinard has been a great friend and has helped me throughout my studies. We have worked together on several projects over the years and she has always helped me with my own thesis work. Dr. Deborah Leonard has been a constant source of advice, both personal and professional. Dr. Catherine Bue, Dr. Anil Chawla, Dr. Olga Gealikman, Deanna Navaroli, Dr. Xiarong Shi, and Khanh-Van Tran and have assisted me throughout my research with their helpful discussions and support.

For all their encouragement during my graduate degree, I would like to thank my friends. Those that are a part of the UMass community understand this process and helped me in every way possible. To those I knew before pursuing my doctoral degree, and the ones I met along the way, thank you for supporting me and providing an escape from the pressures of graduate school.

Finally I would like to thank my family for their love and support while I strived to achieve this goal. My parents, Preston and Claudia Burkart, taught me that through hard work anything is possible. They have been a constant source of encouragement throughout my life. I want to thank my sister, Heather, for her support and being a constant source of relief from the stresses of graduate school. To my extended family, thank you for always encouraging me during this process.

ABSTRACT

White adipose plays a major role in the regulation of whole body metabolism through the storage and hydrolysis of triglycerides and by secretion of adipokines. The function of endocrine cells is highly dependent on the unfolded protein response (UPR), a homeostatic signaling mechanism that balances the protein folding capacity of the endoplasmic reticulum (ER) with the cell's secretory protein load. Here we demonstrate that the adipocyte UPR pathway is necessary for its secretory functions, and can thus play a crucial role in the control of whole body energy homeostasis. ER protein folding capacity is dependent both on the number of available chaperones as well as on their activity, which requires a sufficient ATP supply. In 3T3-L1 adipocytes, mitochondrial biogenesis occurred in parallel with induction of the UPR; therefore, we tested whether it was necessary for efficient ER function. Inhibition of mitochondrial ATP synthesis through depletion of Tfam, a mitochondrial transcription factor, or treatment with inhibitors of oxidative phosphorylation, demonstrate that ER function is sensitive to acute changes in adenine nucleotide levels. In addition, adenylate kinase 2 (AK2), which regulates mitochondrial adenine nucleotide interconversion, is markedly induced during adipocyte and B cell differentiation. AK2 depletion impairs induction of the UPR and secretion in both cell types. Interestingly, cytosolic adenylate kinase 1 (AK1) does not have the same effect upon UPR induction. We show that adenine nucleotides promote proper ER function and alterations in specific aspects of ATP synthesis can impair UPR signaling. Understanding the complex energetic regulation of the UPR may provide insight into the relationship between UPR and disease.

TABLE OF CONTENTS

LIST OF FIGURES

LIST OF TABLES

LIST OF ABBREVIATIONS

2-DOG/2DG – 2-deoxy-D-glucose
Acdc/Acrp30 – Adiponectin
Acaa2 – Acetyl-coenzyme A acyltransferase 2
Acadm – Medium-chain acyl-coenzyme A dehydrogenase
Adn – Adipsin
ADP – Adenine diphosphate
AIP1 – ASK1 interacting protein 1
AK – Adenylate kinase
AK1 – Adenylate kinase 1
AK2 – Adenylate kinase 2
AKT/PKB – thymoma viral proto-oncogene/protein kinase B
AMP – Adenine monophosphate
AMPK – Adenine monophosphate activated kinase
ASK1 – Apoptosis signal-regulating kinase 1
ATF4 – Activating transcription factor 4
ATF6 – Activating transcription factor 6
ATP – Adenine triphosphate
ATP6 – ATP synthase F0 subunit 6
aP2 – Adipocyte protein 2
BCA – Bicinchoninic acid
BCL6 – B cell lymphoma 6
BCR – B cell receptor
BFA/BA – Brefeldin A
BiP – Immunoglobulin heavy chain-binding protein (also known as GRP78)
BMI – Body mass index
β-NAD – Beta nicotinamide adenine dinucleotide
BSA – Bovine serum albumin
bZIP - basic region-leucine zipper
Calretic. – Calreticulin
Cebpa – CCAAT/Enhancer-binding protein alpha
Cebpb – CCAAT/Enhancer-binding protein beta
Cebpd – CCAAT/Enhancer-binding protein delta
CCCP – Carbonyl cyanide M-chlorophenylhydrazone
CHOP/GADD153 – CCAAT/enhancer-binding protein epsilon/DNA damage-inducible transcript 3
Cox1 – Cytochrome C oxidase cubunit 1
CPT1b – Carnitine palmitoyltransferase 1B
CPT2 – Carnitine palmitoyltransferase 2
cDNA – Complementary DNA

cRNA – Complementary RNA
CREB – Cyclic adenine monophosphate response element-binding
Cs – Citrate synthase
Cytb – Cytochrome B
CytC/Cycs – Cytochrome C
DGAT1 – diacylglycerol O-acyltransferase 1
DNP – 2,4-Dinitrophenol
DTT – Dithiothreitol
EDEM – ER degradation-enhancing alpha-mannosidase-like protein
eIF2α – Elongation initiation factor 2 alpha
eIF2αS51A – Elongation initiation factor 2 alpha with alanine substituted for serine 51
ER – Endoplasmic reticulum
ERAD – Endoplamic reticulum associated protein degradation
ERdj3 – Endoplasmic reticulum-localized DnaJ homologue 3
ERdj4 – Endoplasmic reticulum-localized DnaJ homologue 4
ERO1 – Endoplasmic oxidoreductin-1-like protein
ERSE – ER stress response element
Etfdh – Electron-transferring-flavoprotein dehydrogenase
FADH$_2$ – Flavin adenine dinucleotide, reduced
FBS – Fetal bovine serum
FCCP – Carbonylcyanide-P-trifluoromethoxyphenylhydrazone
Fth – Ferritin heavy chain
GADD34 – Growth arrest and DNA damage-inducible protein 34
GADD153 – Growth arrest and DNA damage-inducible protein 153 (also CHOP)
GCN2 – General control non-derepressible 2
GRP78 – Glucose regulated protein, 78 kilodaltons
GRP94 – Glucose regulated protein, 94 kilodaltons
GLUT1 – Glucose transporter 1
GLUT4 – Glucose transporter 4
HFD – High fat diet
HRI – Heme-regulated inhibitor
IEF – Isoelectric focusing
Ins. – Insulin
IRES – Internal ribosome entry site
IRE1 – Inositol-requiring 1
ISR – Integrated stress response
kDA – Kilodalton
KEGG – Kyoto Encyclopedia of Genes and Genomes
KDELR3 – KDEL endoplasmic reticulum protein retention receptor 3
KRH – Krebs-Ringer HEPES
LPS – Lipopolysaccharide
MALDI-TOF – Matrix-assisted laser desorption/ionisation-time of flight
MAM – Mitochondrial associated membranes
MEF – Mouse embryonic fibroblast

MHC – Major histocompatibility complex
mHSP60 – Mitochondrial heat shock protein 60
mtDNA – Mitochondrial DNA
mTOR – Mammalian target of rapamycin
NAD$^+$ – Nicotinamide adenine dinucleotide, oxidized
NADH – Nicotinamide adenine dinucleotide, reduced
ND – Normal diet
ND1 – NADH dehydrogenase subunit 1
Olig – Oligomycin
PBS – Phosphate buffered saline
P-AMPK – Phosphorylated adenine monophosphate activated kinase (activate form)
PERK – Eukaryotic translation initiation factor 2 alpha kinase 3
PDI – Protein disulfide isomerase
PKR – Protein kinase R
PPARa – Peroxisome proliferator activated receptor alpha
PPARg – Peroxisome proliferator activated receptor gamma
Prkag3 – AMPK subunit gamma 3
Prkag3^{225Q} – AMPK subunit gamma 3 with a constitutively active mutation
PTP-1B – Protein-tyrosine phosphatase 1B
Rag2 – Recombination activating gene 2
Redox – Reduction-oxidation
RER – Rough endoplasmic reticulum
Retn – Resistin
RLU – Relative luminescence units
RNA – Ribonucleic acid
RNAi – RNA interference
rRNA – Ribosomal RNA
PBS – Phosphate buffered saline
SER – Smooth endoplasmic reticulum
SCD1 – Stearoyl-coA desaturase 1
SCID – Severe combined immunodeficiency
Scr – Scrambled
SDS – Sodium dodecyl sulfate
SDS-PAGE – Sodium dodecyl sulfate polyacrylamide gel electrophoresis
siRNA – Small interfering RNA
SREBP – Sterol regulatory element binding transcription factor 1
sXBP1 – Spliced X-Box binding protein 1
TBS – Tris buffered saline
T1DM – Type 1 Diabetes Mellitus
T2DM – Type 2 Diabetes Mellitus
Tfam – Transcription factor A, mitochondrial
Tfbm – Transcription factor B, mitochondrial
Th – Thapsigargin
TNFα – Tumor necrosis factor alpha

TRAF2 – TNF receptor-associated factor 2
tRNA – Transfer RNA
Tuni/Tu – Tunicamycin
UCP2 – Uncoupling protein 2
UCP3 – Uncoupling protein 3
UPR – Unfolded protein response
UTR – Untranslated region
WFS1 – Wolfram syndrome 1
WT – Wild type
XBP1 – X-Box binding protein

CHAPTER I
INTRODUCTION

Metabolism is a tightly controlled system involving cross-regulation and signaling between multiple tissues. Each tissue has a distinct role in the system and can alter the activities of the other tissues through chemical and protein factors secreted into the blood stream. Energetic homeostasis is maintained principally through the functions of insulin sensitive tissues, such as the brain, muscle, liver, pancreas, and white adipose tissue (1). If the function of any of these tissues is compromised, it leads to a breakdown in energetic homeostasis. Persistent dysregulation results in a pathology termed the metabolic syndrome. The metabolic syndrome is a cluster of conditions, including obesity, insulin resistance, dyslipidema, hypertension, and Diabetes Mellitus (2). Additionally, studies show that this syndrome is associated with twice the risk of developing cardiovascular disease (1). The prevalence of the metabolic syndrome has reached epidemic proportions throughout the world. Originally only a problem in industrialized nations, there are now increasing incidences of these metabolic diseases even in developing nations. Studies have identified overnutrition and inactivity as two of the major contributing factors to the development of the metabolic syndrome. However, molecular causes also need to be investigated as potential targets for prevention or treatment.

Obesity and Diabetes Mellitus

Two of the main pathologies of the metabolic syndrome, obesity and Diabetes Mellitus (hereafter referred to as diabetes), are often discussed as one condition. Though these are two distinct pathologies, they are believed to have common molecular origins. The body mass index (BMI) is a calculation used to estimate a healthy body weight respective to height. BMI equals the mass of a person in kilograms divided by the square of their height in meters. While a healthy BMI is between 18.5 and 25, human obesity is defined medically as having a BMI equal to or greater than 30. Due to the increased adiposity, obese individuals often suffer from insulin resistance, where the body does not respond properly to insulin signaling, and diabetes. Diabetes is a condition where there is insufficient insulin necessary to maintain glucose homeostasis resulting in high blood glucose levels. The dramatic increase in the number of cases of diabetes worldwide in recent years has promoted interest in determining the cause(s) of this disease to find preventative measures and new treatments. Diabetes is a condition with three distinct pathologies. Gestational diabetes results from an increase in blood glucose levels that occurs in some mothers during pregnancy (3). Glucose homeostasis often returns to normal after birth. Type 1 diabetes (T1DM), or juvenile diabetes, is an autoimmune disease that attacks the insulin-producing β cells of the pancreas (4). Due to the lack of β cells, T1DM patients are dependant on exogenous sources of insulin to maintain glucose homeostasis. There is no cure for T1DM as of now, but there is promising research being conducted on β cell transplantation. Type 2 diabetes (T2DM) was previously referred to as adult-onset, but this is no longer applicable due to increased incidences in children and

adolescents (5). T2DM occurs when the body does not produce sufficient amounts of insulin for proper glucose metabolism, typically due to excessive body weight. The patients may require glucose lowering drugs, exogenous insulin, or both, and can make a full recovery with effective treatment, including diet and exercise.

With increased weight gain, the body is often unable to produce enough insulin to compensate, resulting in T2DM (5). Increased adiposity alone, however, is not the sole cause for the development of diabetes. In fact, it appears that other factors must also occur to promote this pathology, including increased free fatty acids in the blood stream and impaired cellular metabolism. Recent data supports the hypothesis that failure of the adipose tissue to sufficiently expand is more a cause for the disease rather than the general expansion of the tissue itself (2). To further that concept, more work is being done on understanding the function of the adipose organ.

White adipose tissue, traditionally thought to be an inert lipid storage depot, regulates whole body metabolism by monitoring nutrient levels (6,7). It can then act on the central nervous system and peripheral tissues to control caloric intake and utilization through the secretion of adipokines. These hormones and cytokines, including leptin, adiponectin, resistin, retinol binding protein 4, and tumor necrosis factor alpha (TNFα), can also affect blood pressure, lipid and glucose metabolism, inflammation, and atherosclerosis (8-10). The importance of these secreted factors have led to the reclassification of the adipose tissue as an endocrine organ. Given the importance of adipokines to whole body homeostasis, understanding the molecular mechanisms that regulate adipocyte secretion is highly relevant.

Eukaryotic cells have two sources of protein synthesis, the cytosol and the endoplasmic reticulum (11). The majority of cellular proteins are translated and folded within the cytosol. However, a subset of proteins destined for either secretion, such as the adipokines, or insertion into the plasma membrane are synthesized and processed within the endoplasmic reticulum. The endoplasmic reticulum (ER) is composed of a phospholipid bilayer surrounding a lumen to form a network of tubules and vesicles adjacent to the cell's nucleus. There are three types of endoplasmic reticulum, defined by their major function: The rough ER (RER), so named by the presence of ribosomes on the membrane surface, is the location of ER protein synthesis. Smooth ER (SER), lacks ribosomes and therefore has a "smooth" membrane, functions in the synthesis of lipids and steroids, carbohydrate metabolism, and regulation of calcium. The sarcoplasmic reticulum, a specialized form of SER found in smooth and striated muscle cells, regulates the calcium stores necessary for contraction. While the SER and sarcoplasmic reticulum play important and necessary roles in cellular homeostasis, the ER as an organelle is commonly associated with protein folding.

Proteins destined for transport through the secretory pathway require the aid of luminal ER chaperones to achieve their final functional conformation. Importantly, unlike proteins folded in the cytosol, those folded in the ER also have the potential to undergo post-translational modification, such as glycosylation or proteolytic cleavage (12). Adiponectin, a major adipocyte factor, is synthesized as a 247 amino acid polypeptide that undergoes extensive folding to form a trimer stabilized through disulfide bond formation (8,9). It is further processed into higher molecular weight complexes prior to

secretion by adipocytes. Resistin, another adipokine, also undergoes multimeric assembly dependant on disulfide bonds for stabilization (13). The volume of factors synthesized and secreted, along with the complex folding required for some of these proteins, suggest that there is a considerable load on the endoplasmic reticulum of the adipocyte. Perturbations in folding caused by either physiological or pharmacological insult can cause the ER to become overloaded with unfolded proteins. Eukaryotic cells have evolved a system of responses to deal with this stress, termed the "unfolded protein response".

The Unfolded Protein Response

The unfolded protein response (UPR) is a mechanism by which cells can recover from an overburdened ER (14). Most components of the mammalian UPR can be found conserved in eukaryotic systems, from yeast to higher order mammals. Originally discovered as a stress response to low glucose levels in cultured cells (15,16), further studies elucidated its important role in ER homeostasis. The UPR involves a three-pronged approach to allow the cell to recover from ER stress: 1) translational repression to reduce proteins entering the ER, 2) increased chaperone expression to improve ER folding efficiency and capacity, 3) and degradation of misfolded proteins in the ER to lower the ER load. These processes allow cells to respond to a variety of stresses from the physiological burden caused by cellular differentiation or a high volume of secretion, and pharmacological stress, such as from chemically induced impairments or heat shock. Importantly, an impaired UPR, when the cell is unable to respond properly, has been

shown to cause or exacerbate a variety of human ailments, including neurodegeneration, viral infection, and Diabetes Mellitus (17-19).

Key Players in the UPR

There are three major sensors on the ER membrane that monitor when the protein folding capacity is exceeded, IRE1 (inositol requiring enzyme 1), ATF6 (activating transcription factor 6), and PERK (eukaryotic translation initiation factor 2 alpha kinase 3). Each responds by initiating independent branches of the UPR to restore ER homeostasis (Figure 1.1). They each exist in an inactive state as monomers bound to immuonglobulin heavy chain-binding protein (BiP/GRP78) (20,21). BiP, an ER resident chaperone, dissociates upon increased levels of unfolded proteins to aid in protein folding. This allows activation of the sensors through homodimerization of IRE1 and PERK and proteolytic cleavage of ATF6. The universal function of these distinct signaling cascades is to reduce general translation while increasing the expression of select ER chaperones. ER associated protein degredation (ERAD) is also increased upon UPR activation. If these methods fail, and the stress upon the ER remains, all three branches will initiate an apoptotic response.
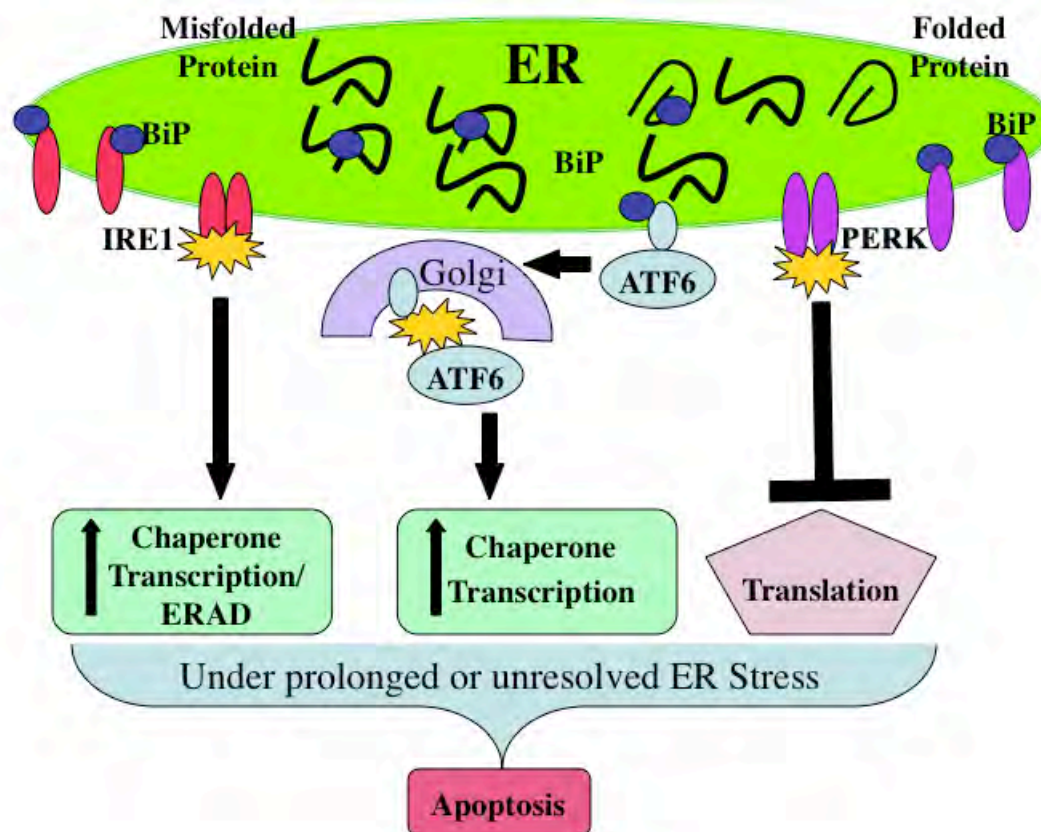
Figure 1.1: Three Main UPR Branches.

The UPR has three major ER resident sensors, IRE1, ATF6, and PERK, which are inactive while bound to BiP. During increased levels of unfolded proteins, BiP releases the sensors in order to aid in protein folding. This allows activation of the sensors and induction of downstream responses to improve the capacity and efficiency of ER folding through upregulation of chaperones, decreased general translation, and degradation of unfolded proteins through ER associated protein degradation (ERAD). If the stress on the ER is not relieved, all three branches of the UPR will initiate apoptosis.

Key Players in the UPR: IRE1/XBP1 Branch

IRE1 is a transmembrane serine/threonine kinase localized to the ER (Figure 1.2). A highly conserved branch of the UPR, yeast IRE1p has two mammalian homologs, IRE1α and IRE1β (22,23). Both isofoms can activate the UPR, however more studies have been completed on the function of IRE1α. The luminal domain of IRE1 acts as a sensor for the ER folding capacity while the cytoplasmic region is required for its kinase and endoribonuclease functions (20,24-26). Upon dimerization after BiP release, IRE1 auto-transphosphorylates, inducing a conformational change and subsequent activation (27). The resulting downstream responses include splicing of X-box binding protein 1 (XBP1) mRNA, which is a transcription factor that increases chaperones and elements of ERAD. A late stage response is the induction of apoptosis via a TNF receptor-associated factor 2 (TRAF2) and caspase 12 pathway.
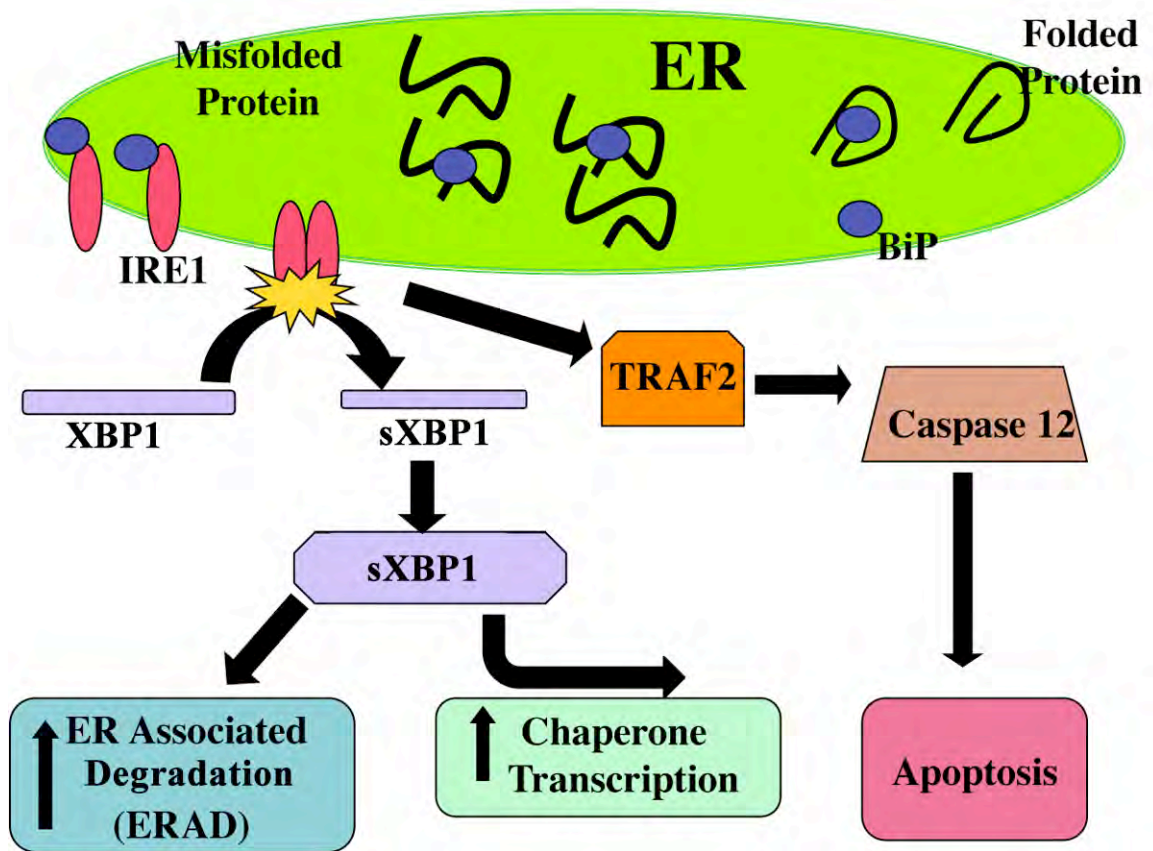
Figure 1.2: The IRE1/XBP1 branch of the UPR.

Upon increased ER stress, BiP dissociates from IRE1 allowing homodimerizaiton and activation. Activated IRE1 splices XBP1 mRNA to form a stable XBP1 mRNA product. Upon its translation, sXBP1 promotes the transcription of ER chaperones. ER degradation is also upregulated. Under conditions of unrelieved stress, IRE1 induces apoptosis via Traf2 mediated caspase 12 cleavage.

IRE1's activation is due specifically to auto-phosphorylation, which opens up an active site allowing nucleotide binding (28). Upon binding, a conformation change is induced allowing for activation of the ribonuclease (RNase) domain of IRE1. The conformational change may involve the binding of either adenine triphosphate (ATP) or adenine diphosphate (ADP) to the kinase domain. ADP has been shown to be a more effective activator *in vitro*, though ATP also is capable of initiating phosphorylation (25). IRE's ability to activate through binding of adenine nucleotides may also serve as a nutritional sensor, regulating protein synthesis and UPR activation based on the energetic state of the cell (29).

IRE1α knockout mice embryos, which die by embryonic day 13, are smaller than their wild type littermates and have severe liver hypoplasia (30). The cause of death appears to be due to dysfunction of the placenta rather than embryonic growth (31). To bypass the lethality, studies on immune function were performed by reconstituting the immune system of recombination activating gene 2 (Rag2) deficient mice with IRE1α$^{-/-}$ hematopoietic stem cells. IRE1α was then shown to be required for two distinct steps in B cell lymphopoiesis: first in the rearrangement of the Ig genes and production of B cell receptors, and second during plasma cell differentiation (30). These murine defects indicate that IRE1α expression and activity plays an important role in cellular health and function.

Acting as an unconventional endoribonuclease, active IRE1 can remove a 26-nucleotide intron from XBP1, creating a stable mRNA product (25). Spliced XBP1 (sXBP) mRNA can then be translated into XBP1, a transcription factor. XBP1 is a

member of the cAMP response element-binding/activating transcription factor (CREB/ATF) basic region-leucine zipper (bZIP) family (32). It was originally identified in a screen for proteins that bound the X-box, a sequence that regulates transcription of the human major histocompatibility complex (MHC) (33). Subsequently, XBP1 has been shown to be able to regulate the expression of several ER chaperones including BiP, ER-localized DnaJ homologues 3 and 4 (ERdj3 and ERdj4) and other UPR effectors including ATF4, CCAAT/enhancer-binding protein epsilon/DNA damage-inducible transcript 3 (CHOP), PERK, protein disulfide isomerase (PDI), ER degradation-enhancing alpha-mannosidase-like protein (EDEM), as well as its own expression in a cell type specific manner (34-36). XBP1 is not only a key player in promoting the induction of the UPR, but it also is physiologically necessary for mouse development and cell differentiation.

Similar to IRE1α, XBP1 knockout mice also exhibit severe liver hypoplasia resulting in embryonic death (37). Rescue experiments have shown that in addition to functional liver formation, XBP1 is required for proper development of other secretory tissues, including the salivary gland and exocrine pancreas (36). Other studies show that XBP1 is not only required for the secretory capacity of plasma cells but also the differentiation of B cells into antibody secreting plasma cells (38). Interestingly, forced XBP1 expression can increase the secretory capacity of primary B cells (36). These data show that the IRE1 branch of the UPR not only affects cellular activity but also has a great impact on whole body function.

Key Players in the UPR: ATF6 Branch

Another branch of the UPR is the ATF6 regulated induction of chaperone mRNA transcription (Figure 1.3). In addition, ATF6 also may regulate the PERK branch of the UPR by inhibiting growth arrest and DNA damage-inducible protein 34 (GADD34), which dephosphorylates eukaryotic translation initiation factor 2 alpha (eIF2α), a modulator of protein translation. Upon prolonged ER stress, ATF6 will induce apoptosis through activating transcription factor 4 (ATF4) regulation of CHOP.
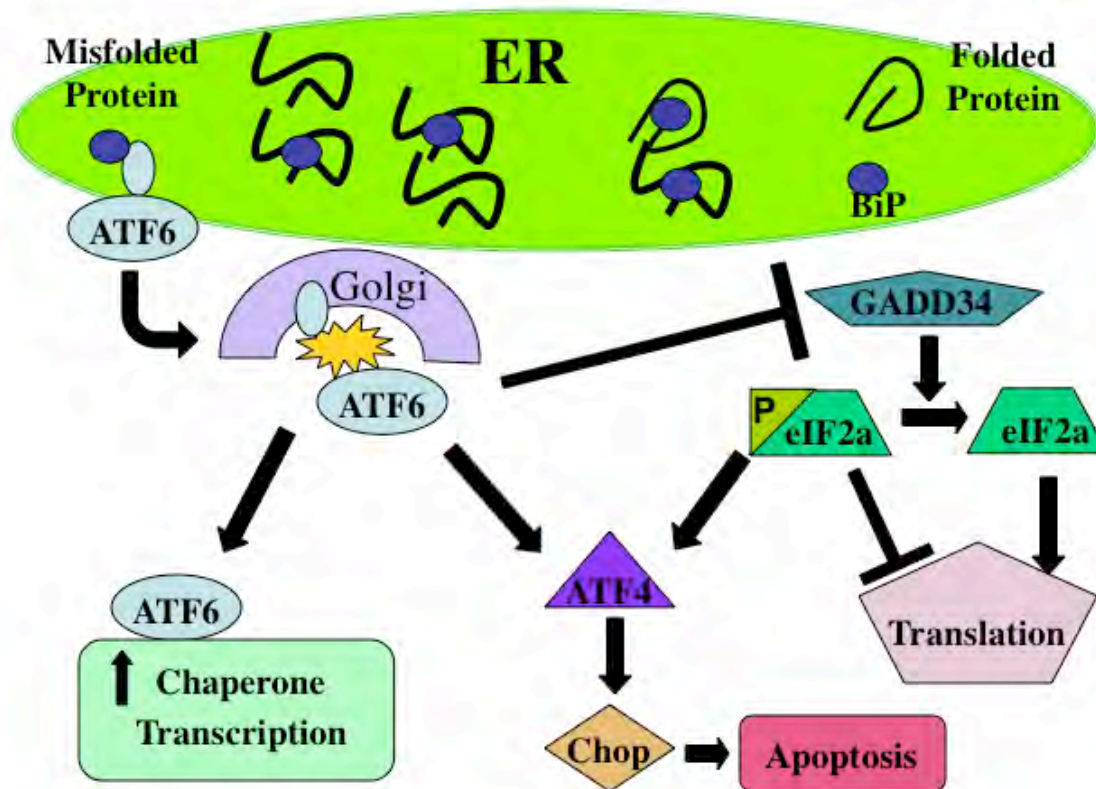
Figure 1.3: The ATF6 branch of the UPR.

BiP dissociates upon increased ER stress allowing ATF6 to translocate to the Golgi and undergo proteolytic cleavage. Activated ATF6 promotes the transcription of ER chaperones. Under conditions of unrelieved stress, ATF6 via ATF4 induces apoptosis through upregulation of CHOP. It can also mediate translational regulation by inhibiting GADD34, which dephosphorylates eIF2α.

The two bZIP-type transcription factors, ATF6α and ATF6β, are constitutively expressed transmembrane proteins located in the ER (39). Upon activation, ATF6 is translocated to the Golgi where it is cleaved by Site-1 and Site-2 proteases (39-41). p50ATF6, the soluble N-terminal portion containing the bZIP domain, is transported to the nucleus where it directly binds the ER stress response element (ERSE) to induce transcription of key UPR effectors including XBP1, BiP, and PDI (42,43).

ATF6α knock out mice show no overt phenotype; they are vital, fertile, and healthy (44). However, upon acute tunicamycin treatment *in vivo*, these mice are unable to protect against ER stress and exhibit increased toxicity and organ failure. The lack of a strong phenotype may be due to the overlap between the ATF6 and PERK/eIF2α branches. During chronic ER stress, ATF6 may prolong the block on translation through suppression of growth arrest and DNA damage-inducible protein 34 (GADD34), which dephosphorylates eIF2α (44). Additionally, if the stress on the ER is not relieved, both ATF6 and PERK are able to activate CHOP mediated apoptosis through upregulation of ATF4 (42).

Key Players in the UPR: PERK/eIF2α Branch

The final ER stress sensor, PERK, is a conserved protein with a luminal domain similar to IRE1 and a kinase domain related to double-stranded RNA-dependent protein kinase (PKR) (Figure 1.4) (45). Once freed from BiP, PERK is auto-phosphorylated, leading to dimerization and trans-phosphorylation (20,46). Both ER stress as well as ischemia can activate PERK, which in turn phosphorylates eIF2α on serine 51

(45,47,48). Phosphorylation of eIF2α inhibits its ability to initiate protein translation causing a decrease in general protein synthesis (49). Upon unrelieved ER stress, PERK, in the same manner as ATF6 can induce apoptosis through the ATF4/CHOP pathway.
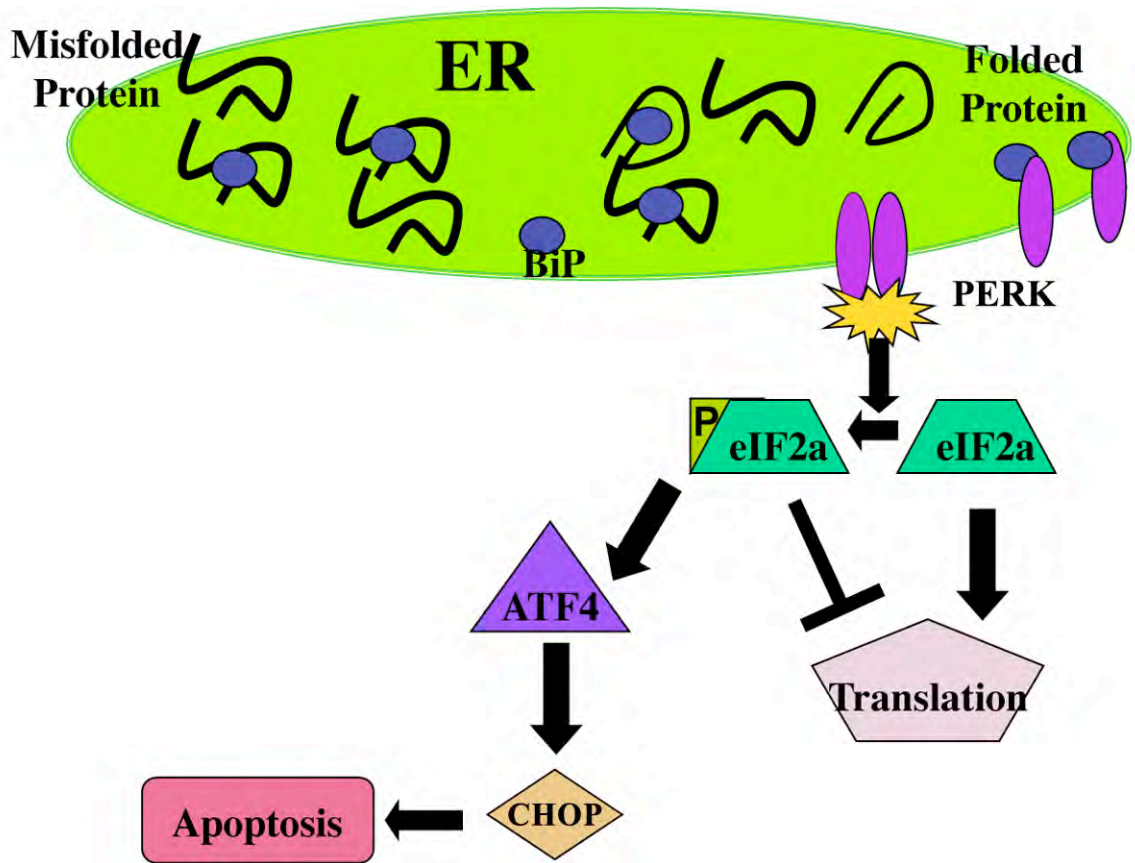
Figure 1.4: The PERK/eIF2α branch of the UPR.

Upon increased ER stress, BiP dissociates from PERK allowing homodimerization and activation. Activated PERK phosphorylates eIF2α, which decreases general translation. Under these conditions, ATF4 is specifically upregulated, which can then induce CHOP and apoptosis.

Although PERK knockout mice are viable, about 30% die prenatally and less than 40% live past the first week of birth (50). At birth they appear healthy and similar to wild type littermates but noticeable changes occur within the first few weeks. They experience severe growth retardation and by the end of the first week they are already about 50% smaller than wild type mice. PERK$^{-/-}$ pancreatic β cells quickly degenerate and the mice develop Diabetes Mellitus. The cause of these effects is believed to be due to dysregulation of eIF2α and protein synthesis (50), although this has not been confirmed and could be due to a different, currently unknown substrate.

In addition to PERK, eIF2α can also be phosphorylated by general control non-derepressible 2 (GCN2), heme-regulated inhibitor (HRI), and PKR (51,52). Though the kinase domains are similar, their regulatory domains differ and therefore they can be activated by various stimuli. In fact, under various stress conditions they can be activated either singly or in combination (53). To determine the physiological role of eIF2α phosphorylation, mice were generated containing an alanine replacement of serine 51 (54). Similar to the PERK$^{-/-}$ mice, eIF2αS51A mice were indistinguishable from wild type mice at birth. Although born at a Mendelian ratio, indicating no prenatal lethality, almost all the homozygous eIF2αS51A mice died within 18 hours. Death was due to hypoglycemia caused by impaired gluconeogenesis in the liver. In addition, similar to what was seen in the PERK$^{-/-}$ mice, these mice had decreased β cell populations and serum insulin levels. These two mice models indicate that the PERK/eIF2α pathway of protein synthesis regulation is necessary for glucose metabolism. Additionally, it

strengthens the hypothesis of ER stress as a monitor and/or regulator of nutritional and energetic status (29).

In addition to its potential function in glucose metabolism, eIF2α phosphorylation has a key role in ER stress due to its regulation of protein synthesis. By decreasing general translation, the load on the ER is reduced allowing recovery and a return to normal folding homeostasis (45,49). Paradoxically, the state of enhanced eIF2α phosphorylation promotes translational upregulation of ATF4 (54,55). Select mRNAs that contain either a secondary open reading frame or an internal ribosome entry site (IRES) can be transcribed upon eIF2α phosphorylation (56). ATF4 has two short open reading frames in its 5' untranslated region (UTR) that prevent initiation at the start codon during unstressed conditions (57). Upon eIF2α phosphorylation, reinitiating ribosomes are able to promote translation of ATF4 (58). Once translated, ATF4 aids in transcription of several members of the UPR including CHOP and GADD34 (59,60). ATF4 and its targets are part of the integrated stress response (ISR), a pro-survival gene expression program (61). Besides ER stress, several different cellular functions are also regulated by ATF4 and the ISR, including amino acid import and protection from oxidative stress.

The ultimate aim of the three branches of the UPR is to increase the folding capacity of the ER to restore homeostasis. A major mechanism for restoring capacity is the upregulation of key ER chaperones, including BiP and glucose regulated protein of 94 kDa (GRP94), as well as enzymes involved in the reduction-oxidation (redox) mechanisms of disulfide bond formation, such as BiP and ERO1α. In conjunction with

that, the amount of unfolded proteins in the ER is reduced through translational attenuation by eIF2α phosphorylation as well as increased proteolysis through ER-associated degradation (ERAD) (62). ERAD involves a series of checkpoints to separate folded from misfolded proteins. Upon prolonged retention in the ER due to problematic folding, ER degradation-enhancing α-mannosidase-like 1 (EDEM) acts to separate misfolded proteins from their chaperone (63). This improves folding capacity in two ways. It makes the chaperones available for further protein folding while allowing the misfolded protein to proceed through ERAD. Once a protein is identified as misfolded, it is ubiquitinated and degraded by the proteosome (64). EDEM is upregulated during the UPR to promote the clearance of misfolded proteins and relieve pressure on the ER during this stressed state (65).

If the mechanisms employed by the ER are unable to restore homeostasis, the final stage of the UPR is the initiation of apoptosis. All three signaling branches have pro-apoptotic targets. IRE1, via TRAF2, can induce caspase 12 cleavage and the caspase signaling cascade (66). PERK and ATF6, potentially through regulation of ATF4, can work synergistically to upregulate CHOP (42). CHOP is a bZIP containing transcription factor that is a member of the CCAAT/enhancer binding protein (C/EBP) family (67). While it promotes proper cellular function by its role in the differentiation of several cell types, it can also induce apoptosis through p38 dependent and independent mechanisms (67-71). Upon unresolved UPR, a release of calcium from the ER triggers the canonical mitochondrial initiated apoptotic pathway (72-74). Importantly, the switch between cytoprotective to cytotoxic activity is due to the duration of ER stress and variations in

signaling kinetics (75). Upon prolonged ER stress, the signaling pathways are attenuated and apoptosis begins. Artificially sustaining IRE1 activity can prevent UPR initiated apoptosis; a potential mechanism to promote cell survival and recovery during UPR driven disease states.

UPR and Disease

While the role of the UPR is to promote the proper function of the ER, it has been shown to play a key role in human health and disease. Several conditions, including neurodegeneration, tumor growth, the immune response, and diabetes, have been linked to improper or impaired UPR activation. A major focus has been on the pro-apoptotic feature of the UPR and its relationship to disease. Recently, direct links between UPR signaling and function/dysfunction has been shown to play a role in these maladies.

Many unrelated neurodegenerative diseases are caused by an accumulation of unfolded proteins that aggregate into deposits, termed lewy bodies (76). Brains afflicted with Alzheimer's disease, characterized by aggregates of amyloid β protein, have been shown to display increased UPR activity, leading to cellular toxicity (77,78). Interestingly, chaperones are not upregulated indicating that even with increases in activation, the UPR is not functioning properly (79). Notably, one chaperone, BiP, has been shown to bind to and promote proper folding of the amyloid precursor proteins thereby decreasing their plaque-forming potential (80). The UPR is similarly activated in Parkinson's disease, which has aggregation of α-synuclein (81). In a mouse model generated by treatment with a neurotoxin, XBP1 overexpression has been shown be

cytoprotective (82). Therefore, improving UPR efficiency could serve as a preventative and/or therapeutic treatment for these and possibly other neurological diseases.

Similar to Alzheimer's and Parkinson's diseases, increased UPR activation has also been seen in solid tumors (83). In these tumors, the PERK branch is activated by hypoxia in an apparent hypoxia inducible factor 1 (HIF1)-independent manner (84). Notably, optimal tumor growth is prevented upon depletion of either PERK or XBP1 (85,86). Under these conditions, tumors are more sensitive to hypoxia and cell death thereby signifying the UPR as a potential therapeutic target. Unlike how enhanced UPR could improve neurodegeneration, cancer researchers are looking to inhibit the UPR as a potential treatment.

Upon viral infection, membrane proteins and lipids are usurped for viral packaging leading to increased stress on the host cell's ER (18). The role of the UPR during infection is varied dependant on viral stain. It can promote viral activity by increasing ER efficiency and thereby aiding in viral replication. Hepatitis B has a promoter that is indirectly activated by IRE1 and sXBP1 activity (87). Additionally, in order to block the host immune response, the cytomegalovirus US11 protein induces degradation of MHCs via UPR activation (88). Conversely, the increased burden on the cell by uninhibited viral replication can induce the UPR leading to decreased translation, an antiviral response. In fact, PERK and eIF2α depleted cells have been shown to support higher viral titers (89,90). It has been discovered that several other viruses manipulate the UPR either to promote infection or impair the host's antiviral response (18). Thus, both

stimulatory or inhibitory compounds of the UPR should be developed as either type could be useful antiviral treatments, dependant on the infecting viral strain.

As indicated earlier, the UPR has been linked to several metabolic conditions, including obesity and diabetes. As more data portrays the UPR as a molecular cause of the metabolic syndrome, it has become a potential therapeutic target. While T1DM often results from an autoimmune attack on the pancreatic β cells, some cases have been shown to be due to genetic defects. The Wollcott-Rallison syndrome is a form of T1DM caused by a mutation in PERK resulting in pancreatic β cell death (91). Additionally Wolfram Syndrome, another T1DM condition, is triggered by mutations in WFS1 (92). WFS1, a UPR responsive gene, helps maintain ER homeostasis and its inactivity may lead to the β cell dysfunction seen in these patients (93). The Akita mouse, a model of T1DM, has a missense mutation in the insulin 2 gene (94). This mutation causes the protein to be misfolded and retained in the ER, resulting in ER stress and apoptosis (95). Therefore, UPR activity in β cell function and survival is an important consideration for the treatment or prevention of some forms of T1DM.

Obesity and T2DM have also been linked to altered UPR activity in several tissues. Obesity causes increased UPR activation in the liver and adipose tissues (96). This activation has been linked to decreased insulin signaling in the liver. Chronic ER stress has been seen in both the *db/db* T2DM mouse model and patients with T2DM (97). Hyperglycemia during diabetes leads to increased proinsulin production; this added strain on the ER can trigger the UPR and if not released can result in the β cell death seen in uncontrolled T2DM (98). Interestingly, treatment of *ob/ob* mice with chemical

chaperones relieves ER stress in the liver and adipose tissue and restores glucose homeostasis and insulin sensitivity (99). This indicates that impaired protein folding may be a cause of T2DM, and improving UPR efficiency rather than blocking the activation of the UPR might be a potential treatment. These data indicate that alterations in the adipocyte UPR could directly influence adipokine secretion and thereby whole body energy homeostasis.

Mitochondria

The ER protein folding and the UPR are not the only cellular functions being examined as potential causes of the metabolic syndrome. As energetics are often dysregulated in obesity and diabetes, numerous studies have been done on the role of mitochondria in these diseases. Mitochondria fulfill the energetic needs of the cell, as well as numerous other roles required for important cellular functions. This multiplicity of roles is reflected in the variation in the mitochondrial proteome seen among different tissues (100,101) and during differentiation (102).

The major function of mitochondria is the generation of ATP through oxidative phosphorylation. It however performs other roles including signaling, apoptosis, and regulation of cell growth (103). Mitochondria have four compartments each with distinct functions: the outer and inner membranes, the intermembrane space, and the matrix (104). Their membrane structure is constantly changing through fission and fusion events, and the dynamics have been correlated with mitochondrial activity (103). Mitochondria are the only organelles with their own genome, which encodes for 37 genes, including 13 proteins involved in oxidative phosphorylation, 22 transfer RNAs

(tRNAs), and 2 ribosomal RNAs (rRNAs). Mitochondrial DNA (mtDNA) transcription requires nuclear encoded proteins, Transcription factor A and B, mitochondrial (Tfam and Tfbm), and mitochondrial RNA polymerase (105). Tfam has also been shown to promote the replication and maintenance of mtDNA. Mutations or malfunctions in mtDNA have been implicated in several human diseases including diabetes mellitus, anemia, pancreatic dysfunction, and several neurological diseases, including Alzheimer's and Parkinson's diseases (106). Although some of these have a non-metabolic cause, such as an autoimmune response, the majority is often due to impaired oxidative phosphorylation leading to decreased ATP production.

In most cells, oxidative phosphorylation is the major source of energy production, in the form of ATP (104). In eukaryotes, the proteins involved in this metabolic pathway are located in the mitochondria, while similar protein complexes in prokaryotes are located in the inner membrane. In mitochondria, these protein complexes form the electron transport chain, which transfers electrons via reduction-oxidation reactions to provide energy for the movement of protons from the matrix to the intermembrane space. This influx of protons generates an electrochemical gradient across the inner membrane. The final complex involved in oxidative phosphorylation is ATP synthase, which uses the force of protons crossing the inner membrane back into the matrix to phosphorylate ADP, generating ATP. Mitochondrial oxidative phosphylation can be impaired through inhibition of any of the protein complexes within the electron transport chain, including oligomycin, which blocks ATP synthase. In addition, the proton gradient can be disrupted by addition of chemical ionophores, such as FCCP or 2,4-Dinitrophenol, or the

uncoupling protein family, all of which transport protons across the inner membrane thereby "uncoupling" proton transfer from ATP synthesis. Regulation of ATP synthesis is critical as maintenance of a sufficient ATP supply is necessary for cellular function and survival.

ATP synthesis is tightly controlled based upon the energetic needs of the cell. The cell has several mechanisms by which it regulates energy levels. AMP activated protein kinase (AMPK), is a key regulator of cellular energetics (107). Under conditions of reduced energy levels, signaling by AMPK decreases ATP consuming pathways, including protein synthesis, and increases ATP generating ones, such as fatty acid oxidation. These mechanisms of energy conservation continue until homeostatic adenine nucleotide levels are restored.

Adenylate Kinase

The concentrations of ATP and other adenine nucleotides within the cell are also regulated by an ancient family of proteins, the adenylate kinases (EC. 2.7.4.3). Members of this family are present throughout the phylogenic tree, from plants to bacteria and humans. Adenylate kinase (AK) catalyzes the reversible phosphoryl transfer reaction AMP + ATP ⇔ 2ADP. It is necessary for the survival of bacteria and lower eukaryotes (108-110). AK has been thought to provide the principal homeostatic mechanism to maintain adenine nucleotide ratios under different conditions of ATP production and utilization. It has also been proposed that AK provides a mechanism to channel the high energy phosphate of ATP from sites of ATP production to sites of utilization through the operation of phosphotransfer networks (111). Higher eukaryotes have genes coding for

up to 9 enzymes bearing similarity to AK. They differ in cellular and subcellular distribution as well as even substrate affinity indicating that each has a specific cellular function.

The most well characterized isoform is AK1, a cytosolic enzyme found in the skeletal muscle, brain, and erythrocytes (112,113). AK1, along with creatine kinase and nucleoside diphosphokinase, help maintain stable intracellular ATP concentrations (114). They are thought to promote energy transfer from ATP generating sites to ATP consuming regions. In skeletal muscle over 95% of the total adenylate kinase activity corresponds to AK1 (115). It has been shown to aid in transferring ATP from the mitochondria to myofibrils (116). However, mice lacking AK1 have normal growth and contractile ability (114,115,117). Given the importance of AK activity in prokaryotes, and the fact that AK1 is by far the predominant AK activity in muscle, it was rather surprising that these mice were able to maintain ATP levels. These results suggest that compensatory mechanisms are elicited in these mice to adapt to the lack of this enzyme. In fact, alterations in creatine kinase flux and increased glycolytic metabolism were observed. Interestingly, it was also observed that the rate of ATP synthesis, assessed by ^{18}O redistribution into high-energy phosphate-containing metabolites, was significantly increased in muscles from AK1$^{-/-}$ mice in response to contraction, indicating more ATP had to be produced to maintain normal contractility. Therefore, the efficiency of ATP use was lower in AK1$^{-/-}$ mice compared to controls, especially under stress (114,115). Proteomic analysis has shown an increase in AK1 in the muscle of obese versus lean women (118). This increase in AK1 is believed to compensate for the impaired

mitochondrial function during obesity. These results are consistent with a proposed role of AK in improving the efficiency of ATP utilization in cells through the operation of phosphotransfer networks (111), or other yet unknown mechanisms.

There are three mitochondrial members of the adenylate kinase family, AK2, AK3, and AK4. AK2 is found in the mitochondrial intermembrane space of liver, kidney, spleen, and heart (112). There are two isoforms, AK2A and AK2B, differentiated only by a small sequence variation in the C terminal region and slightly different tissue distribution (113,119). Interestingly, there is large discrepancy between the expression of the mRNA and of the protein of AK2, indicating a significant post-transcriptional regulation (120). AK3 and AK4 are localized to the mitochondrial matrix, where AK3 is more ubiquitously expressed while AK4 is in kidney, heart, liver, and brain (121). Unlike the other adenylate kinases, AK3 catalyzes the reaction AMP + GTP $\Leftrightarrow$ ADP + GDP (122). AK4 has shown no enzymatic activity but can interact with the mitochondrial adenine transporter (121). It is believed that AK2 and AK3 work together shuttling adenine nucleotides within the mitochondria to promote oxidative phosphorylation (123). In this way, they work together to enhance the efficiency of mitochondrial ATP synthesis.

Physiologically, AK2 has been shown to be required for *Drosophila* growth and development (124). Maternally derived AK2 is sufficient for embryonic development, however growth arrest occurs during the third larval stage followed by death. Recently, mutations in AK2 have been identified as the basis for reticular dysgenesis, a rare form of severe combined immunodeficiency (SCID) characterized by a complete lack of

granulocytes and almost complete deficiency of lymphocytes in the blood (125,126). Mechanistic analysis showed that zebrafish lacking AK2 also had impaired leukocyte development (126). Cells from the SCID patients showed enhanced apoptosis, abnormal levels of reactive oxygen species, and altered mitochondrial membrane potential, indicating that mitochondriopathy might be the underlying cause of this disease (126). Interestingly, patients with reticular dysgenesis also suffer from sensorineural deafness. It was found that AK2 is located in the stria vascularis region of the inner ear and therefore is most likely also responsible for this symptom of the disease (125). The effect of this enzyme on hematopoiesis illustrates the importance of adenine nucleotide regulation. Further studies on the role of adenylate kinases and energetic regulation will help in understanding their importance not only within cellular functions but perhaps also in human disease.

Mitochondria and the ER

3T3-L1 adipocyte differentiation is accompanied by the induction of the UPR and initiation of adiponectin secretion (127). This induction coincides with a robust increase in mitochondrial biogenesis (102). Adiponectin secretion by 3T3-L1 adipocytes is compromised by mitochondrial poisons and enhanced by increased mitochondrial capacity (128), suggesting a high energy requirement for its processing. These findings suggest the possibility that these two events are functionally linked, with mitochondrial function being required for UPR induction and efficient secretion in differentiated adipocytes.

Mitochondria and the endoplasmic reticulum are physically joined by junctions between their two membranes (129). The regions of ER that co-sediment with the mitochondria, termed mitochondrial associated membranes (MAM), have a different composition than non-sedimenting ER (130). These regions show enhanced phospholipid synthesis and may be the means by which the phospholipids are transferred between the two organelles. These junctions may also improve mitochondrial uptake of calcium released by the ER (131,132). The specificity of the mitochondrial calcium transporters is too low for efficient import. However, the closeness of the two organelles and the higher concentration of calcium near the ER membrane would allow more efficient mitochondrial import. Other molecules that need to travel between the two organelles are adenine nucleotides. ATP is necessary for ER chaperone function and the resulting ADP must return to the mitochondria for oxidative phosphorylation. ATP import from the cytosol has been shown to occur via a transporter, however the protein has not been identified yet (133). A large percentage of cellular ATP is required for protein folding and synthesis in both the cytoplasm as well as the ER. Therefore, direct ER/mitochondrial exchange via the MAMs would be a more efficient means of nucleotide transport. The crosstalk between the mitochondria and ER becomes more important as new data emerges. It is already known that these two organelles have roles in similar cellular functions, including calcium signaling and apoptosis. Additionally, both have been implicated in metabolic diseases and neurodegenerative conditions, such as Alzheimer's and Parkinson's diseases. Greater understanding of the role of mitochondria in the energetics of the ER and the UPR would supply insight not only into

basic cellular function, but could also provide information about the root cause of several

human diseases and potential targets for prevention and treatment.

SPECIFIC AIMS

The goal of this body of work is to examine the role energetics play in protein folding and the induction of the unfolded protein response. Previous studies have illustrated the relationship between ER and mitochondrial functions within the cells, mainly focusing on calcium regulation and signaling. Additionally, both mitochondrial biogenesis and induction of the UPR have been shown during 3T3-L1 differentiation. Physiologically, numerous studies have linked the UPR to Diabetes Mellitus and several neurodegenerative diseases. Separately, mitochondrial dysfunction has also been proposed as a cause for these same diseases. These similarities led us to question whether it could be a joint breakdown in both organelles resulting in the disease.

Although it is known that ER function requires ATP for chaperone function, the full extent of the energetics of ER function has not been examined. Therefore we sought to look at the role of mitochondrial ATP synthesis on ER function. ATP is not only synthesized by mitochondrial oxidative phosphorylation, but can also be produced through adenylate kinase activity. Interestingly, both UPR impairment, such as by IRE1 or XBP1 depletion, and mutations in AK2 result in profound alterations in hematopoiesis. Therefore, we also asked whether AK generated ATP would also be required for ER function. Thus, the specific aims of this study are:

1) To examine the induction of the UPR during 3T3-L1 differentiation and its role in adipocyte secretion.

2) To determine the effect of ATP generated from mitochondrial oxidative phosphorylation on UPR function.

3) To ascertain whether adenine nucleotide regulation by AK affects the UPR.

CHAPTER II

CONCURRENT UPREGULATION OF THE UPR AND MITOCHONDRIAL BIOGENESIS DURING 3T3-L1 DIFFERENTIATION

The following data includes unpublished results as well as data taken from:

Shi, X., **Burkart, A.**, Nicoloro, S. M., Czech, M. P., Straubhaar, J., and S. Corvera (2008) Paradoxical Effect of Mitochondrial Respiratory Chain Impairment on Insulin Signaling and Glucose Transport in Adipose Cells. *J Biol Chem* 283, 30658-30667.

Burkart, A., Shi, X., Chouinard, M., and S. Corvera (2010) Adenylate Kinase 2 Links Mitochondrial Energy Metabolism to the Induction of the Unfolded Protein Response. *Submitted*.

The analysis of the mitochondrial DNA and some of the Tfam siRNA transfections were performed by Xiarong Shi. Microarray experiments on 3T3-L1 differentiation were performed by Sarah Nicoloro with Juerg Straubhaar performing statistical analysis on the resulting data. I performed the remaining experiments contained within this chapter.

Summary

The white adipose cell plays a major role in the regulation of whole body metabolism, through the storage and hydrolysis of triglycerides, thereby affecting systemic energy levels and insulin sensitivity. The 3T3-L1 cell line undergoes mitochondrial biogenesis during adipocyte differentiation to allow for efficient fatty acid metabolism; however, the induction of other metabolic pathways besides fatty acid catabolism may indicate that the cell has a greater energetic role than solely triglyceride storage. Adipocytes are able to control satiety and energy metabolism through the secretion of proteins, such as adiponectin, leptin, and resistin. Secretory function in cell types such as pancreatic β cells and antibody producing B cells is highly dependent on the unfolded protein response (UPR). Other labs, as well as our own, show that 3T3-L1 differentiation involves upregulation of the UPR, including key proteins such as the endoplasmic reticulum chaperone BiP, and the transcription factors XBP1 and CHOP. Here we demonstrate that adiponectin secretion is preceded by the induction of the unfolded protein response (UPR) in differentiating 3T3-L1 adipocytes. Additionally, impairment of XBP1 activation results in a parallel impairment of adiponectin expression, indicating that the adipocyte UPR pathway is necessary for its secretory functions, and can thus play a crucial role in the control of whole body energy homeostasis. Since mitochondrial biogenesis is occurring in parallel to induction of the UPR, we tested whether it was necessary for ER function. Depletion of Tfam, a mitochondrial transcription factor, and treatment with chemical inhibitors, shows that ER

function is sensitive to acute changes in adenine nucleotide levels through mitochondrial manipulations.

Background

White adipocytes play a central role in the regulation of whole body metabolism by sensing nutrient levels, and responding with the secretion of peptide factors that act on the central nervous system and peripheral tissues to control caloric intake and utilization (6,7). These factors include the hormone leptin, as well as the protein adiponectin (8-10). The levels and oligomeric structure of serum adiponectin positively correlates with insulin sensitivity (134,135). Moreover, insulin sensitizers of the thiazolidinedione family stimulate adiponectin secretion and this effect could contribute to the therapeutic actions of these drugs (136). Given the importance of adiponectin to whole body homeostasis, understanding the molecular mechanisms that regulate its secretion from adipocytes is highly relevant.

Adiponectin is synthesized as a 247 amino acid polypeptide that undergoes extensive folding to form a trimer stabilized through disulfide bond formation (8,9). In addition to trimeric adiponectin, higher molecular weight complexes are formed and secreted by adipocytes, indicating that the process of adiponectin folding in the endoplasmic reticulum is likely to be complex. Earlier proteomic analysis of 3T3-L1 adipocyte differentiation revealed a pronounced increase in the mRNA levels for the ER chaperone ERO1α (102), a protein involved in disulfide bond formation during protein folding (137). It has also been recently shown that the UPR is upregulated during 3T3-L1

adipocyte differentiation (127). These studies prompted us to investigate whether further adaptations of the ER folding machinery would be necessary for the establishment of adipocyte secretory functions.

Protein folding capacity in the endoplasmic reticulum is achieved through a series of mechanisms collectively termed the "unfolded protein response" (UPR) (98,138-140). These mechanisms can be induced by artificial pressure upon the secretory pathway, such as that which occurs when cells express proteins that are difficult to fold or when drugs, such as tunicamycin, impair the enzymatic machinery required for folding (19). Under these extreme conditions, three branches of the UPR are activated, each initiated through activation of the transmembrane endoplasmic reticulum signaling proteins ATF6, IRE1, and PERK. ATF6 is cleaved by Golgi membrane endopeptidases to produce a bZIP domain that translocates into the nucleus. IRE1, through its intrinsic endoribonuclease activity cleaves the mRNA for the transcription factor XBP1, resulting in translation of a stable product. These induce transcriptional and translational responses that enhance the folding capacity of the ER. The serine/threonine protein kinase PERK phosphorylates and inactivates eIF2α, resulting in temporary arrest of general protein translation thus transiently limiting protein synthesis.

Specific branches of the UPR are active in cells that sustain chronically elevated protein flux through the ER, such as the pancreatic β cell and the salivary gland, and these cells are particularly sensitive to alterations in the UPR pathway (141). Thus, PERK knockouts or knock-ins of non-phosphorylatable mutants of the PERK substrate eIF2α result in rapid post-natal β cell failure and diabetes (142). The IRE1 branch of the UPR is

activated upon differentiation of plasma cells, and is necessary at the latest stages of differentiation to enable the secretion of immunoglobulins (30,143). Here we provide evidence for the induction of the XBP1 branch of the UPR during the process of adipocyte differentiation, and its requirement for adiponectin secretion. These data indicate that alterations in the adipocyte UPR could directly influence adipokine secretion and thereby whole body energy homeostasis.

We have previously reported that differentiation of 3T3-L1 preadipocytes is accompanied by a robust increase in mitochondrial biogenesis (102), which coincides with the induction of the UPR and initiation of adiponectin secretion. Adiponectin secretion by 3T3-L1 adipocytes is compromised by mitochondrial poisons and enhanced by increased mitochondrial capacity (128), suggesting a high energy requirement for its processing. These findings suggest the possibility that these two events are functionally linked, with mitochondrial biogenesis being required for UPR induction and to sustain adiponectin secretion in differentiated adipocytes.

Mitochondria play an essential role in fulfilling the energetic needs of the cell, as well as numerous other roles required for cell function. This multiplicity of roles is reflected in the variation in the mitochondrial proteome seen among different tissues (100,101), or during differentiation (102). To investigate the relationship between mitochondrial biogenesis and the induction of the UPR, we focused on manipulating oxidative phosphorylation through two methods, Tfam depletion and chemical inhibitors. Previous work from our laboratory has shown that Tfam, a factor involved in mtDNA transcription and replication (144) can be silenced during 3T3-L1 adipocyte

differentiation, mitigating the increase in oxidative phosphorylation that accompanies normal mitochondrial biogenesis (145). In addition, we used chemical compounds such as FCCP, a mitochondrial uncoupler, and oligomycin, which blocks the mitochondrial ATP synthase, to induce inhibitory manipulations of oxidative phosphorylation. We find that acute impairments of oxidative phosphorylation results in diminished UPR activation, however more prolonged alterations through Tfam depletion has little effect on ER function, suggesting that the observed changes are due to the differential regulation of ER function or compensation through other mechanisms.

Results

The 3T3-L1 cell line is a well-characterized model system for adipocyte differentiation and function. Treatment of these cells with a hormone cocktail induces a phenotypic change from a fibroblastic pre-adipocyte to a quiescent adipocyte (Figure 2.1A). Upon differentiation, the 3T3-L1 takes on characteristics of a primary adipocyte including lipid accumulation, insulin sensitivity, and the expression of adipocyte specific proteins. Previously, our lab has shown that mitochondrial biogenesis occurs during differentiation, as demonstrated by the increased protein expression of cytochrome C and heat shock protein 60 (HSP60) (Figure 2.1B and (102)). The increased protein expression accompanies increased mitochondrial mass and increased function as assessed by oxygen consumption (102). Mass spectrometry analysis was performed on proteins increased during differentiation purified from a crude mitochondrial isolation; interestingly,

ERO1α, an ER resident protein was co-purified and shown to be significantly increased (102). We sought to determine whether the increase in ERO1α represented a general improvement in the secretory capacity of the cell as a function of adipogenesis.

The adipocyte, a known secretory cell, regulates whole body metabolism through secretion of adipokines and other proteins, such as tumor necrosis factor alpha (TNFα) (146,147). Adiponectin is an adipokine found in human serum at concentrations of 10-20 μg/mL (148). It is also produced and secreted at copious levels by 3T3-L1 adipocytes and we used it as a marker of secretory ability throughout differentiation. The cell begins expressing adiponectin at low levels on day 3 of differentiation (data not shown). However, secretion does not begin until day 4 of differentiation and peaks around day 7 (Figure 2.1C).
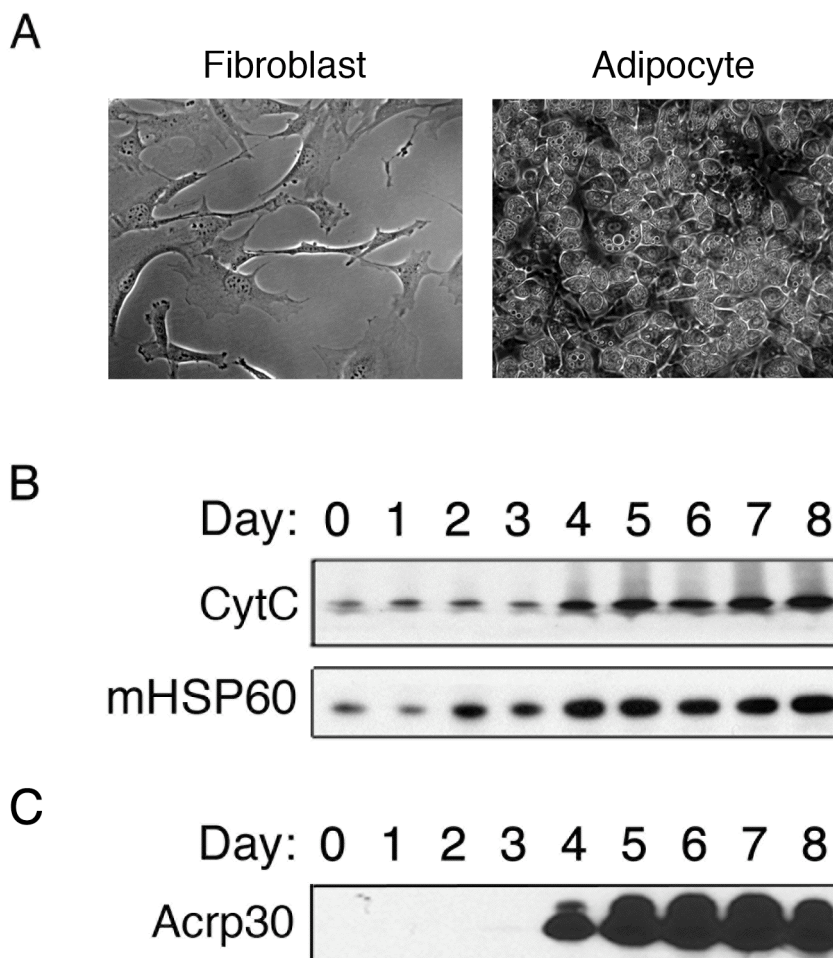
Figure 2.1: Differentiation of 3T3-L1 adipocytes.

A. Bright field image of 3T3-L1 fibroblasts (left) and adipocytes (right). B. 3T3-L1 cells were harvested just prior to addition of hormonal cocktail (day 0), and at indicated days of differentiation thereafter. Cell extracts were analyzed by western blotting with antibodies to the proteins indicated. C. Culture media was analyzed by western blotting with anti-adiponectin (Acrp30). All data is representative of three independent experiments.

The UPR is a combination of responses that work jointly to expand the folding efficiency and capability of the ER (43,98,138,139). It is elicited in cells when demand for secretory capacity is high, such as during the differentiation of B lymphocytes into antibody-secreting plasma cell (38,143). It entails the activation of transcriptional mechanisms that increase the levels of ER chaperones, including BiP. Affymetrix chip databases of RNA isolated from 3T3-L1 cells at different times of differentiation were queried with a list of probe sets for secretory and ER resident proteins. As expected, differentiation was accompanied by more than 10-fold increases in RNA expression for adiponectin, adipsin, and resistin (Table 1). In addition, other secretory proteins involved in extracellular matrix deposition and angiogenesis were also greatly induced. We anticipated the ER capacity to expand in order to process this increased secretory load. In fact, mRNA levels of resident proteins of the endoplasmic reticulum were also increased (Table 1). Enzymes which regulate lipid metabolism were increased, such as stearoyl-coA desaturase 1 (SCD1) and diacylglycerol O-acyltransferase 1 (DGAT1). As found in a previous study (102), ERO1-like, a protein involved in oxidative protein folding, is also upregulated. Thus, both the secretory load as well as a transcriptional response for endoplasmic reticulum components increase during differentiation.

Secretory Proteins	Symbol	FC
Adipocyte, C1Q and collagen domain containing	Acdc	205.43
Adipsin	Adn	120.26
Apolipoprotein C-1	Apoc1	34.45
Resistin	Retn	21.95
Haptoglobin	Hp	18.43
Carboxylesterase 3	Ces3	16.83
Angiotensinogen	Agt	10.31
Vascular endothelial growth factor A	Vegfa	7.89
Orosomucoid 1	Orm1	7.87
Retinoic acid receptor responder (tazarotene induced) 2	Rarres2	6.45
Growth hormone releasing hormone	Ghrh	3.56
ER Resident Proteins	**Symbol**	**FC**
Stearoyl-Coenzyme A desaturase 1	Scd1	69.96
Carboxylesterase 3	Ces3	16.83
Diacylglycerol O-acyltransferase 1	Dgat1	12.80
Expressed sequence AU018778	AU018778	8.03
ERO1-like (S. cerevisiae)	Ero1l	4.43
Longevity assurance homolog 4 (S. cerevisiae)	Lass4	4.19
P450 (cytochrome) oxidoreductase	Por	3.37

Table 2.1: mRNA expression during 3T3-L1 differentiation.

Databases containing mRNA expression of 3T3-L1 pre-adipocytes and adipocytes were generated and analyzed as previously described (102,149). Genes annotated as being either extracellular or as residing in the endoplasmic reticulum, and showing a minimum of a 3-fold increase during differentiation are listed. The expression levels are an average of three independent experiments ($p< 0.05$). Full gene expression profiles can be obtained through www.diabetesgenome.org

The kinetics of induction of these mRNAs during differentiation were then analyzed. The most pronounced increase in mRNA for most secreted proteins, including adiponectin, adipsin, and resistin, occurred between day 2 and day 4 of differentiation (Figure 2.2A). Interestingly, the mRNA for XBP1 began to increase between day 0 and day 2, prior to the induction of the secreted proteins, and continued to increase through day 4. The active form of XBP1 (sXBP1) is the translation product of an mRNA spliced by IRE1, an ER-resident endoribonuclease (43,150). To determine whether increased levels of sXBP1 protein parallel the changes in XBP1 mRNA, total extracts of 3T3-L1 cells obtained during differentiation were analyzed by western blotting (Figure 2.2B). An increase in sXBP1 protein was detected at day 2 of differentiation, and this increased to maximum level at day 3, after which it decreased moderately and remained present throughout differentiation (Figure 2.2B). In this regard, adipocyte differentiation is similar to differentiation of B cells into plasma cells, where XBP1 is induced prior to the increase in expression of IgM transcripts (143).

To determine whether downstream targets of XBP1s were induced, we analyzed the levels of BiP, a protein chaperone, and ERO1α after the induction of differentiation. The levels of both proteins increased during differentiation (compare day 0 and day 2), reaching a maximum at day 5 (Figure 2.2B). Notably, increases in both the mRNA and protein of XBP1, as well as BiP and ERO1α protein levels, precede the secretion of adiponectin that is elicited during 3T3-L1 cell differentiation.

Together with other forms of cellular stress, ER stress is associated with the activation of the transcription factor CHOP/GADD153, a member of the C/EBP family

(151). CHOP is induced at least in part through the actions of ATF4 (59), and can heterodimerize with other members of the C/EBP family, enhancing or repressing their ability to act upon specific promoters (68). In 3T3-L1 cells, CHOP has been reported to be induced early in differentiation, and to act to suppress the action of C/EBPα (67). CHOP mRNA also becomes elevated later in differentiation, to an extent influenced by glucose availability (152,153). Western blotting with antibody to CHOP (Figure 2.2B) revealed a detectable increase in CHOP protein levels as cells reach post-confluency (day –2 to day 0). This is followed by a decrease in CHOP protein levels at early stages of differentiation (day 0 to day 2). CHOP levels then gradually increased through day 7. These results confirm those reported by others (67,152,153), and are consistent with the induction of the UPR during adipogenesis.
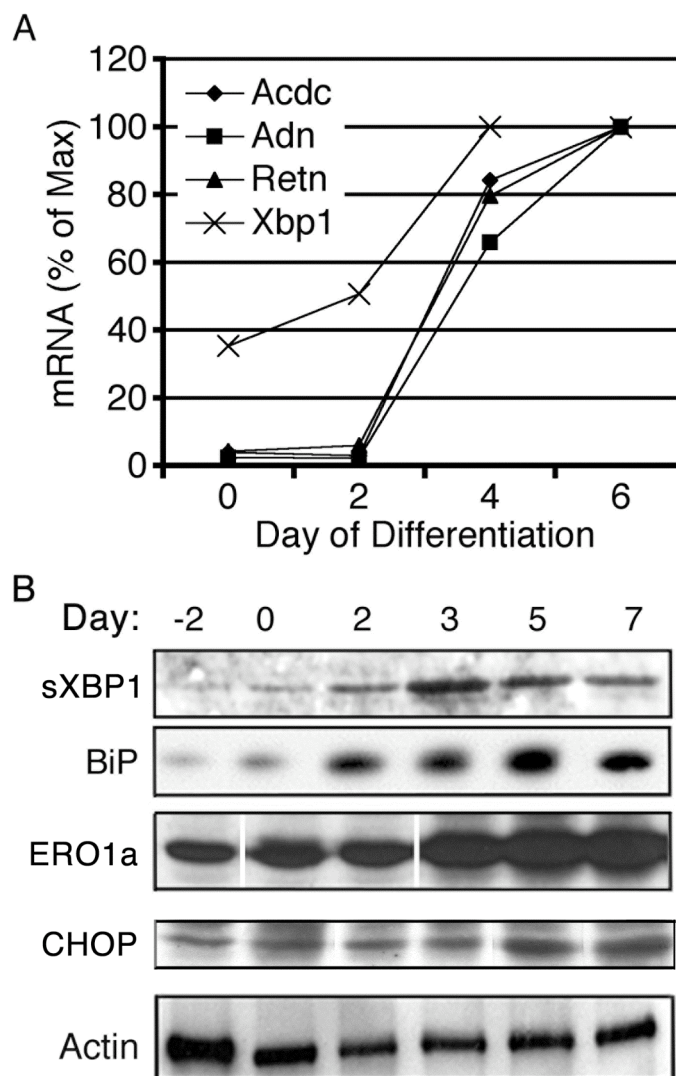
Figure 2.2: UPR induction during 3T3-L1 differentiation.

A. RNA was isolated from 3T3-L1 cells at days 0, 2, 4, and 6 during differentiation. Databases containing this mRNA expression data were generated and analyzed as previously described (102,149). The expression levels of secretory proteins, Adiponectin (Acdc), Adipsin (Adn), and Resistin (Retn), and the UPR marker XBP1 (Xbp1) are shown. The expression levels are an average of three independent experiments (p< 0.05). Full gene expression profiles can be obtained through www.diabetesgenome.org B. 3T3-L1 cells were at full confluence (day –2), just prior to addition of hormonal cocktail (day 0), and at indicated days of differentiation thereafter. Cell extracts were analyzed by western blotting with antibodies to the proteins indicated. Blots are representative of three independent experiments.

XBP1 has been shown to be required for expression and folding of IgM in plasma cells (154). To determine the functional role of XBP1 in adipocyte differentiation and function, XBP1 was depleted during the early stages of 3T3-L1 adipocyte differentiation. When cells were exposed to an interfering RNA oligonucleotide directed to XBP1 at day 2 of differentiation, the mRNA levels of XBP1 and spliced XBP1 measured at day 5 were decreased to approximately 20% and 40% respectively (Figure 2.3A) and the protein was decreased about 50% (Figure 2.3B), compared to scrambled levels. To determine the effect of XBP1 depletion on adipocyte differentiation, lipid accumulation was examined. XBP1 depletion by siRNA had no effect on lipid accumulation based upon either visual examination of lipid droplets stained with Oil Red O (Figure 2.3C) or quantification of Oil Red O staining (Figure 2.3D). As an additional functional parameter of adipogenesis, we analyzed insulin stimulated glucose uptake, which depends on the appropriate expression of the insulin-signaling pathway as well as trafficking elements specific to the adipocyte (155). Although basal glucose uptake was decreased in response to XBP1 depletion, insulin produced a robust stimulation of glucose uptake in XBP1 depleted cells (Figure 2.3E). Thus, XBP1 depletion did not affect the development of lipid accumulation and insulin responsiveness, two key parameters of adipocyte differentiation.

Figure 2.3: Effect of siRNA to XBP1 on mRNA expression.

3T3-L1 cells were transfected by electroporation at day 2 of differentiation with either non-targeting scrambled (Scr) siRNA or siRNA targeting XBP1. Experiments were performed 72 hours later. A. The degree of knockdown was determined for mRNA expression by qRT-PCR. B. The degree of knockdown was determined for protein expression by western blot. C. Representative fields of Oil Red O stained cells. D. Quantification of Oil Red O staining by absorbance in a multimode plate reader. E. Glucose uptake expressed as a function of basal glucose uptake in cells treated with Scr siRNA. * indicates p<0.05 by paired two-tailed Student t-test. All values are means of a minimum of three independent experiments.

To further investigate any effects that XBP1 depletion had on the differentiating adipocyte, we examined the expression of several proteins involved in ER function or the UPR, including BiP and ERO1α, as well as transmembrane and secreted proteins that need to be processed by the ER, including adiponectin, glucose transporter 4 (GLUT4), and glucose transporter 1 (GLUT1), in addition to perilipin, mitochondrial HSP60, and β-actin by western blot analysis. There was no apparent change in the expression levels of these proteins upon XBP1 depletion (Figure 2.4A). These results show the specificity of the silencing oligonucleotides to the XBP1 mRNA, and also indicate that the diminished level of XBP1 mRNA does not have a generalized effect on ER or mitochondrial chaperones (BiP, ERO1α, mHSP60) nor on adipocyte-specific protein expression (GLUT4 and perilipin).

To test the hypothesis that the UPR is required to meet the increased demand in secretory capacity during differentiation, the effect of disruption of XBP1 expression on adiponectin secretion was analyzed. The rate of adiponectin accumulation in the media of cells exposed to either Scr or XBP1-directed siRNA was measured by western blot (Figure 2.4B). A 35% decrease in adiponectin secretion was measured in cells depleted of XBP1 (Figure 2.4C). Adiponectin forms trimers stabilized by disulfide bonds that can then form larger complexes of up to 16-18 peptides (8,9). These higher molecular weight complexes are secreted by adipocytes into the circulation. Since all oligomeric forms of adiponectin are decreased to the same extent, XBP1 depletion does not seem to preferentially affect the more complex oligomers (data not shown). This decrease was also not due to a generalized decrease in secretory function, as total ^{35}S-methionine

labeled proteins detected in the media were not significantly decreased by XBP1 depletion (data not shown). Thus, the induction of XBP1 during adipocyte differentiation appears to be mostly required for the adaptation of this cell for secretion of adiponectin. In this regard, XBP1 function in adipocytes is similar to that seen in B cells, where it promotes the synthesis, maturation, and secretion of IgM heavy chains, but not other secretory proteins, such as class I and class II MHC, and Ig light chains (154).
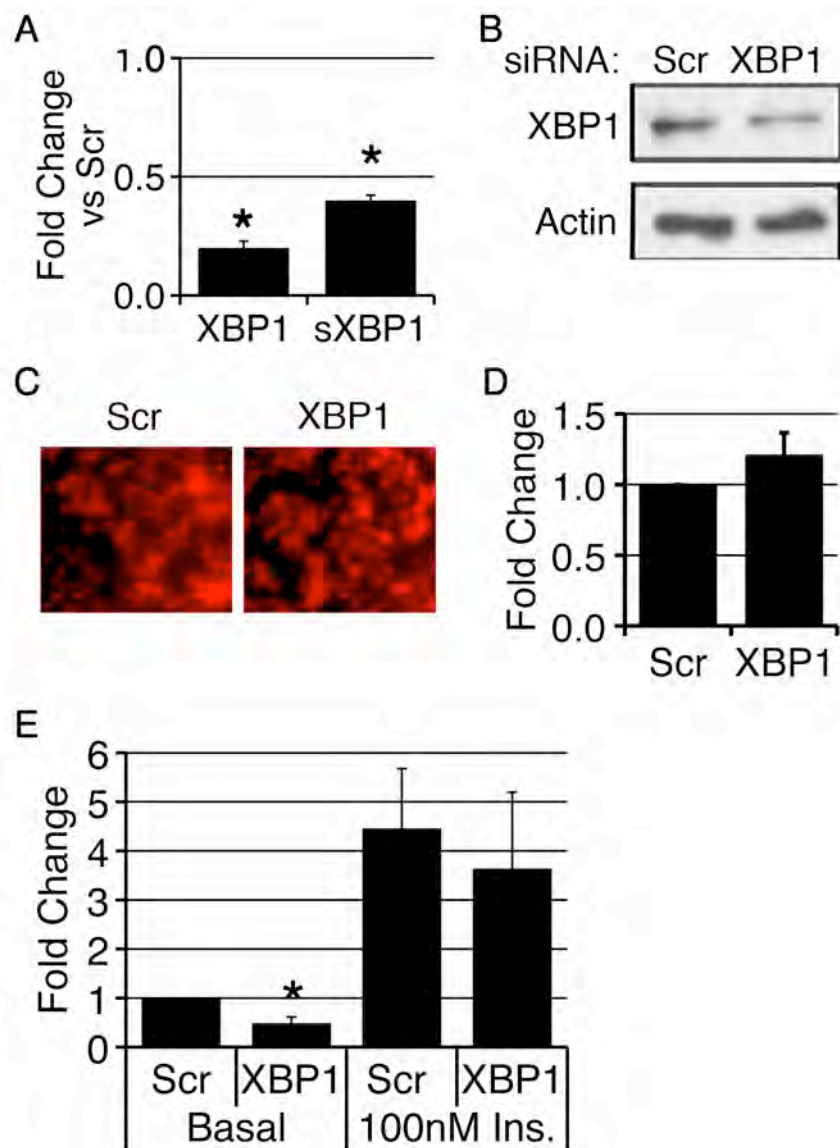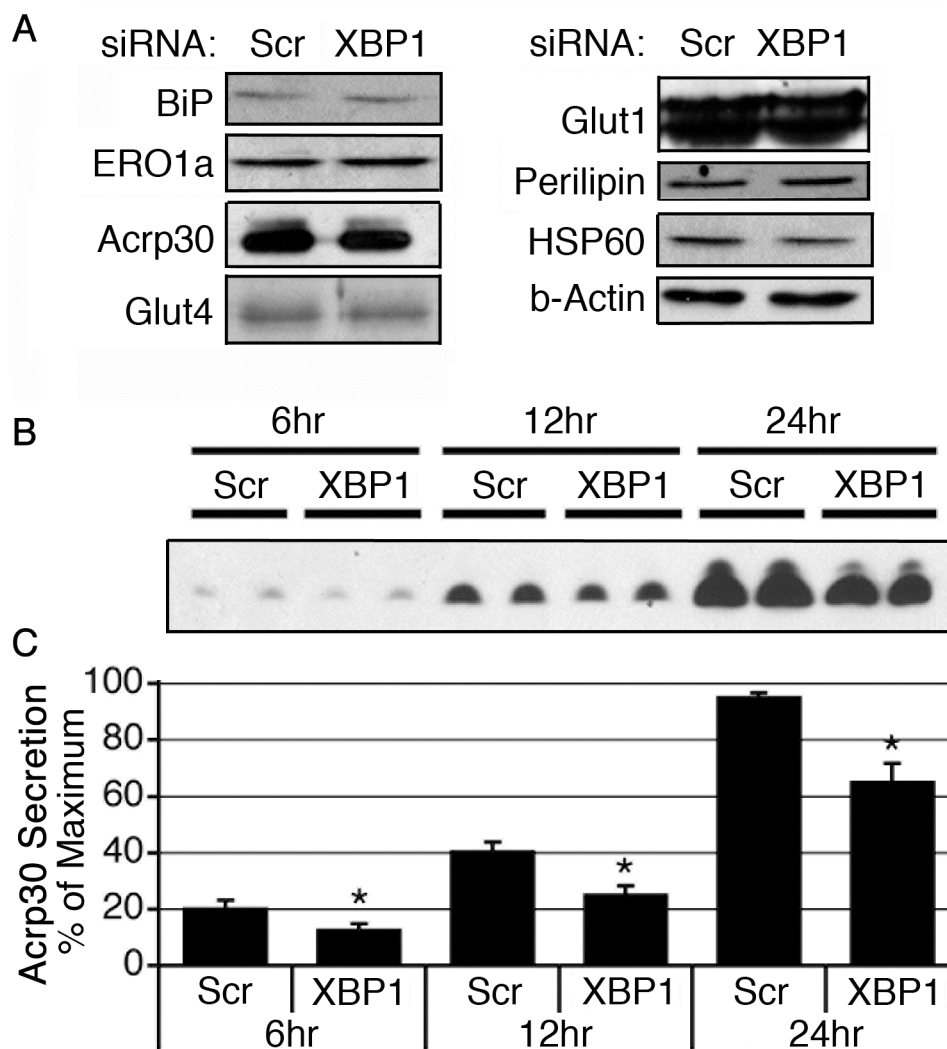
Figure 2.4: Effect of siRNA to XBP1 on adiponectin secretion.

3T3-L1 cells were transfected by electroporation at day 2 of differentiation with either non-targeting scrambled (Scr) siRNA or siRNA targeting XBP1. Experiments were performed at day 5 of differentiation. A. Cell extracts were analyzed by western blotting with antibodies to the proteins indicated. B. Media was replaced and samples of the media were taken at times indicated and analyzed by western blotting with anti-adiponectin antibodies. C. Quantification of the western blot analyses shown in B by densitometry. * indicates $p < 0.05$ by paired two-tailed Student t-test. Blots are representative of 3 independent experiments, values are the means of three independent experiments.

As described earlier, mitochondrial biogenesis occurs in parallel with increased protein secretion and the upregulation of the UPR during 3T3-L1 differentiation. We decided to test whether this increase in mitochondrial mass and function was necessary for the enhanced secretory capacity of the cell. We have previously shown that siRNA-mediated depletion of Tfam, a nuclear-encoded transcription factor for mitochondrial DNA, does not impair the increase in mitochondrial mass seen during adipocyte differentiation, but does lead to impaired respiratory chain function (145). This impairment is due to reduced transcription of the respiratory chain subunits encoded by mitochondrial DNA. We used this model system of reduced mitochondrial function to closely examine UPR function and protein secretion. siRNA targeted depletion led to a decrease in Tfam mRNA expression and mtDNA content by 60% and 40% respectively (Figure 2.5A and B). This caused a decrease in oxygen consumption and ATP levels similar to what was published previously (data not shown and (145)). The depletion in Tfam did not alter lipid accumulation indicating that differentiation proceeded normally (Figure 2.5C). Additionally, there was no obvious change in mitochondrial structure as assessed by HSP60 immunostaining (Figure 2.5D). These data confirm what was seen previously, that Tfam depletion does not affect general adipocyte function or mitochondrial mass.

Figure 2.5: Tfam depletion does not inhibit induction of UPR.

Cells were transfected with scrambled (Scr) or Tfam targeting (Tfam) siRNA at day 2 of differentiation. Experiments were performed on day 5 of differentiation. A. Level of Tfam mRNA determined by qRT-PCR. B. Level of mtDNA copy number. C. Lipid accumulation based upon Oil Red O staining (red) with Hoeschst stained nuclei (blue). D. Mitochondrial morphology determined by HSP60 immunostaining (red) with Hoeschst stained nuclei (blue). * indicates $p<0.05$ by paired two-tailed Student t-test. Images are representative of 3 independent experiments. Values are the means of a minimum of three independent experiments.

We then examined the effect Tfam depletion has on the UPR. We first examined the structure of the ER based upon immunocytochemistry with an anti-calreticulin antibody and found no obvious differences between scrambled and Tfam-directed siRNA treated cells (Figure 2.6A). Next we analyzed the effect of Tfam depletion on the expression of several UPR markers. The decrease in Tfam expression did not impair basal sXBP1 mRNA levels, nor the basal mRNA levels of the UPR sensors, PERK, ATF6, and IRE1α (Figure 2.6B). Analysis of proteins involved in the control of post-translational processing in the ER revealed a decrease in mRNA levels for ERO1α, which re-oxidizes protein disulfide isomerase to support disulfide bond formation (156). ERO1α levels are sensitive to oxygen tension (157), suggesting that its decrease may reflect alterations in the redox state caused by impairment in the respiratory chain function of Tfam depleted cells. Similar to the affects seen on mRNA expression, Tfam depletion did not have a significant effect on protein levels of two key markers of the UPR, sXBP1 and BiP (Figure 2.6C). Taken together these data indicate that decreased respiratory chain function through Tfam depletion does not significantly impair the induction of the UPR induced by differentiation in 3T3-L1 cells.
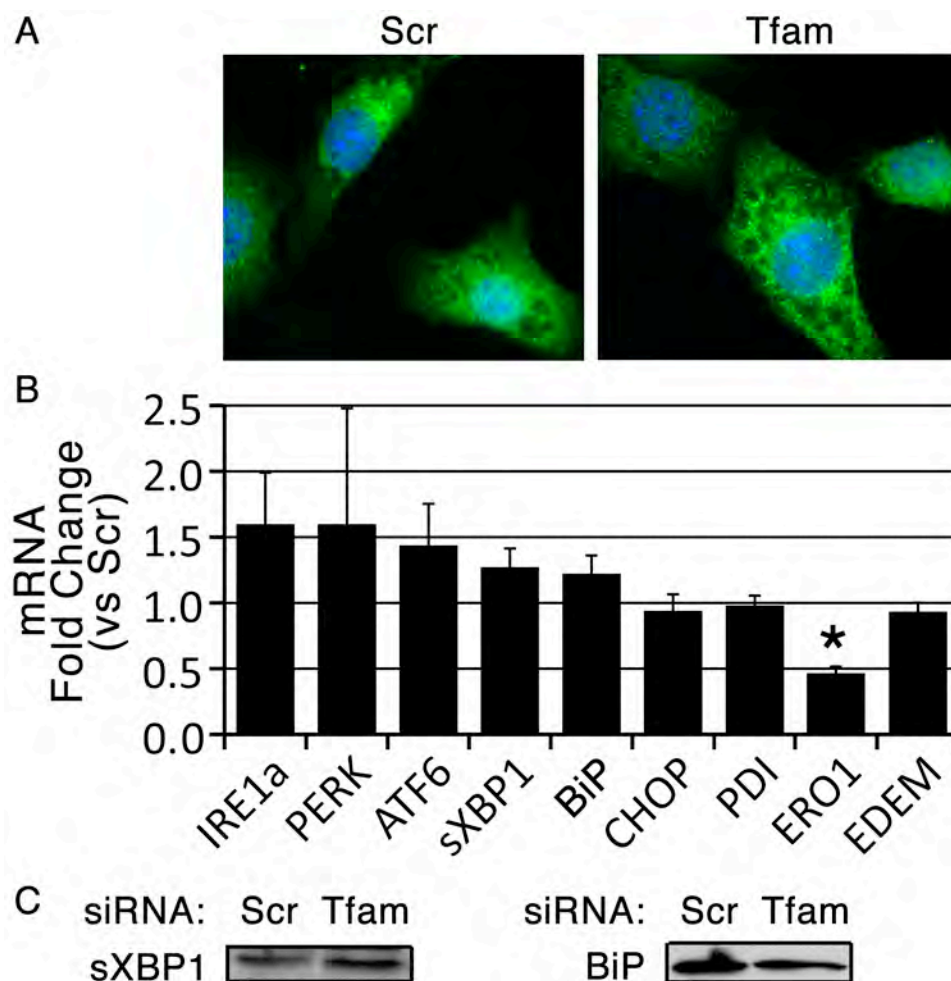
Figure 2.6: Basal UPR upon Tfam depletion.

Cells were transfected with scrambled (Scr) or Tfam targeting (Tfam) siRNA at day 2 of differentiation. Experiments were performed on day 5 of differentiation. A. ER morphology determined by calreticulin immunostaining (green) with Hoeschst stained nuclei (blue). B. Fold change of mRNAs for specific UPR proteins determined by qRT-PCR upon depletion of Tfam relative to scrambled. C. Protein levels for UPR markers by western blotting. * indicates $p < 0.05$ by paired two-tailed Student t-test. Images and blots are representative of 3 independent experiments. Values are the means of a minimum of three independent experiments.

To determine whether impaired respiratory chain function would affect the induction of the UPR by increased misfolded protein load in fully differentiated cells, we examined the effects of tunicamycin, which blocks N-linked glycosylation causing the accumulation of unfolded proteins. IRE1 activation was monitored through the splicing of XBP1 mRNA. Tfam depletion had no effect on the integrated magnitude of tunicamycin-induced XBP1 splicing over a 24-hour period (Figure 2.7A). The induction of BiP mRNA was used as a marker to assess the regulation of UPR chaperones. Again, there was no effect on the tunicamycin-induced increase in BiP mRNA upon Tfam depletion (Figure 2.7B). These experiments suggest that respiratory chain activity and oxidative phosphorylation are not rate limiting for UPR induction in response to enhanced secretory load in 3T3-L1 adipocytes. These results are also consistent with previous reports of a lack of requirement for electron transport for BiP induction in response to thapsigargin-induced ER stress (158).
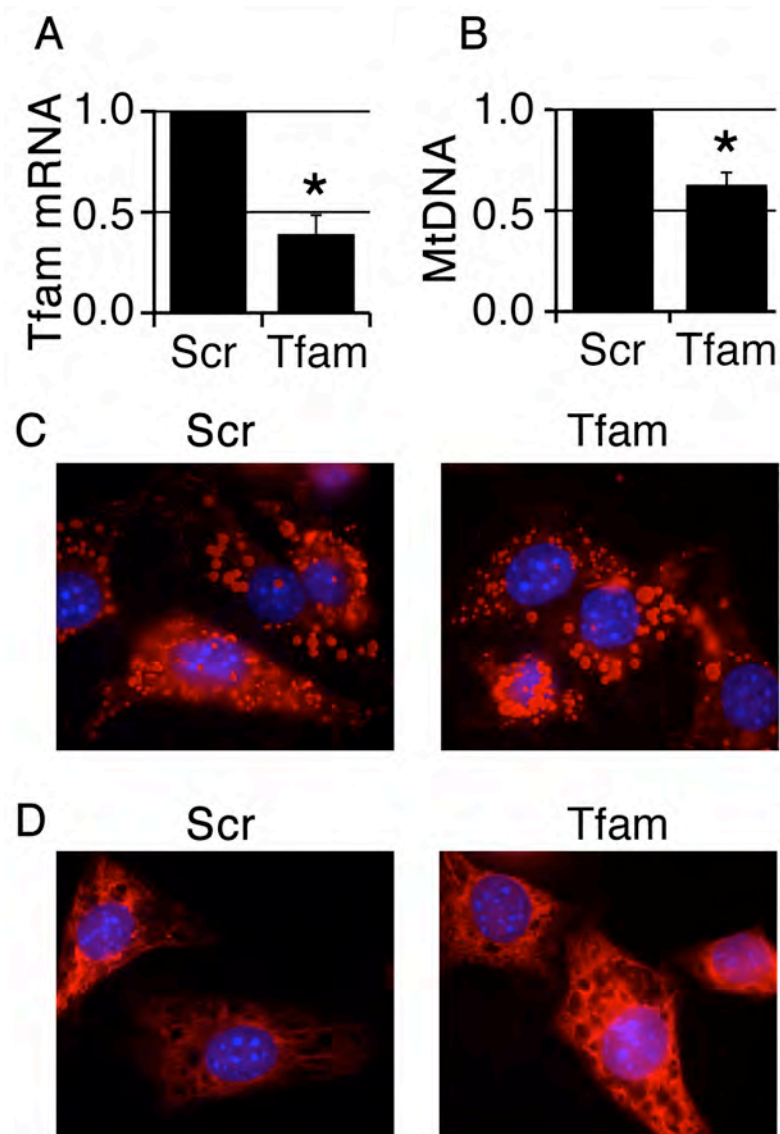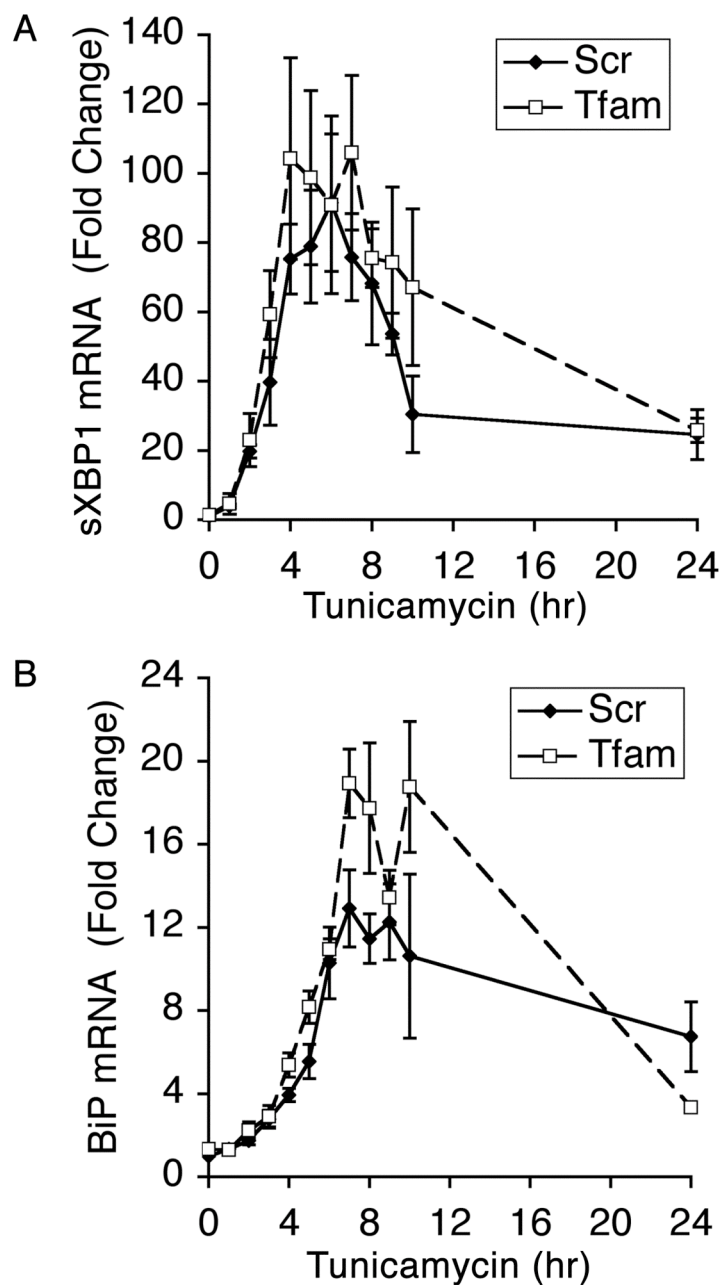
Figure 2.7: Tfam depletion does not inhibit induction of UPR.

Cells were transfected with scrambled (Scr) or Tfam targeting (Tfam) siRNA at day 2 of differentiation. Experiments were performed on day 5 of differentiation. A. Time course of IRE1 activation by tunicamycin, measured by qRT-PCR of spliced XBP1 (sXBP1). B. Time course of BiP accumulation upon tunicamycin treatment determined by qRT-PCR of BiP mRNA. All values shown are means of a minimum of three independent experiments.

These results raise the question of the mechanisms by which nucleotides can exert such profound effects on endoplasmic reticulum function in previous studies. To better understand the relationship between energy levels and UPR function, we acutely manipulated ATP levels using FCCP or oligomycin, which impair oxidative phosphorylation by dissipating the proton gradient or by directly inhibiting the mitochondrial ATP synthase respectively. As was expected, FCCP increases oxygen consumption in 3T3-L1 adipocytes to the maximum respiratory capacity while oligomycin induces an almost complete block in cellular respiration (Figure 2.8A). At these concentrations, incubation with oligomycin and FCCP induced only a partial decrease in ATP levels, 25% and 50% respectively (Figure 2.8B), comparable to the approximate 50% decrease in ATP synthesis seen in Tfam depleted cells (145). Therefore these inhibitors are affecting mitochondrial oxidative respiration and ATP synthesis as expected. To assess these manipulations on the UPR, we examined IRE1 activation. Treatment with the mitochondrial inhibitors induced a 2-fold increase in XBP1 splicing (Figure 2.8C), similar to previously published accounts (128). Previously, Koh et al. have shown that incubation with CCCP, another mitochondrial uncoupler, or oligomycin causes impairment of adiponectin secretion (128), and here we confirm the effect of oligomycin and find that FCCP also has a similar effect (Figure 2.8D). In addition, DNP, another uncoupler of the proton gradient, can impair adiponectin secretion in a dose dependant manner (Figure 2.8E). Therefore, acute manipulation of mitochondrial driven ATP synthesis can affect ER function and secretion.
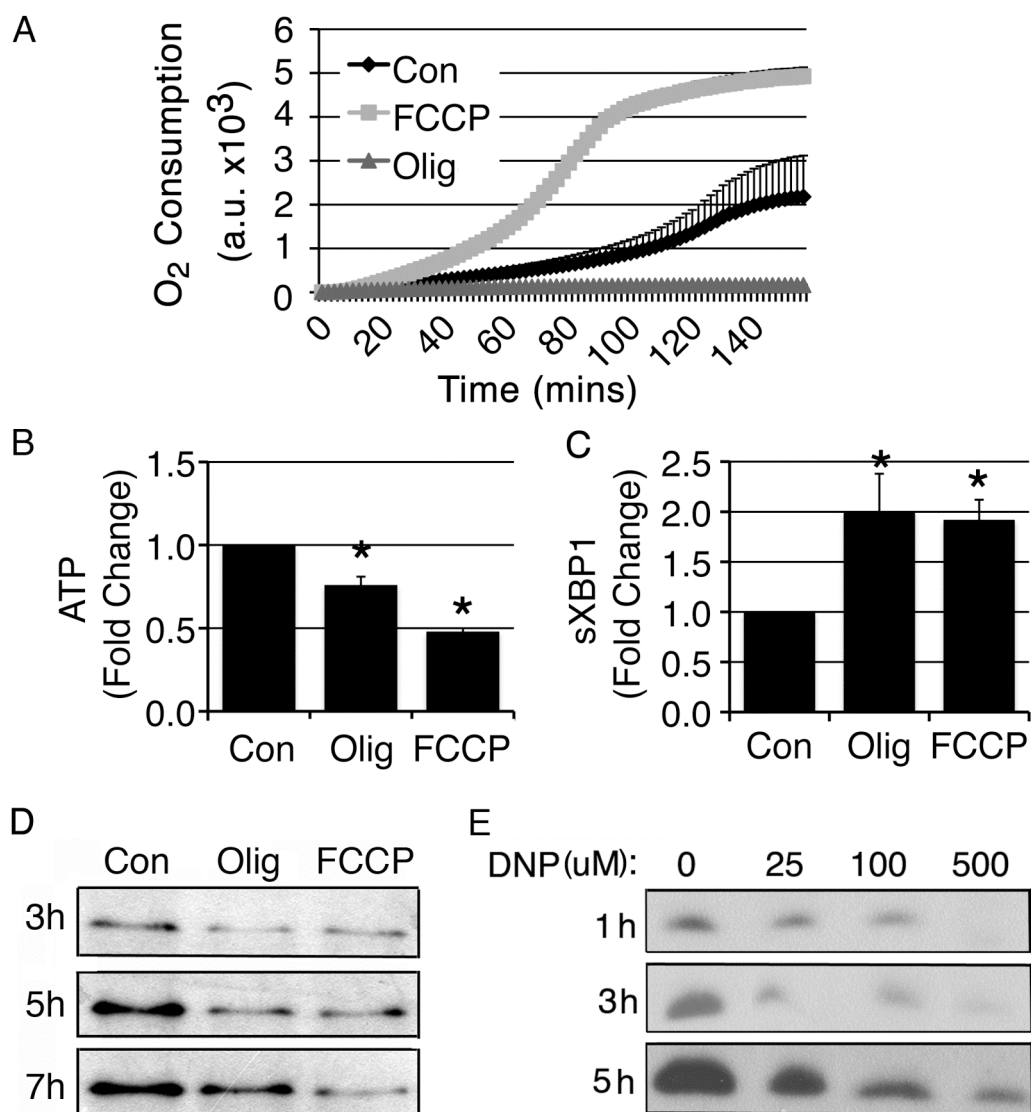
Figure 2.8: Chemical inhibitors of oxidative phosphorylation affect ER function.

A. 3T3-L1 adipocytes at day 7 of differentiation were exposed to oligomycin (Olig) or FCCP and O_2 consumption was measured. B. Cells were exposed to oligomycin (Olig) or FCCP for 2-4 hours and ATP levels in whole cell extracts was measured. Values are expressed as a function of the value in untreated cells (Con). C. Fold change of spliced XBP1 (sXBP1) mRNA levels was measured by qRT-PCR for 3T3-L1 adipocytes at day 7 of differentiation treated with oligomycin (Olig) or FCCP for 2-4 hours compared to untreated (Con). D. Adiponectin secretion from cells treated with oligomycin (Olig) or FCCP as indicated. E. Adiponectin secretion from cells treated with DNP as indicated. * indicates $p<0.05$ by paired 2-tailed Student t-test. All values shown are means of a minimum of three independent experiments.

To further test how impaired mitochondrial function would affect the UPR upon increased protein load, we treated 3T3-L1 cells with tunicamycin. Upon tunicamycin treatment, sXBP1 mRNA increases approximately 6 fold, however oligomycin and FCCP almost completely blocked this induction (Figure 2.9A). Interestingly, incubation with 2-deoxyglucose (2DG), an inhibitor of glycolysis, had no effect on sXBP1 induction and actually trended higher than cells treated with tunicamycin alone (Figure 2.9A). To further examine the kinetics of this blockage, we treated cells with tunicamycin either in the presence of oligomycin at the beginning of treatment or with it added 5.5 hours after tunicamycin treatment began. As expected, tunicamycin-induced XBP1 splicing was completely blocked by oligomycin (Figure 2.9B). Moreover, addition of oligomycin to cells following tunicamycin treatment rapidly stops ongoing XBP1 splicing activity (Figure 2.9B). These results indicate that mitochondrial ATP production is critically required for the induction and maintenance of the UPR in response to an increased misfolded protein load.

A

B
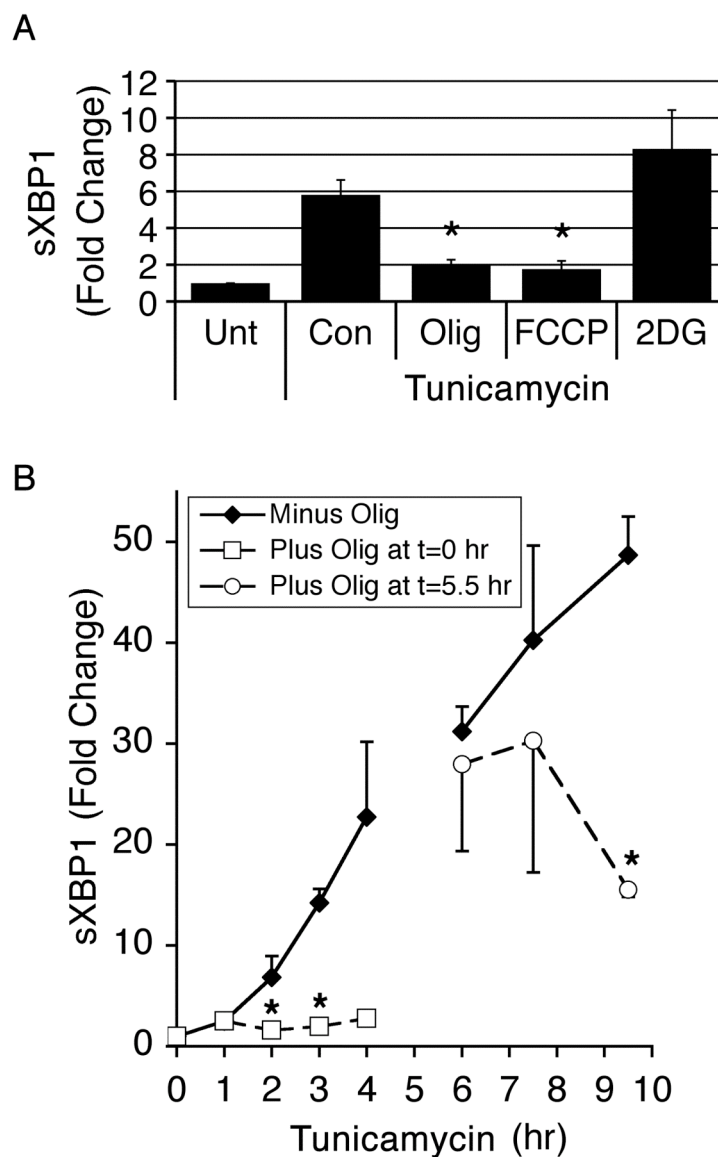
Figure 2.9: IRE1 activation is highly sensitive to ATP levels.

A. Fold change of tunicamycin induced spliced XBP1 (sXBP1) mRNA levels was measured by qRT-PCR for 3T3-L1 adipocytes at day 7 of differentiation treated with oligomycin (Olig), FCCP, or 2-deoxyglucose (2DG) for 2-4 hours compared to untreated (Con). B. Cells were treated with tunicamycin for times indicated. Some were treated with oligomycin (Olig) present from the start (t=0 hr) or added after 5.5 hours of incubation. Spliced XBP1 (sXBP1) was then measured by qRT-PCR at the times indicated. Values are expressed as a function of untreated levels. * indicates p< 0.05 by paired 2-tailed Student t-test. All values shown are means of a minimum of three independent experiments.

Conclusions

In summary, we find that expansion of the ER through activation of the UPR pathway occurs during adipocyte differentiation, and is required for proper secretory function. A previous study found that the chemical chaperone 4-phenylbutyrate (4-PBA) inhibits both the activation of the UPR and differentiation in the 3T3-L1 cell line (127). We find that adipogenesis proceeds normally upon XBP1 knockdown, though secretory function is affected. This discrepancy could be due to the fact that XBP1 knockdown results in only a partial decrease in protein levels, or the other branches of the UPR may be promoting adipogenesis. Since the adequate secretion of adipokines is crucial in the control of whole body metabolism, defects in the adipocyte UPR, specifically in the IRE1/XBP1 pathway, could lead to alterations in energy utilization and whole body energy metabolism. Indeed, the requirement for the UPR in the control of whole body energy metabolism is evident in mice lacking the protein kinase PERK or harboring a replacement of eIF2α with a non-phosphorylatable mutant. This disruption of the translation control branch of the UPR results in neonatal or perinatal lethality due to disruption of carbohydrate metabolism (54,159). While defects in hepatic gluconeogenesis and β cell insulin production are the precipitating causes of death, the adipocyte UPR may also be involved in the failure to fulfill the organism's metabolic needs under these conditions.

While it appears evident that the UPR plays a role in regulating the metabolic needs of an organism, we asked whether the metabolic status could also regulate the UPR on a cellular level. Protein synthesis and folding put an energetic strain on the cell due to

their requirement of approximately 15-20% of the total cellular ATP (160,161). In addition, UPR activity is sensitive to ATP levels since adenine nucleotides are able to activate IRE1 through induction of a conformational change promoted by trans-autophosphorylation (25,28). Once properly folded, exiting the ER is also a nucleotide dependant step; ATP is required for the release of BiP from the folded proteins (162). Taken together, it appears that changes in adenine nucleotide levels could have a severe impact on ER function and protein folding on several levels.

To address the metabolic regulation of UPR induction we used two approaches in the 3T3-L1 cell line: 1) constitutive reduction of mitochondrial respiratory chain function through Tfam depletion during differentiation 2) acute inhibition of oxidative phosphorylation by chemical compounds. Impaired ATP production through Tfam depletion does not appear to affect basal expression of UPR markers or tunicamycin induced UPR activity. Therefore, there may be a mechanism compensating for this chronic state of diminished ATP. However, the acute depletion of ATP by chemical inhibitors of oxidative phosphorylation appears to be either too severe or occurs too quickly for compensation and therefore we see the dramatic effects on induction of the UPR. These combined results indicate that while there is a metabolic regulation of UPR function, it does not appear to simply be the cell's total ATP levels. Moreover, there may be pools of nucleotides available for ER function and oxidative phosphorylation may not be the only metabolic pathway involved in their synthesis. Deficiencies in protein folding and impaired UPR have been shown to lead to apoptosis and multiple human pathologies, including neurodegeneration and metabolic disorders. Therefore, further understanding of

the regulation of the UPR by ATP and mitochondrial function as well as any mechanism by which the cell compensates for impaired mitochondrial function may be beneficial in treating these diseases.

Experimental Procedures

Primary Antibodies: Anti-ACRP30/adiponectin (Affinity Bioreagents, Inc.), anti-BiP (Transduction Laboratories), Anti-cytochrome C (BD Pharmingen), anti-CHOP (Santa Cruz), anti-calreticulin (Calbiochem), anti-GLUT1 (Abcam), anti-GLUT4 (Santa Cruz), anti-HSP60 (Assay Designs), anti-Perilipin (Fitzgerald Industries) and anti-mouse IgM (μ-chain specific) and anti-β-actin (Sigma). Anti-ERO1-Lα and XBP1 was kindly provided by Dr. Fumihiko Urano.

Cell Culture: All cells were obtained from American Type Culture Collection and grown under 10% CO_2. 3T3-L1 cells were cultured in complete media defined as: Dulbecco modified Eagle medium (DMEM) supplemented with 10% fetal bovine serum (FBS), 100 U of penicillin/mL, 100 μg of streptomycin/mL, and 50 μg of Normocin/mL (InvivoGen), which was replaced every 48 hours unless otherwise stated. 3T3-L1 cells were grown on 150 mm dishes. For differentiation, three days after reaching confluence (day 0) media was replaced with complete media containing 0.5 mM 3-isobutyl-1-methylxanthine (Sigma), 0.25 μM dexamethasone (Sigma), and 1 μM insulin (Sigma). 72 hours later, media was replaced with complete media.

Chemical Treatments: Cells were treated with 6 µM tunicamycin, 10 µg/mL oligomycin, or 5 µM FCCP for times indicated.

XBP1 siRNA Transfection: siRNA for XBP1 was purchased from Dharmacon in a duplex form (sense sequence is 5'-GCUGGAAGCCAUUAAUGAAUU-3'). 3T3-L1 cells were grown and differentiated as described above. On day 2, medium was collected and cells were lifted with 1x trypsin with 1% collagenase and transfected with either 20 nmol XBP1 or scrambled siRNA into approximately 10^7 cells by electroporation. Cells were resuspended in the collected day 2 medium and re-plated; 24 hours later, the differentiation medium was replaced by complete medium. Experiments were performed 72 hours post-transfection.

Tfam siRNA Transfection: siRNA oligos against mouse Tfam mRNA was purchased from Dharmacon in a duplex form with 3'-dTdT protective overhangs (sense sequence is 5'-GAAUGUGGAUCGUGCUAAAdTdT-3'). 3T3-L1 cells were grown and differentiated as described above. On day 2, medium was collected and cells were lifted with 1x trypsin with 1% collagenase and transfected with either 5 nmol Tfam or scrambled siRNA into approximately 10^7 cells by electroporation. Cells were resuspended in the collected day 2 medium and re-plated; 24 hours later, the differentiation medium was replaced by complete medium. Experiments were performed 72 hours post-transfection.

Quantitative RT-PCR: Total RNA was extracted by using TRIzol reagent (Invitrogen). For quantitative mRNA analysis, 2 µg of the total RNA was reverse-transcribed by using an iScript complementary DNA (cDNA) Synthesis kit (Bio-Rad). Ten percent of each RT reaction was subjected to quantitative real-time PCR analysis using an iQ SYBR green supermix kit and Real-Time PCR detection system following the manufacturer's instructions (MyiQ, Bio-Rad). Ferritin heavy chain (Fth) or β-actin was used as an internal housekeeping gene. Relative gene expression was calculated by the $2^{-\Delta\Delta CT}$ method (163). Briefly the threshold cycle number (Ct) of the target genes was subtracted from the Ct value of Fth or β-actin and raised 2 to the power of this difference.

Mitochondrial DNA Measurement: Total DNA was extracted by DNeasy® tissue kit. Primer pairs corresponding to Nd1 (mitochondrial) and or β-actin (nuclear) were used to amplify a mitochondrial and nuclear DNA fragment, respectively. The $2^{-\Delta\Delta CT}$ method was used to analyze the relative mtDNA level.

Affymetrix Gene Chip Analysis: Analysis was performed as previously described (102,149). Total RNA was prepared from three sets each of 3T3-L1 cells at day of differentiation indicated. Poly(A)+ mRNA was isolated from each set of total RNA by using an Oligotex mRNA kit (Qiagen) according to the manufacturer's instructions. Double-stranded cDNA synthesis was reverse transcribed from 5 µg of isolated mRNA by using the SuperScript choice system (Invitrogen) according to the manufacturer's

protocol in addition to using an oligo(dT) primer containing a T7 RNA polymerase promoter site. Biotin-labeled complementary RNA (cRNA) was transcribed by using a BioArray RNA transcript labeling kit (Enzo). Fragmented cRNA was hybridized to the murine genome U74 array (MG-U74A, MG-U74B, and MG-U74C) per Affymetrix protocols. The GeneChips were washed with a GeneChip Fluidics Station 400 and were scanned with an HP GeneArrayScanner (Affymetrix). Raw expression data was analyzed with the Bioconductor statistical environment (164) using RMA (165) and MAS5, a Bioconductor implementation of the MAS 5.0 algorithm (Affymetrix). The "fold change" for each gene was determined by dividing the mean of the average difference from three independent experiments.

Immunoblot Analysis: Cell monolayers were washed twice with ice-cold phosphate-buffered saline (PBS) and scraped into 1% sodium dodecyl sulfate (SDS) in PBS. Protein concentration was determined by a bicinchoninic acid (BCA) protein assay (Pierce), and equal amounts of protein were separated by SDS-polyacrylamide gel electrophoresis (PAGE) and transferred to nitrocellulose. Samples of the cell culture medium were taken just prior to media replacement every 24 hours, or as indicated in figure legends, spun 5 minutes at 500*xg,* and equal volumes were separated by SDS-PAGE and transferred to nitrocellulose. The membranes were blocked with 5% nonfat-milk in Tris-buffered saline with 0.1% Tween and incubated with primary antibodies overnight. They were then incubated with anti-rabbit or anti-mouse IgG horseradish peroxidase conjugated antibodies (Promega) and detected using enhanced chemiluminescence (Perkin Elmer

Life Sciences, Inc.). Films were scanned at 300 dpi, and band intensities were quantified

by using Photoshop software as follows. Images were inverted to render the bands white;

bands were next selected by using the rectangular marquee tool and then delineated by

using the color range tool until the whole band was selected. The histogram function was

used to determine the number of pixels in the selection, which was multiplied by the

average pixel intensity.

ATP Assay: Cells were plated into a 96 well opaque plate and treated as indicated. ATP

concentration was determined using the CellTiter-Glo® luminescent assay (Promega)

according to manufacturer's instructions. Luminescence was read using a Tecan Safire2

multimode microplate spectrophotometer.

Brightfield Imaging: All images were obtained using a conventional wide-field

microscope fitted with a 60x Nikon PlanApo objective.

Oil Red O Staining and Quantification: Cells were washed twice in 1x PBS and fixed in

4% formaldehyde for one hour. Cells were washed in dH_2O three times before being

stained with 5 mg/mL Oil Red O in 60% triethyl-phosphate for 30 minutes. Cells were

washed in dH_2O six times before proceeding with analysis. All images were obtained

using a conventional wide-field microscope fitted with a 60x Nikon PlanApo objective.

Oil Red O staining was quantified using a Tecan Safire2 multimode plate reader. Cells

stained with Oil Red O were read at an excitation wavelength of 530 nm and an emission wavelength of 580 nm.

Fluorescent Imaging: Cells were seeded on coverslips, fixed in 4% formaldehyde for 15 minutes at room temperature, permeabilized with 0.5% Triton X-100 plus 1% FBS in 1xPBS, and stained with primary antibodies overnight at 4°C. Alexa Fluor® 488 or 594 donkey anti-mouse or rabbit secondary antibodies were used to detect bound primary antibody. For staining of nuclei, cells were incubated with 1 µg/mL Hoechst 33258 pentahydrate (bis-benzimide) for 10 minutes. All images were obtained using a conventional wide-field microscope fitted with a 100x Nikon PlanApo objective.

2-Deoxyglucose Uptake Assay: Cells were plated in a 24-well dish. Cells were starved for 2 hours in Krebs-Ringer HEPES (KRH) buffer (130 mM NaCl, 5 mM KCl, 1.3 mM CaCl$_2$, 1.3 mM MgSO$_4$, and 25 mM HEPES, pH 7.4) supplemented with 2 mM sodium pyruvate and 1% bovine serum albumin (BSA) prior to a 30 minute stimulation with 100 nm insulin. Uptake was initiated by the addition of [^{3}H]2-deoxy-D-glucose to a final assay concentration of 100 µM for 5 minutes at 37°C. Assays were terminated by three washes with ice-cold 1xPBS, and the cells were solubilized with 0.4 mL of 1% Triton X-100, and ^{3}H content was determined by scintillation counting. Nonspecific deoxyglucose uptake was measured in the presence of 20 µM cytochalasin B and subtracted from each sample to obtain specific uptake.

Oxygen Consumption: Cells were trypsinized and resuspended in KRH buffer supplemented with 1% fatty acid free BSA. Approximately 7.5×10^4 cells in 150 μL of KRH buffer were added to wells in a BD Oxygen Biosensor System plate (BD Biosciences) in triplicate. Chemical reagents were then added to the cells. Plates were sealed and fluorescence intensity was recorded for 120 minutes (2 minute intervals) at an excitation wavelength of 485 nm and emission wavelength of 630 nm on a Tecan Safire2 multimode microplate spectrophotometer maintained at 37°C.

CHAPTER III

ADENYLATE KINASE 2 LINKS MITOCHONDRIAL ENERGY METABOLISM TO THE INDUCTION OF THE UPR

The following data includes unpublished results as well as data taken from:

Burkart, A., Shi, X., Chouinard, M., and S. Corvera (2010) Adenylate Kinase 2 Links Mitochondrial Energy Metabolism to the Induction of the Unfolded Protein Response. *Submitted*.

Isolation of mouse tissues was performed by My Chouinard. She also assisted in the generation and maintainence of the primary myoblast cultures. I performed the remaining experiments contained within this chapter.

Summary

The unfolded protein response (UPR) is a homeostatic signaling mechanism that balances the protein folding capacity of the endoplasmic reticulum (ER) with the cell's secretory protein load. ER protein folding capacity is dependent on the abundance of chaperones, which is increased in response to UPR signaling, and on a sufficient ATP supply for their activity. An essential branch of the UPR entails the splicing of XBP1 to form the XBP1 transcription factor. XBP1 has been shown to be required during adipocyte differentiation, enabling mature adipocytes to secrete adiponectin, and during differentiation of B cells into antibody-secreting plasma cells. Here we find that adenylate kinase 2 (AK2), a mitochondrial enzyme that regulates adenine nucleotide interconversion within the intermembrane space, is markedly induced during adipocyte and B cell differentiation. Depletion of AK2 by RNAi impairs adiponectin secretion in 3T3-L1 adipocytes, IgM secretion in BCL1 cells, and the induction of the UPR during differentiation of both cell types. Interestingly, depletion of adenylate kinase 1 (AK1) a cytosolic enzyme in the muscle that also regulates nucleotide interconversion does not have the same effect upon UPR induction. These results reveal a new mechanism by which adenine nucleotides fulfill the energetic requirements for ER function, and suggest that specific mitochondrial defects may give rise to impaired UPR signaling. The requirement of AK2 for UPR induction may explain the pathogenesis of the profound hematopoietic defects of reticular dysgenesis, a disease associated with mutations of the AK2 gene in humans.

Background

Obesity and its many associated co-morbidities are caused by an imbalance between food intake and energy expenditure (166-169). Addressing this problem requires an understanding of the mechanisms by which fuel consumption, energy production, and energy utilization are coordinated. In cells, energy production in the form of adenine nucleotides, ATP and ADP, is tightly coupled with energy utilization for motility or anabolic processes (170). Even in cells that have acute high-energy requirements, such as skeletal and cardiac myocytes and neurons, ATP synthesis is highly coordinated with ATP utilization, such that the steady state levels of ATP remain constant over a wide range of workloads. In these cells, carbohydrate or lipid fuels are channeled to oxidative phosphorylation in mitochondria, where ATP is primarily synthesized, and this process is enhanced dramatically in response to increased ATP utilization.

Among the important molecular mechanisms by which energy flux is regulated in a single cell are enzymatic activities that utilize, are regulated by, or alter the levels of adenine nucleotides. For example, an increase in the AMP/ATP ratio ensuing from enhanced ATP utilization is sensed by AMP-activated protein kinase (AMPK), which then triggers an increase in fuel consumption that facilitates the restoration of homeostatic ATP levels (171-175). In addition, AMPK activation results in decreased energy expenditure by minimizing the activity of many anabolic pathways.

An enzyme that influences adenine nucleotide levels is adenylate kinase (AK), which catalyzes the reversible phosphoryl transfer reaction AMP + ATP $\Leftrightarrow$ 2ADP. The adenylate kinases are an ancient family of proteins (EC. 2.7.4.3), present from bacteria to

humans. A single isoform of adenylate kinase is present in bacteria and lower eukaryotes and is essential for life (108-110). AK has been thought to provide the principal homeostatic mechanism to maintain adenine nucleotide ratios under different conditions of ATP production and utilization. It has also been proposed that AK provides a mechanism to channel the high energy phosphate of ATP from sites of ATP production to sites of utilization through the operation of phosphotransfer networks (111). The human genome encodes for 9 genes bearing similarity to AK that differ in cellular and subcellular distribution.

AK1 is localized to the cytosol and is found in skeletal muscle, brain, and erythrocytes (112,113). In skeletal muscle over 95% of the total adenylate kinase activity corresponds to AK1 (115). Given the importance of AK activity in prokaryotes, and the fact that AK1 is by far the predominant AK activity in muscle, it was rather surprising that mice lacking AK1 are ostensibly normal, capable of exerting enhanced contractile force, highly tolerant to fatigue, and able to maintain normal steady-state levels of ATP (114,115,117). These results suggest that compensatory mechanisms are elicited in these mice to adapt to the lack of this enzyme. Interestingly, muscles from AK1$^{-/-}$ mice had a higher rate of ATP synthesis in response to contraction, indicating more ATP had to be produced to maintain normal contractility. This suggests that the efficiency of ATP use was lower in AK1$^{-/-}$ mice compared to controls (114,115). These results are consistent with a proposed role of adenylate kinase for improving the efficiency of ATP utilization in cells through the operation of phosphotransfer networks (111), or other yet unknown mechanisms.

AK2 has not been as well characterized as AK1. Human AK2 is found in the mitochondrial intermembrane space of liver, kidney, spleen, and heart (112). There are two isoforms, AK2A and AK2B, of identical amino acid sequences except for at the C-terminal region (113,119). Interestingly, there is large discrepancy between the expression of the mRNA and of the protein of AK2, indicating a significant post-transcriptional regulation (120). AK2 has been shown to be required for *Drosophila* development (124). Recently, mutations in AK2 have been identified as the basis for a profound failure of lymphopoiesis in humans (125,126).

We have previously reported that differentiation of 3T3-L1 preadipocytes is accompanied by a robust increase in mitochondrial biogenesis (102), which coincides with the initiation of adiponectin secretion. Additionally, it has been shown that the UPR is upregulated during 3T3-L1 adipocyte differentiation (127). These findings suggest the possibility that these two events are functionally linked, with mitochondrial function being required for UPR induction and to sustain adiponectin secretion in differentiated adipocytes. As we have shown in the previous chapter, mitochondrial oxidative phosphorylation is able to partially regulate induction of the UPR, however it appears that there could be other compensatory mechanisms as well.

Here we report that in addition to a general increase in mitochondrial mass and oxidative phosphorylation (102), adipocyte differentiation is associated with a striking increase in the levels of AK2. In its role in regulating the interconversion of adenine nucleotides, it has the ability to compensate for impaired oxidative phosphorylation. Thus, we investigated the effects of AK2 depletion on the induction of the UPR. We find

that, while optimal oxidative phosphorylation appears unnecessary, AK2 is required for the induction of the UPR. To determine whether this was a universal role for AK family members, we tested whether a decrease of AK1 would also show the same results. Interestingly, although AK1 depletion produced significant metabolic alterations, the UPR was relatively unaffected. These results reveal a novel mechanism by which mitochondrial energy metabolism and ER homeostasis are linked, which may explain the profound hematopoietic defects associated both with UPR deficiency (30) and with genetic deficiency of AK2 (125,126).

Results

Previous reports have shown that human AK2 is expressed in liver, kidney, spleen, and heart (112). Here we find that the protein expression in the mouse differs from the human studies, as it is highly enriched in white adipose tissue, liver, pancreas, and kidney (Figure 3.1A). We find that during 3T3-L1 differentiation, AK2 begins to express at around day 4 and continues to increase through day 8 (Figure 3.1B). This parallels the mitochondrial biogenesis that is occurring during this time frame, exemplified by cytochrome c expression (Figure 3.1B). Based upon immunocytochemistry, we find that AK2 is mainly localized in the mitochondria, co-localizing with MitoTracker® Red staining (Figure 3.1C). While there appears to be AK2 staining in the nucleus, it is unclear if it is physiologically relevant or a non-specific artifact of the staining.
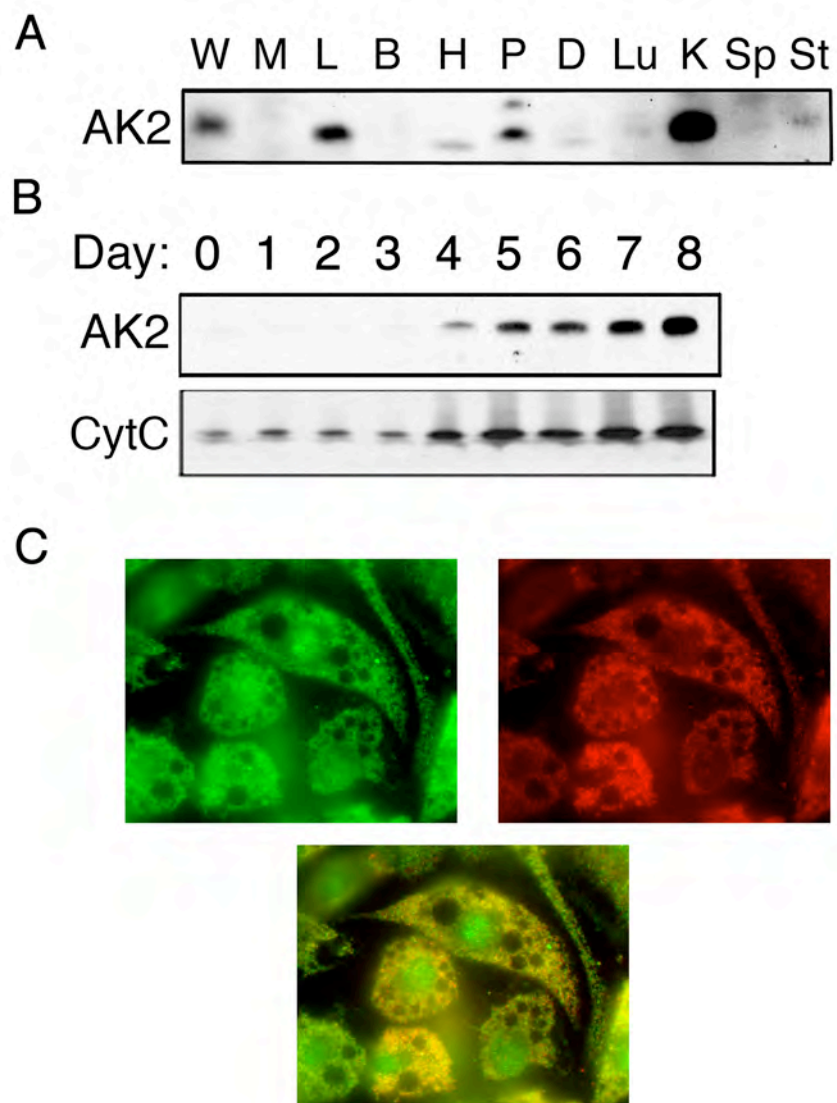
Figure 3.1: AK2 expression in mouse tissues and 3T3-L1 adipocytes.

A. Western blotting of mouse tissues with an antibody to mouse AK2. W, white adipose tissue; M, muscle; L, liver; B, brain; H, heart; P, pancreas; D, diaphragm; Lu, lung; K, kidney; Sp, spleen; St, stomach. B. 3T3-L1 cells were harvested just prior to the addition of hormonal cocktail (day 0), and at indicated days thereafter. Cell extracts were analyzed by western blotting with antibodies to the proteins indicated. C. Localization of AK2 by immunostaining (green) and mitochondria by MitoTracker® Red staining (red). Co-localized areas are shown in yellow in the bottom panel. Data shown are representative of a minimum of three independent experiments.

To analyze the function of AK2 in 3T3-L1 adipocytes, AK2-directed RNAi oligonucleotides were introduced at day 2 of differentiation, to match the experimental conditions used in the analysis of Tfam in the previous chapter. At day 5 of differentiation, AK2 mRNA levels were decreased by 90%, and protein levels by an average of 60% (Figure 3.2A and B). This depletion of AK2 had no apparent effect on differentiation as estimated by lipid accumulation (Figure 3.2C). We also measured the mRNA levels of proteins involved in adipocyte differentiation such as C/EBPα, C/EBPβ, C/EBPδ, PPARα, and PPARγ, or reflective of differentiation such as AP2 and GLUT4, or secreted by adipocytes, including adiponectin, adipsin, and resistin. There was no significant change in many of the mRNAs we examined; however, the mRNA expression of GLUT1, which is responsible for basal glucose uptake, and CEBPα did decrease (Figure 3.2D). These data indicate that AK2 is not necessary for differentiation of 3T3-L1 adipocytes.
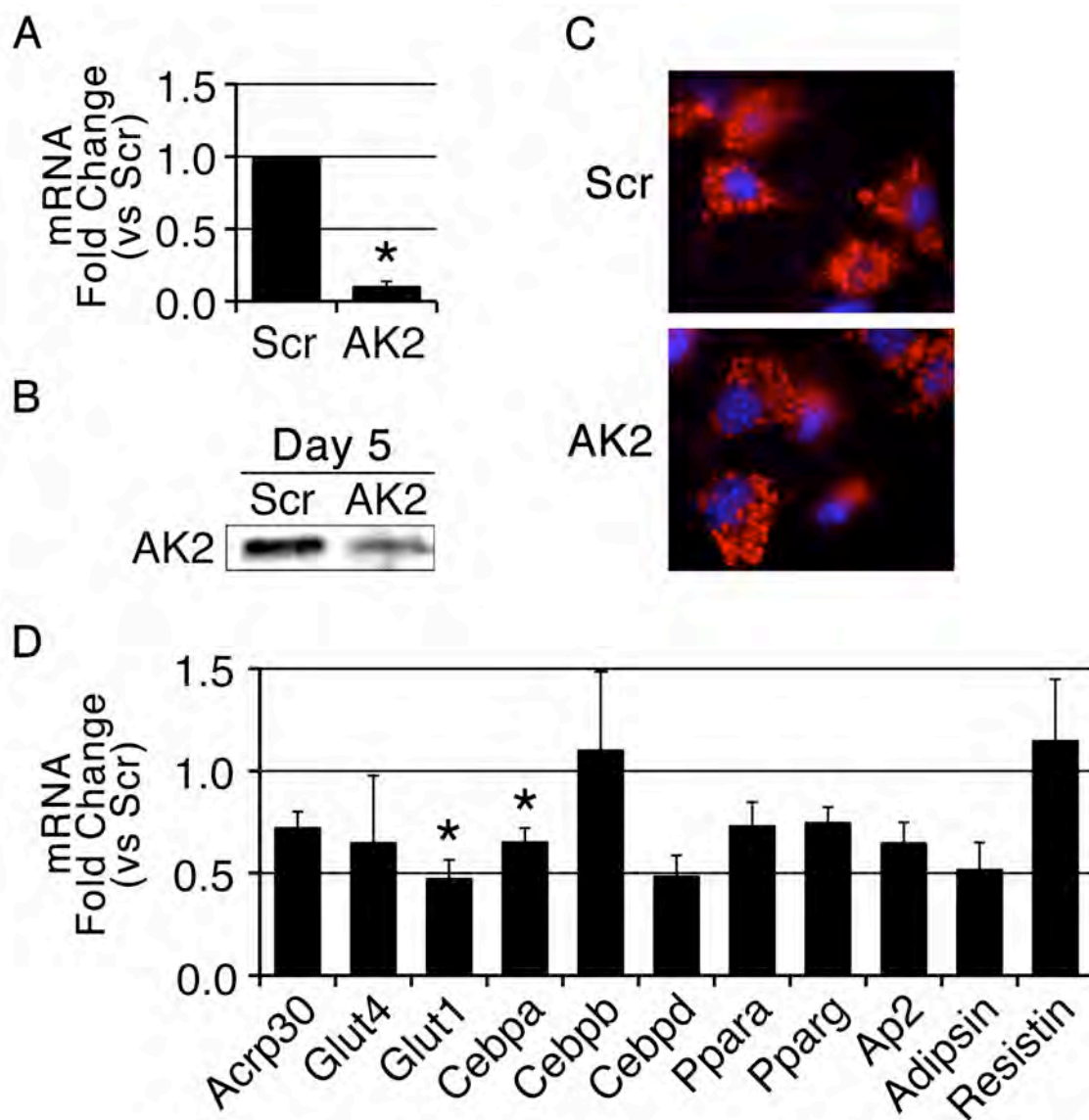
Figure 3.2: Depletion of AK2 does not affect 3T3-L1 differentiation.

Scrambled (Scr) or AK2 targeting (AK2) siRNA was transfected at day 2 of differentiation and experiments were performed at day 5. A. The mRNA change was determined by qRT-PCR. B. The change in protein was determined by western blot analysis. C. Lipid accumulation was determined by Oil Red O staining (red). Nuclei are depicted by Hoescht staining (blue). D. Fold change of mRNAs for adipocyte proteins determined by qRT-PCR upon depletion of AK2 relative to scrambled. * indicates $p<0.05$ by paired 2-tailed Student t-test. Data shown are means of a minimum of three independent experiments.

To further examine the role of AK2 in this model system, we tested whether AK2 plays a role in maintaining the cell's metabolic status. AK2 depletion had a measurable effect on energy homeostasis, reflected by a slight but significant decrease in basal oxygen consumption (Figure 3.3A). In addition, oxygen consumption with either glucose or palmitate provided as a substrate was decreased by AK2 depletion (Figure 3.3A). Notably, glucose was not able to stimulate oxygen consumption upon AK2 depletion. In addition, there was a 20% decrease in lactate levels upon AK2 depletion (Figure 3.3B). This may indicate that upon AK2 depletion glucose metabolism is decreased. These effects were accompanied by small changes in mRNA levels of a few mitochondrial components involved in oxidative phosphorylation and fatty acid β-oxidation, but overall the mRNA expression of mitochondrial enzymes was largely unaffected (Figure 3.3C). There was no obvious affect of AK2 depletion upon mitochondrial structure as assessed by the incorporation of MitoTracker® Red (Figure 3.3D). However, the small effects presented here resulted in a decrease in ATP levels of approximately 15%, with no significant changes in ADP or AMP (Figure 3.3E). Therefore, while AK2 depletion did not affect mitochondrial protein levels or structure, it did slightly alter the metabolic state.
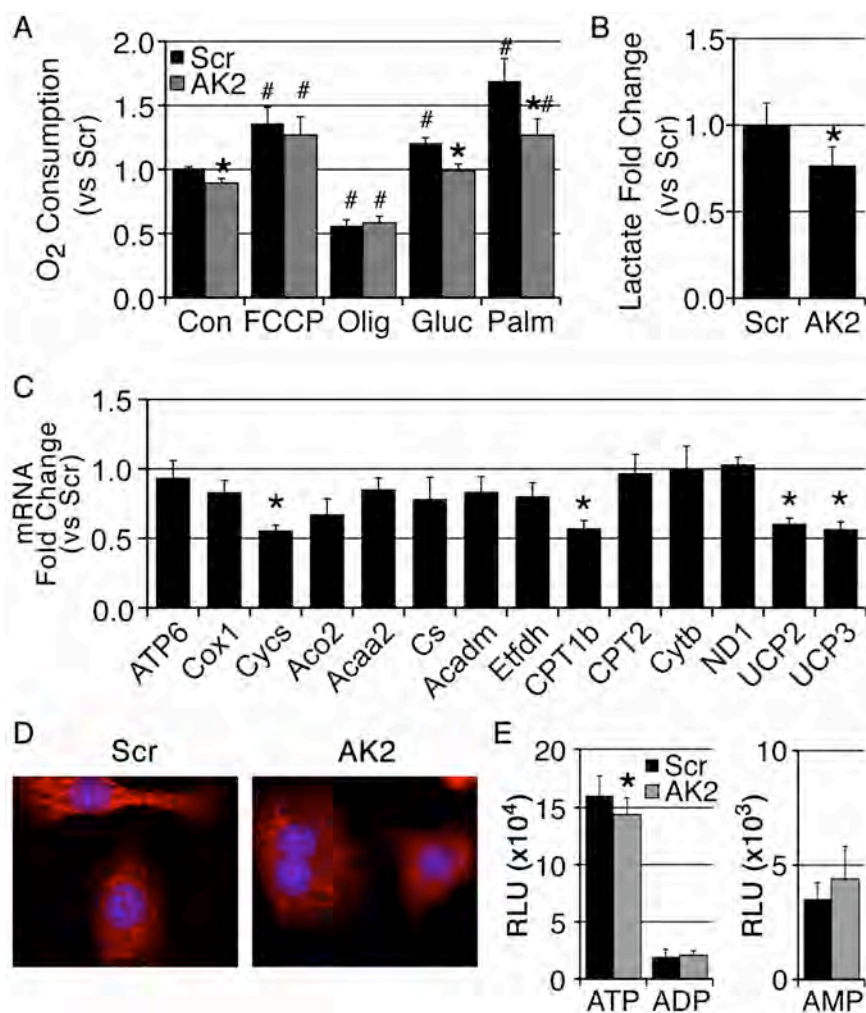
Figure 3.3: Depletion of AK2 alters the metabolic status of day 5 3T3-L1 cells.

Scrambled (Scr) or AK2 targeting (AK2) siRNA was transfected at day 2 of differentiation and experiments were performed at day 5. A. Rate of oxygen consumption expressed as fold change of the control scrambled cells. B. Basal lactate levels expressed as fold change of scrambled. C. Fold change of mRNAs for mitochondrial proteins determined by qRT-PCR upon depletion of AK2 relative to scrambled. D. Mitochondrial morphology by MitoTracker® Red staining. Nuclei are depicted by Hoescht staining (blue). E. Level of adenine nucleotides isolated from cell lysates by TCA extraction expressed as relative luminescent units (RLU). * indicates $p < 0.05$ between Scr and AK2 by paired 2-tailed Student t-test. # indicates $p < 0.05$ between control and treated cells by paired 2-tailed Student t-test. Data shown are means of a minimum of three independent experiments.

We then sought to determine whether depletion of AK2 would affect the UPR or ER function. There was no noticeable change in calreticulin staining upon AK2 depletion indicating that the ER structure was unaffected (Figure 3.4A). We then examined the basal levels of key elements of the UPR. Strikingly, the mRNAs for all three ER stress sensors, IRE1α, PERK, and ATF6, were decreased by >50%, and total and spliced XBP1 mRNAs were decreased by 80% in AK2-depleted cells (Figure 3.4B). The transcription factor CHOP, which is responsive to sustained UPR signaling, was also significantly decreased, and similar to what was observed in Tfam knockdown cells, the levels of ERO1α was reduced (Figure 3.4B compare to Figure 2.6B). Unlike the mRNA expression, IRE1α protein levels did not change and we were unable to view the phosphorylation state in order to determine activation (Figure 3.4C). However, the decreased level of spliced XBP1 indicates that IRE1 activity is inhibited. Although BiP mRNA did not change significantly, the protein level decreased indicating there is an effect on components downstream of XBP1 splicing. In addition, ERO1α protein expression was also decreased whereas the calcium binding protein calreticulin was unaffected. Despite unaltered levels of adiponectin seen in western blotting of cell extracts (Figure 3.4C), AK2 depletion and its concomitant perturbations in differentiation-induced UPR signaling correlated with a significant decrease in adiponectin secretion (Figure 3.4D). Thus, AK2 depletion during adipocyte differentiation leads to impaired induction of the UPR and the development of secretory function.
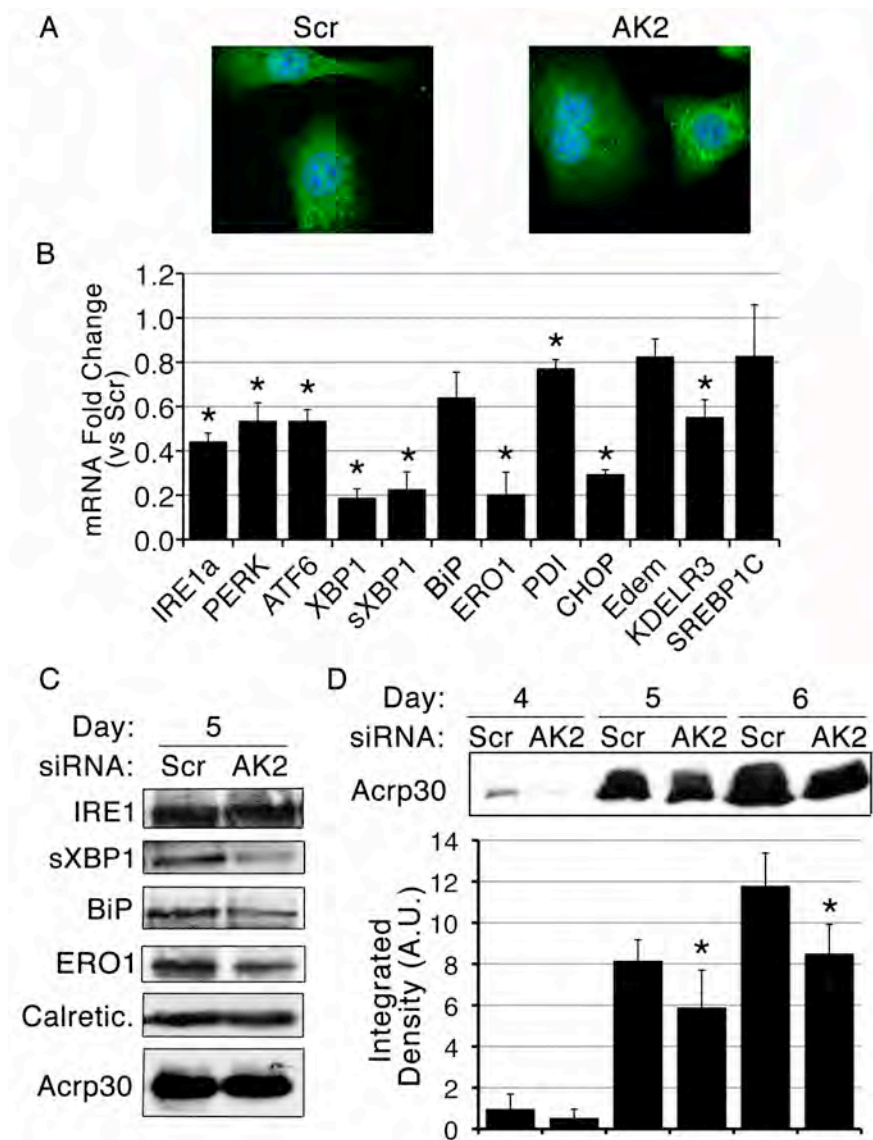
Figure 3.4: Depletion of AK2 reduces UPR induction and secretion.

Scrambled (Scr) or AK2 targeting (AK2) siRNA was transfected at day 2 of differentiation and experiments were performed at day 5. A. ER morphology by calreticulin immunostaining. Nuclei are depicted by Hoescht staining (blue). B. The mRNA change of UPR markers was determined by qRT-PCR. C. The change in protein was determined by western blot analysis. D. Culture media was removed at days 4, 5, and 6 of differentiation as indicated and secretion of adiponectin (Acrp30) over the previous 24 hours was determined by western blot analysis. A representative blot is shown (top panel) as well as the average of all experiments (bottom panel). * indicates $p < 0.05$ by paired 2-tailed Student t-test. Data shown are means of a minimum of three independent experiments.

To determine whether AK2 depletion affects the induction of the UPR in mature adipocytes we examined the effects of tunicamycin treatment. Cells at day 5 of differentiation, at which mitochondrial biogenesis is already maximal (102,145), were transfected with scrambled or AK2-directed oligonucleotides. At day 7, AK2 mRNA and protein levels were depleted by > 80% (Figure 3.5A and B). The ability of the adipocyte to accumulate and store lipid was unaffected as demonstrated by Oil Red O staining (Figure 3.5C). In addition, there was no obvious effect on the structure of the endoplasmic reticulum by AK2 depletion based upon calreticulin staining (Figure 3.5D top panels). Also, AK2 knockdown did not appear to alter mitochondria structure and membrane potential as demonstrated by MitoTracker® Red incorporation (Figure 3.5D bottom panels).
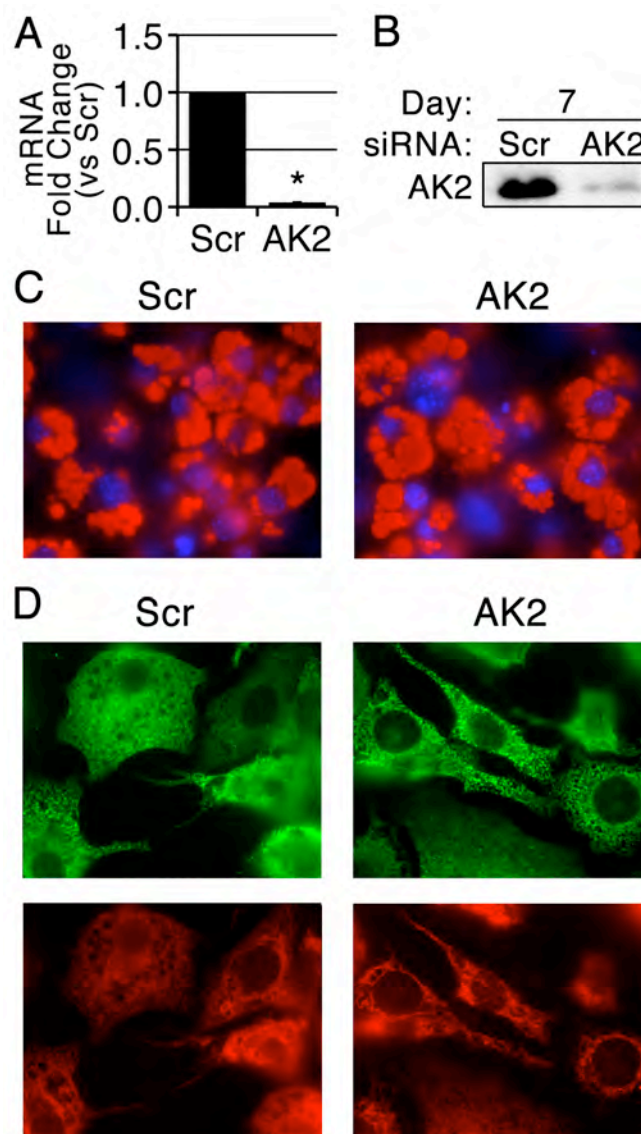
Figure 3.5: Depletion of AK2 does not affect general adipocyte function.

Scrambled (Scr) or AK2 targeting (AK2) siRNA was transfected at day 5 of differentiation and experiments were performed at day 7. A. The mRNA change was determined by qRT-PCR B. The change in protein was determined by western blot analysis. C. Lipid accumulation depicted by Oil Red O staining (red). Nuclei are depicted by Hoescht staining (blue). D. ER morphology by calreticulin immunostaining (top panel) and mitochondrial morphology by MitoTracker® Red staining (bottom panel) * indicates p<0.05 by paired 2-tailed Student t-test. Data shown are means of a minimum of three independent experiments.

We next examined the effect of AK2 depletion on the metabolic status of these fully differentiated cells. Insulin sensitivity was unaffected based upon insulin stimulated 2-deoxyglucose uptake, however basal uptake was increased (Figure 3.6A). There was no effect of AK2 depletion on basal lactate production though it did trend down (Figure 3.7B). Functionally, the mitochondrial showed diminished basal oxygen consumption upon AK2 depletion (Figure 3.6C). Additionally, uncoupled respiration as well as substrate (glucose and palmitate) stimulated respiration was decreased by siRNA knockdown of AK2. Interestingly, similar to the day 2 knockdown cells, glucose did not stimulate an increase in respiration in AK2 depleted cells. Though basal glucose uptake is increased, it appears that the glycolytic metabolism of AK2 depleted cells is impaired. Similar to what was seen upon AK2 depletion early in differentiation, the result of these metabolic changes is a decrease in ATP levels (Figure 3.6D). Although ADP was again unaffected, the levels of AMP approximately doubled upon AK2 depletion (Figure 3.6D).
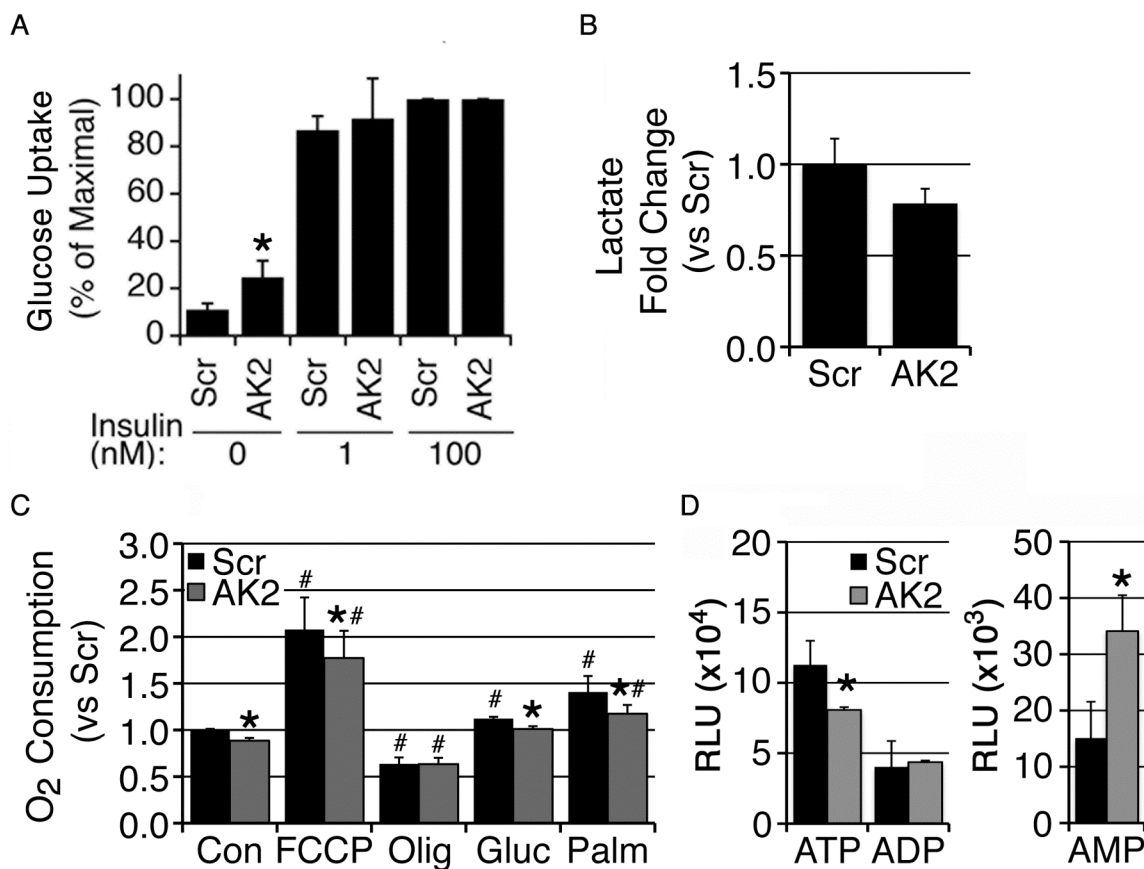
Figure 3.6: Depletion of AK2 alters the metabolic status of day 7 3T3-L1 cells.

Scrambled (Scr) or AK2 targeting (AK2) siRNA was transfected at day 5 of differentiation and experiments were performed at day 7. A. 2-deoxyglucose uptake assay expressed as a percentage of maximal uptake. B. Basal lactate levels expressed as fold change of scrambled. C. Rate of oxygen (O_2) consumption expressed as fold change of the control scrambled cells. D. Level of adenine nucleotides isolated from cell lysates by TCA extraction expressed as relative luminescent units (RLU). * indicates $p<0.05$ between Scr and AK2 by paired 2-tailed Student t-test. # indicates $p<0.05$ between control and treated cells by paired 2-tailed Student t-test. Data shown are means of a minimum of three independent experiments.

Next we examined whether AK2 depletion in response to tunicamycin would have an effect once the secretory components had been allowed to reach their normal levels for mature adipocytes. Upon tunicamycin treatment of day 7 adipocytes, we found XBP1 splicing was delayed and reached a lower maximal level in AK2 depleted cells (Paired 2-tailed Student t-tests yielded a $p = 0.00058$, with means of 35.5 and 23.1 times basal values (t=0) for Scr and AK2 groups, respectively) (Figure 3.7A). This decrease was physiologically relevant, as BiP mRNA and protein accumulation were also significantly impaired ($p = 0.0029$, with means of 5.8 and 3.6 times basal values for Scr and AK2 groups, respectively) (Figure 3.7B). CHOP induction, a later, smaller response to tunicamycin treatment, was also diminished in AK2 depleted cells, indicating that the requirement for AK2 may extend to other branches of the UPR ($p = 0.00028$, with means of 3.4 and 2.2 times basal values for Scr and AK2 groups, respectively) (Figure 3.7C). In addition, the ability of the adipocytes to secrete adiponectin was impaired proportional to the decrease in AK2 expression (Figure 3.7D). Regression analysis on this data yielded an adjusted R^2 of 0.326, and a significance of 0.012. These experiments suggest that AK2 activity is necessary for the induction of the UPR in response to increased secretory protein load.
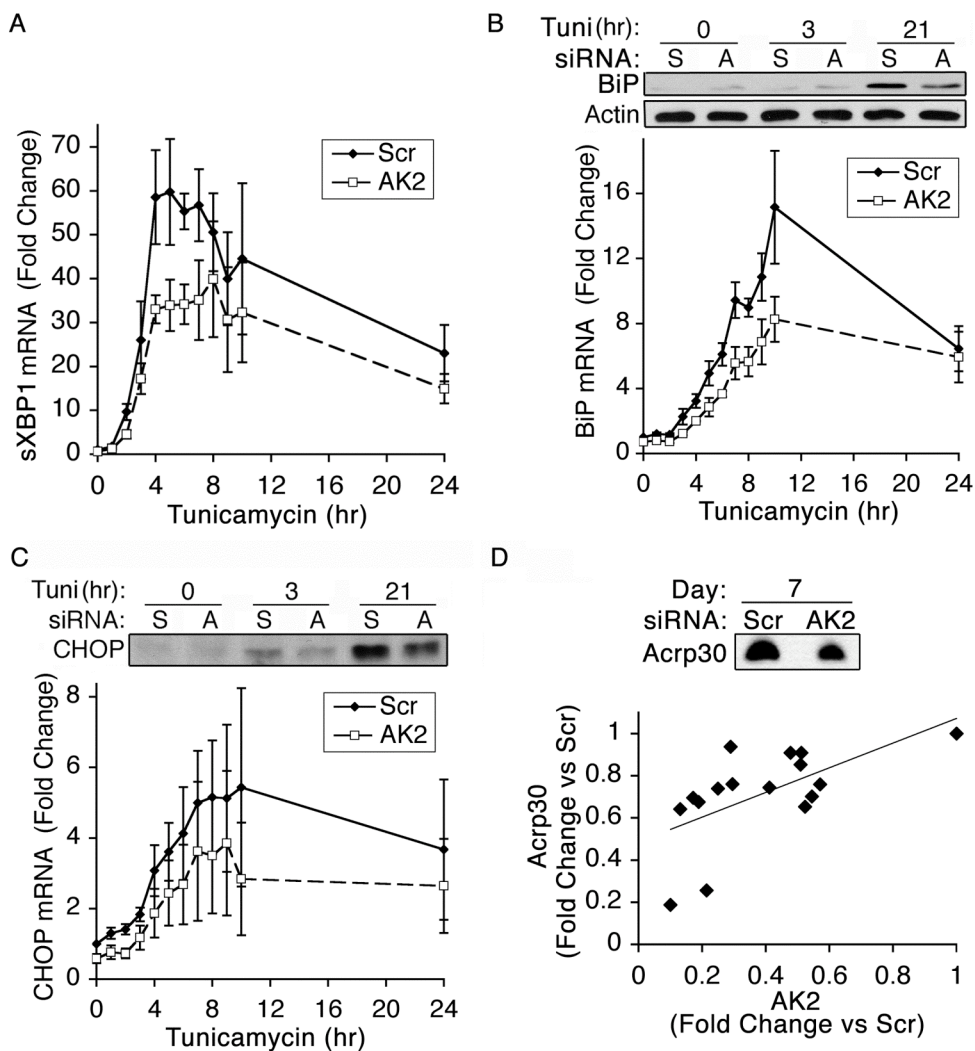
Figure 3.7: Depletion of AK2 decreases UPR induction and secretion.

Scrambled (Scr) or AK2 targeting (AK2) siRNA was transfected at day 5 of differentiation and experiments were performed at day 7. A. Time course of tunicamycin induced spliced XBP1 (sXBP1) mRNA measured by qRT-PCR. B. Time course of BiP accumulation upon tunicamycin (Tuni) treatment measured by western blotting of BiP and β-actin (upper panel) and qRT-PCR of BiP mRNA (bottom panel). C. Time course of CHOP accumulation upon tunicamycin (Tuni) treatment measured by western blotting (upper panel) and qRT-PCR of CHOP mRNA (bottom panel). D. Cell lysates and culture media from multiple experiments were analyzed by western blot with antibodies to AK2 and adiponectin (Acrp30). Band intensities were expressed as the ratio between AK2 and Scr and plotted against each other. Regression analysis yielded an adjusted R^2 of 0.326, and a significance of 0.012. * indicates $p<0.05$ by paired 2-tailed Student t-test. All values shown are means of a minimum of three independent experiments.

Splicing of XBP1 has been shown to be required for terminal differentiation of B cells into antibody producing plasma cells (30,38). To investigate whether the role of AK2 in 3T3-L1 adipocytes could be generalized to other secretory cells, we first examined the expression levels of AK2 during B cell differentiation. Western blot analysis of extracts from BCL1 cells, a B cell lymphoma line, revealed a marked induction of AK2 protein upon LPS-induced differentiation (Figure 3.8A). Thus, like 3T3-L1 adipocytes, BCL1 differentiation is accompanied by the induction of AK2 protein. Interestingly, there is minimal change in AK2 mRNA levels suggesting that AK2 induction may involve post-transcriptional regulation during this period (Figure 3.8B).

siRNA mediated silencing of AK2 prior to LPS stimulation completely blocked AK2 protein (Figure 3.8C), and reduced AK2 mRNA expression to approximately 25% of the level of the scrambled cells (Figure 3.8D). This depletion in AK2 did not impair differentiation, as assessed by the unchanged levels of BCL6 (Figure 3.8D), nor did it result in detectable alterations in mRNA levels of mitochondrial proteins (Figure 3.8E). Oxygen consumption upon AK2 depletion was unchanged either under basal conditions or upon incubation with substrate (Figure 3.8F). Interestingly, the B cells nucleofected with scrambled siRNA responded to glucose with a small but significant increase in respiration, which was not seen upon AK2 depletion, while both responded to palmitate. There was no effect on lactate production under basal conditions (data not shown). Therefore similar to the 3T3-L1 cells, it appears that upon AK2 depletion, B cells have altered glucose metabolism. Additionally, depletion of AK2 did result in decreased cellular ATP levels, although ADP and AMP levels were unchanged (Figure 3.8G).

Therefore, AK2 does not seem to be required for differentiation of B cells into plasma cells but may affect the nucleotide equilibrium and cellular energetics of these cells.
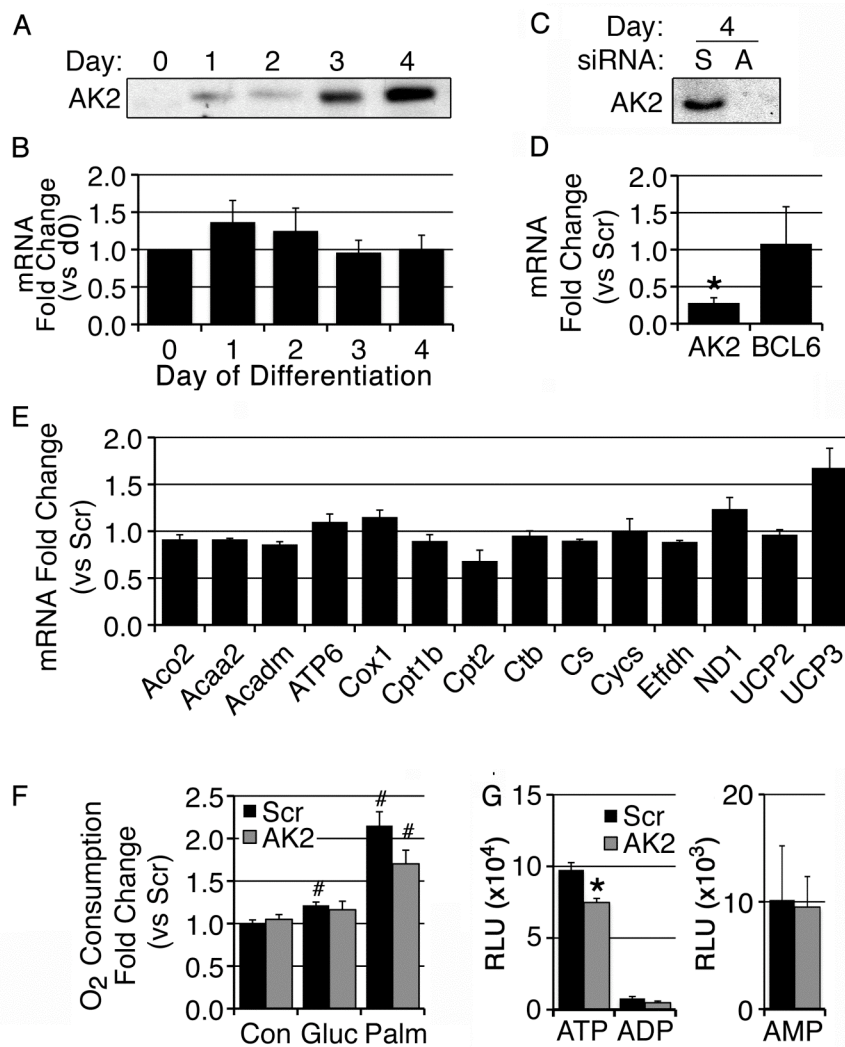
Figure 3.8: AK2 expression during BCL1 differentiation and siRNA knockdown.

A-B. AK2 expression in BCL1 cells during LPS induced differentiation at days indicated. A. Protein expression by western blot. B. mRNA expression by qRT-PCR. C-G. BCL1 cells were nucleofected with either scrambled (Scr) or AK2 directed (AK2) siRNA then induced to differentiate 24 hours later by incubation with LPS. C. Western blot analysis for AK2 protein expression in scrambled (S) or AK2-directed (A) siRNA transfected cells. D. Fold change of mRNAs for AK2 and BCL6 determined by qRT-PCR upon depletion of AK2 relative to scrambled at day 4 of differentiation. E. Fold change of mRNAs for mitochondrial proteins determined by qRT-PCR upon depletion of AK2 relative to scrambled at day 4 of differentiation. F. Rate of oxygen consumption expressed as fold change of the control scrambled cells. G. Level of adenine nucleotides isolated from cell lysates by TCA extraction expressed as relative luminescent units (RLU). * indicates $p < 0.05$ by paired 2-tailed Student t-test. # indicates $p < 0.05$ between control and treated cells by paired 2-tailed Student t-test. All values shown are means of a minimum of three independent experiments.

We then assessed the role of AK2 in the secretory function of the plasma cell. AK2 depleted cells displayed a profound decrease in IgM levels, seen in whole cell extracts, as well as in the amount of antibody secreted into the media (Figure 3.9A). This defect is likely to be due to an impaired induction of the UPR, as the mRNA levels IRE1α, sXBP1, and BiP were significantly decreased in AK2 knockdown cells (Figure 3.9B). A pronounced impairment in the induction of BiP protein with differentiation was also seen in AK2 knockdown cells (Figure 3.9C, upper panel) while calreticulin expression was relatively unaffected (Figure 3.9C, lower panel). These experiments indicate that AK2 protein is required for the induction of the UPR during B cell differentiation, which is in turn required for secretory function of these cells.
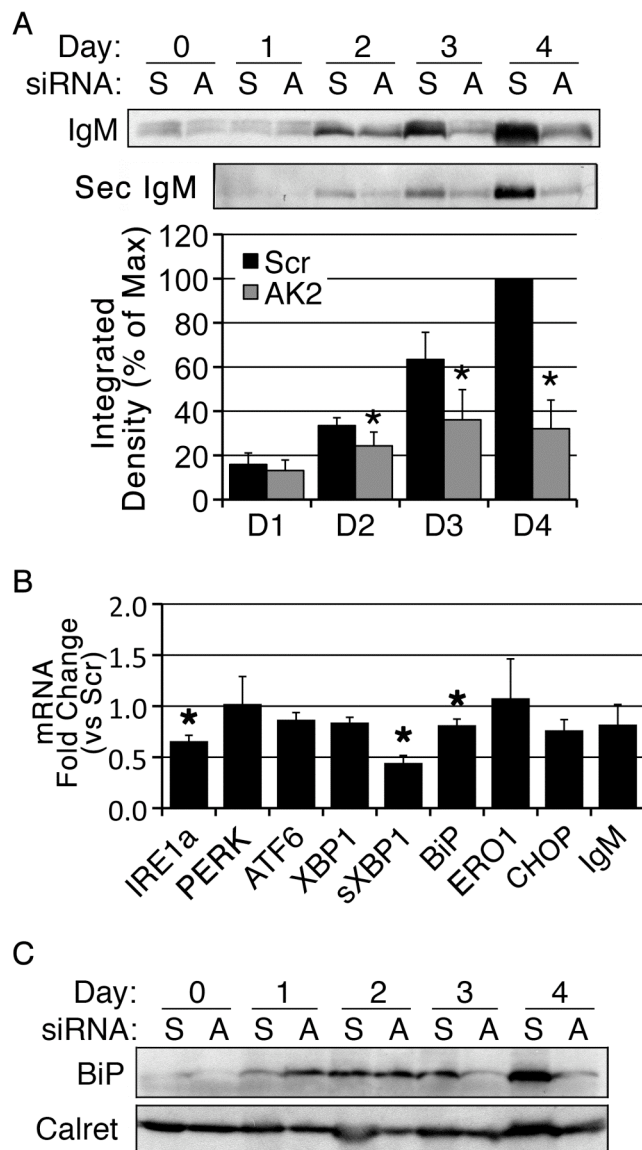
Figure 3.9: AK2 depletion decreases UPR induction and IgM secretion.

BCL1 cells were nucleofected with either scrambled (Scr or S) or AK2 directed (AK2 or A) siRNA then induced to differentiate 24 hours later by incubation with LPS. A. Western blot analysis for IgM protein expression in cell lysate (top panel) or culture media (middle panel) in transfected cells during BCL1 differentiation. Bottom panel shows the quantification of IgM secretion through analysis by densitrometry. B. Fold change of mRNAs for UPR proteins and IgM determined by qRT-PCR upon depletion of AK2 relative to scrambled. C. Western blot analysis with antibodies against BiP and calreticulin (calret) transfected cells during BCL1 differentiation. * indicates $p < 0.05$ by paired 2-tailed Student t-test. All values shown are means of a minimum of three independent experiments.

AK2 plays a profound role in regulating the UPR in both adipocytes and plasma cells. However, since other mitochondrial manipulations such as Tfam depletion did not have a similar affect on secretory ability as shown in the previous chapter, we asked whether other adenylate kinases could also regulate ER function. To test this, primary myotubes were depleted of AK1 to determine any metabolic changes or altered cellular response to tunicamycin induced ER stress. We first examined the tissue distribution of mouse AK1. We found AK1 in the mouse to be highly expressed in skeletal muscle and the diaphram (Figure 3.10A). To determine the functional role of AK1, we studied the effects of siRNA-mediated AK1 depletion in primary myocytes derived from satellite cells from 3-4 week old C57BL/6J mice. Myocytes obtained by this procedure produce a uniformly differentiated cell type regardless of the fiber-type, anatomic location, and embryonic origin of the donor muscles (176). Myoblasts were differentiated into myotubes (Figure 3.10B), and treated with either scrambled or AK1-targeted siRNA oligonucleotides. A decrease in AK1 mRNA of approximately 90% (Figure 3.10C) and of more than 80% in protein levels (Figure 3.10D) was seen with AK1 specific oligonucleotides compared with the scrambled siRNA controls.
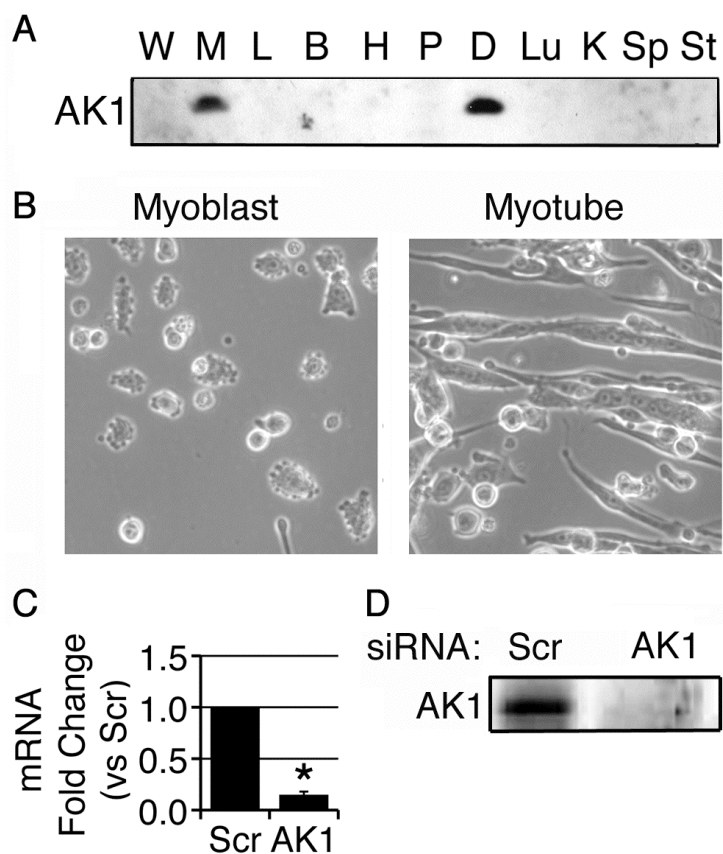
Figure 3.10: AK1 depletion in primary myotubes.

A. Western blot analysis of mouse tissues with an antibody to mouse AK1. W, white adipose tissue; M, muscle; L, liver; B, brain; H, heart; P, pancreas; D, diaphragm; Lu, lung; K, kidney; Sp, spleen; St, stomach. B. Phase images of primary myoblasts and myotubes. C. Expression of AK1 mRNA expression by qRT-PCR from cells transfected with scrambled or AK1 siRNA. D. Western blot analysis of AK1 protein from cells transfected with either scrambled or AK1 siRNA. * indicates $p < 0.05$ by paired 2-tailed Student t-test. All values shown are means of a minimum of three independent experiments.

To determine the functional role of AK1, we examined the metabolic changes elicited upon siRNA transfection. Myotubes depleted of AK1 showed increased basal glucose uptake, averaging a 1.3-fold increase over control myotubes exposed to scrambled siRNA (Figure 3.11A), and a significant increase in basal oxygen consumption (Paired 2-tailed Student t-tests yielded a $p<0.001$) (Figure 3.11B). These results indicate that AK1 depletion in cells elicits acute metabolic changes that increase fuel utilization. In addition, decreased AK1 levels led to lower cellular ATP levels (Figure 3.11C), while ADP and AMP trended higher but were not significantly altered. These changes in nucleotide levels led to increased levels of phosphorylated AMPK indicating increased activation (Figure 3.11D). These findings suggest that the cell is under energetic stress probably due to depleted energy stores and is responding through AMPK and altered metabolic activity to compensate for the lower ATP.
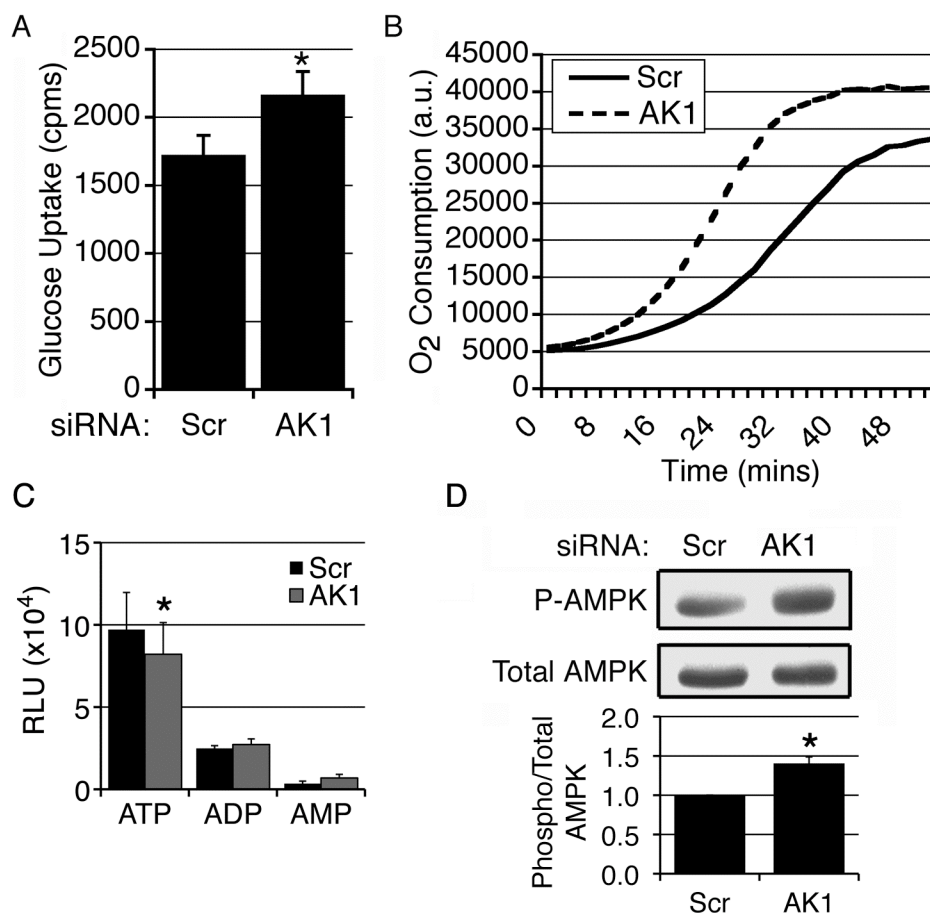
Figure 3.11: AK1 depletion affects primary myotube metabolism.

Primary myotubes were transfected with either scrambled (Scr) or AK1-targeting (AK1) siRNA. A. 2-deoxyglucose uptake in cells transfected with either scrambled or AK1 siRNA. B. Representative graph of oxygen consumption from cells transfected with either scrambled or AK1 siRNA C. Level of adenine nucleotides isolated from cell lysates by TCA extraction expressed as relative luminescent units (RLU). D. Western blot analysis on AMPK protein expression and activation illustrated by phosphorylation from cells transfected with either scrambled or AK1 siRNA and starved overnight in KRH buffer. Lower panel shows the ratio of phosphorylated AMPK to total AMPK based on densitometry of data from blots. * indicates $p<0.05$ by paired 2-tailed Student t-test. All values shown are means of a minimum of three independent experiments.

We then examined whether this alteration in metabolic state would affect the ability of the cells to induce the UPR upon tunicamycin treatment. We found that under basal conditions, there was no change in the mRNA expression of key UPR markers upon AK1 depletion (Figure 3.12A). Therefore, the metabolic changes seen are not affecting the function of the ER or UPR during an unstressed state. To determine how the cell would respond upon increased protein load in the ER, myotubes were treated with tunicamycin to induce ER stress. Myotubes have a functional UPR upon tunicamycin treatment as illlustrated by the increased sXBP1 and BiP mRNA in scrambled siRNA transfected cells (Figure 3.12B). Since CHOP mRNA was also greatly increased, the cells may be unable to handle the increased stress and were proceeding with apoptosis. Upon AK1 depletion, there was no change in the induction of any of the UPR markers as determined by mRNA expression through qRT-PCR analysis. Therefore, unlike what we find in AK2 depleted cells, the nucleotide regulation by AK1 is not required for UPR function.
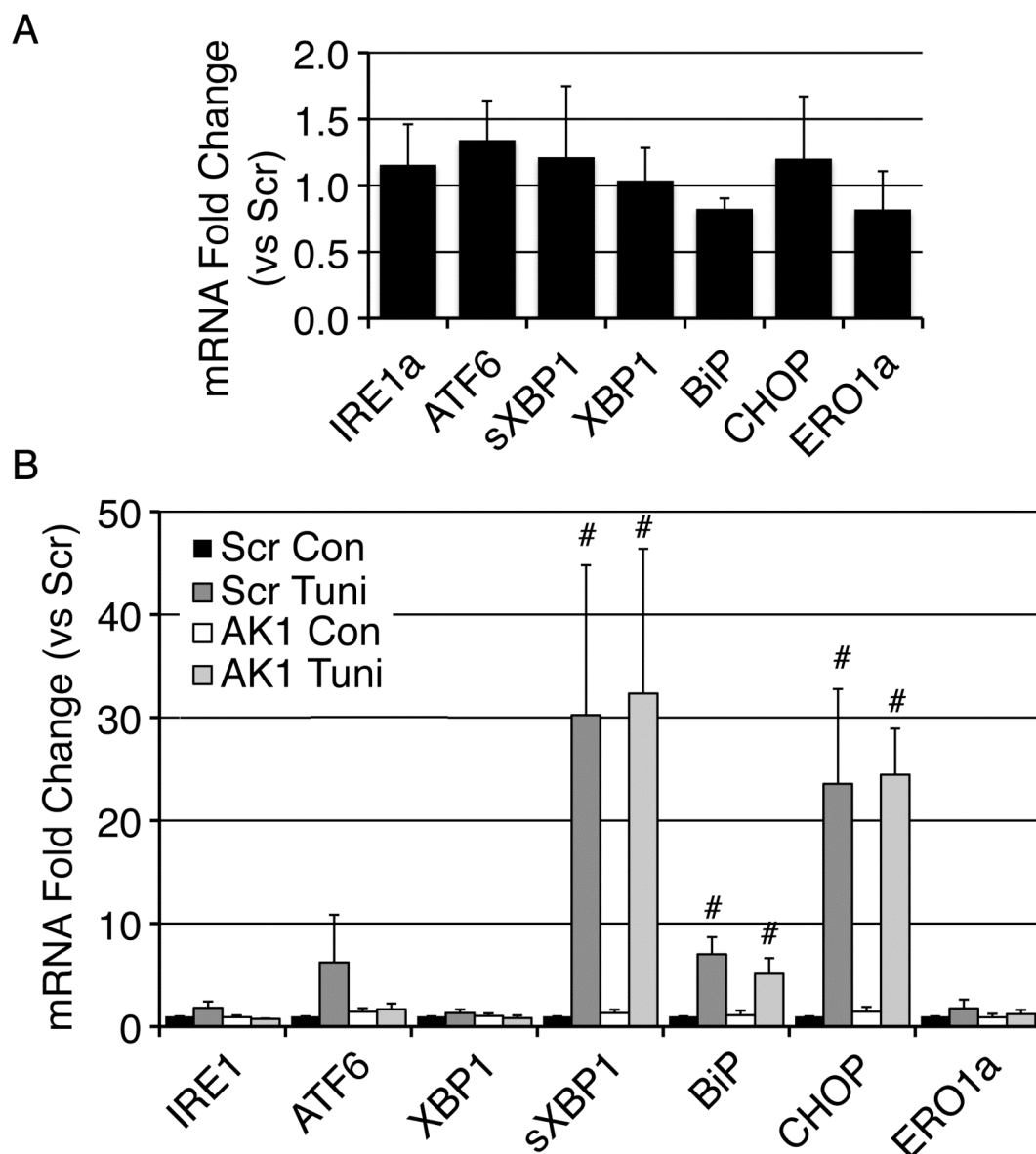
Figure 3.12: AK1 depletion in primary myotubes does not affect UPR induction.

Primary myotubes were transfected with either scrambled (Scr) or AK1-targeting (AK1) siRNA. A. Basal expression of UPR markers determined by qRT-PCR. B. Cells were treated without (Con) or with tunicamycin (Tuni) for 3 hours. Expression of UPR markers was determined by qRT-PCR. # indicates $p<0.05$ between Con and Tuni by paired 2-tailed Student t-test. All values shown are means of a minimum of three independent experiments.

Conclusions

AK2 is a member of a conserved, ancient protein family involved in the interconversion of adenine nucleotides through the reversible reaction ATP+AMP⇔2ADP (120,177,178). Several isoforms of AK exist in humans, and they differ in subcellular localization and tissue distribution (179). The most studied of mammalian AKs is AK1, a cytoplasmic protein expressed specifically in muscle and heart. Studies in knockout mice have suggested that AK1 functions to maximize ATP utilization efficiency during muscle contraction, perhaps by distributing ATP from sites of production to sites of consumption via phosphotransfer reactions (111,114,115). Here we show that while AK1 depletion is able to alter the metabolic status of myotubes, it does not seem to affect induction of the UPR upon tunicamycin treatment.

In contrast to AK1, AK2 is localized to the mitochondrial intermembrane space, where it is imported by a co-translational mechanism that requires a membrane electrochemical potential (180). Previous studies of apoptosis in cultured Jurkat cells have found that AK2 can be released from mitochondria concomitantly with cytochrome c (181,182). This release occurs early in the apoptotic program, prior to changes in mitochondrial membrane potential (183). Additionally, a non-catalytic function for AK2 in promoting apoptosis has been shown in cultured HeLa cells (184). However, its specific role in the regulation of adenine nucleotide metabolism in mammalian cells remained unexplored. AK2 could use increased ADP levels, produced by diminished or uncoupled respiratory chain activity, to generate ATP, serving to delay or mitigate energy depletion. At the same time, the AMP generated by this reaction can serve as a signal to

AMP-sensitive protein kinase to accelerate catabolic reactions to fuel the activity of the respiratory chain (185-187). Another function of AK2 can be proposed, where, under conditions of adequate respiratory chain activity and ATP production, AMP is recruited for the local production of ADP, serving both to maximize the pool of high-energy adenine nucleotides, and as a local signal that cellular energy levels are sufficient. In this way, AK2 has a unique capacity to buffer changes in adenine nucleotide levels and allow the cell to quickly adapt for decreased energy levels while also signaling for the cell to adapt to these changes.

One function of the cell that requires a large amount of energy is protein synthesis. Under conditions of low energy, the levels of AMP/ATP signal activation of AMPK that causes a decrease in protein translation through phosphorylation of eIF2α (188). This signal could also be directly interpreted by the ER, through the unique ability of IRE1 to bind adenine nucleotides (25,28). IRE1 would then respond accordingly, reflecting conditions that would allow a robust response to ER stress without compromising other vital energy intensive cellular functions. The physical proximity between mitochondria and ER membranes may facilitate local energetic signaling among these organelles, in a manner analogous to the communication of calcium signals (189). In this model, IRE1 may function as a checkpoint for cellular energy status, attenuating or promoting UPR signaling in response to cellular energy conditions.

Here we find that AK2 plays an important role in determining the extent and duration of ER stress signaling. The small (15%) decrease in ATP levels with a concurrent increase in AMP levels upon AK2 depletion has a significant impact upon the

UPR and ER function. Thus, a protein that may ensure the maintenance of mitochondrial energetic status in the presence of ER stress appears essential for an adequate cellular response to such stress. Energy status in turn can play a key role in determining the ultimate fate of a cell after ER stress (75). Due to the profound effect that AK2 depletion has on secretion of key extracellular proteins, in an organism, the consequences of AK2 depletion may extend far beyond the cells directly affected. AK2 has been shown to be required for survival of bacteria, yeast, and *Drosophila* (108-110,124). However, higher organisms such as Zebrafish morphants expressing a non-functional AK2 survive though embryogenesis though they have a defect in the development of lymphoid cells (126). Additionally, it has been recently shown that mutations in the AK2 gene are the genetic basis for reticular dysgenesis, a rare form of human severe combined immunodeficiency (SCID) (126). These patients are almost completely devoid of mature lymphoid cells as well as granulocytes. Although the unfolded protein response has been well characterized in the differentiation of mature lymphoid cells, such as B cells and T cells (38,190), its potential role in the maturation of progenitor immune cells is not known. It has been shown that in mice lacking IRE1, the hematopoietic stem cells can reconstitute all lineages of blood cells including pro-B cells (30). However, the pro-B cells of these mice are deficient in VDJ recombination of Ig genes and unable to express B cell receptor (BCR), indicating a role for components of the UPR earlier in B lymphopoiesis. Therefore, the mechanism for which AK2 mutations are causing the human SCID disease may be through its effects on the activation of the unfolded protein response.

Experimental Procedures

Primary Antibodies: Anti-ACRP30/adiponectin (Affinity Bioreagents, Inc.), anti-AMPK and anti-phospho-AMPK (Cell Signaling Technology), anti-BiP (Transduction Laboratories), Anti-cytochrome C (BD Pharmingen), anti-CHOP (Santa Cruz), anti-calreticulin (Calbiochem), anti-GLUT1 (Abcam), anti-GLUT4 (Santa Cruz), anti-HSP60 (Assay Designs), anti-Perilipin (Fitzgerald Industries) and anti-mouse IgM (μ-chain specific) and anti-β-actin (Sigma). Chicken IgY against AK1 was generated by immunization with full-length purified mouse AK1. Chicken IgY and Rabbit IgG against AK2 were generated by immunization with full-length purified mouse AK2. Anti-ERO1-L$^\alpha$ and XBP1was kindly provided by Dr. Fumihiko Urano.

Cell Culture: All cell lines were obtained from American Type Culture Collection and grown under 10% CO_2. 3T3-L1 cells were cultured in complete media defined as: Dulbecco modified Eagle medium (DMEM) supplemented with 10% fetal bovine serum (FBS), 100 U of penicillin/mL, 100 µg of streptomycin/mL, and 50 µg of Normocin/mL (InvivoGen), which was replaced every 48 hours unless otherwise stated. 3T3-L1 cells were grown on 150 mm dishes. Three days after reaching confluence (day 0), media was replaced with culture media containing 0.5 mM 3-isobutyl-1-methylxanthine (Sigma), 0.25 µM dexamethasone (Sigma), and 1 µM insulin (Sigma). 72 hours later, media was replaced with culture media. BCL1 cells were cultured in RPMI 1640 media supplemented with 10 mM HEPES, 1 mM sodium pyruvate, 2.5 g/L D-glucose, 10% fetal bovine serum (FBS), 100 U of penicillin/mL, 100 µg of streptomycin/mL, and 55

µM B-mercaptoethanol. Cells were induced to differentiate by stimulating with 20 µg/mL Lipopolysaccharide (LPS).

Chemical Treatments: Cells were treated with 6 µM tunicamycin, 10 µg/mL oligomycin, 5 µM FCCP, 2.5 mM glucose, or 10 µM palmitate as indicated.

Primary Cell Isolation and Culture: Satellite cells were obtained as previously described (191) with slight modifications. Whole leg muscles from 3-4 week old C57BL/6J mice were dissected and finely minced, and individual cells were separated using 2.4 U/mL dispase and 1% collagenase and then filtering through a 0.7 mm mesh strainer. Cells were plated onto collagen-coated dishes and fed daily with Ham's (F-10) media supplemented with 20% FBS, 400 U of penicillin/mL, 400 mg of streptomycin/mL, 1% Normocin, and 0.25 ng/mL bFGF. Cells were differentiated to myotubes by feeding with DMEM supplemented with 4% horse serum, 400 U of penicillin/mL, 400 mg of streptomycin/mL, and 1% Normocin for 4 days.

siRNA Transfection of 3T3-L1 cells: siRNA oligos to mouse AK2 were obtained and used as a SMARTpool from Dharmacon. Experiments were performed 48 hours post-transfection or as indicated in the figure legends. For day 2 transfections, medium was collected and cells were lifted with 1x trypsin with 1% collagenase and transfected with 20 nmoles of either AK2 or scrambled siRNA into approximately 10^7 cells by electroporation. Cells were resuspended in the collected day 2 medium and re-plated; 24

hours later, the differentiation medium was replaced by complete medium and the medium was refreshed every 2 days afterward. For day 5 transfections, cells were lifted with 1x trypsin with 1% collagenase, and 20 nmoles of siRNA was introduced into approximately 10^7 cells in suspension by electroporation. Cells were re-plated and 48 hours later experiments were performed.

siRNA Nucleofection of BCL1 cells: siRNA oligos to mouse AK2 were obtained and used as a SMARTpool from Dharmacon. Cells were suspended and 0.5 nmoles of siRNA were introduced into approximately 2.5×10^6 cells. Nucleofection was performed using the Amaxa Nucleofector® Kit V and program G-015. Cells were re-plated, 24 hours later media was replace and cells were induced to differentiate.

siRNA Transfection of Myotubes: siRNA oligos to mouse AK1 were obtained and used as a SMARTpool from Dharmacon. Differentiated primary myotubes were fed with DMEM supplemented with 4% horse serum, and immediately transfected with 5 nM of either scrambled or AK1 siRNA using HiPerFect transfection reagent per the manufacturer's protocol (Qiagen). Experiments were performed 48 hours post-transfection.

Quantitative RT-PCR: Total RNA was extracted by using TRIzol reagent (Invitrogen). For quantitative mRNA analysis, 2 µg of the total RNA was reverse-transcribed using an iScript cDNA Synthesis kit (Bio-Rad). Ten percent of each RT reaction was subjected to quantitative real-time PCR analysis using an iQ SYBR green supermix kit and Real-Time

PCR detection system following manufacturer's instructions (MyiQ, Bio-Rad). Ferritin heavy chain (Fth) or β-actin were used as an internal housekeeping gene. Relative gene expression was calculated by the $2^{-\Delta\Delta CT}$ method (163). Briefly the threshold cycle number (Ct) of the target genes was subtracted from the Ct value of Fth or β-actin and raised 2 to the power of this difference.

Immunoblot Analysis: Cell monolayers were washed twice with ice-cold phosphate-buffered saline (PBS) and scraped into 1% sodium dodecyl sulfate (SDS) in PBS. Protein concentration was determined by BCA (Pierce), and equal amounts of protein were separated by SDS-PAGE and transferred to nitrocellulose. Samples of the cell culture medium were taken just prior to media replacement every 24 hours, or as indicated in figure legends, spun 5 minutes at 500*xg,* and equal volumes were separated by SDS-PAGE and transferred to nitrocellulose. The membranes were blocked with 5% nonfat-milk in Tris-buffered saline with 0.1% Tween and incubated with primary antibodies overnight. They were then incubated with anti-rabbit or anti-mouse IgG horseradish peroxidase conjugated antibodies (Promega) or anti-chicken IgY horseradish peroxidase conjugated antibodies (Sigma) and detected using enhanced chemiluminescence (Perkin Elmer Life Sciences, Inc.). Films were scanned at 300 dpi, and band intensities were quantified by using Photoshop software as follows. Images were inverted to render the bands white; bands were next selected by using the rectangular marquee tool and then delineated by using the color range tool until the whole band was selected. The histogram

function was used to determine the number of pixels in the selection, which was multiplied by the average pixel intensity.

Adenine Nucleotide Assay: Levels of adenine nucleotides were measured by a coupled enzymatic assay (192). Cells were washed twice with 1x PBS and then scraped into 20 mM HEPES with 3 mM $MgCl_2$ pH 7.75. An equal volume of 10% TCA was added, lysate was incubated 3 minutes and then spun at 5000*xg* for 5 minutes Supernatant was transferred to a new tube and neutralized by diluting 1:5 with 1 M Tris pH 7.5. 10 µL of sample was added to 12 wells each of an opaque 96-well plate. 90 µl of 20 mM HEPES with 3 mM $MgCl_2$ pH 7.75 was added to each well. To eight wells of each sample, 1.5 mM phosphoenolpyruvate (PEP) and 2.3 U/mL pyruvate kinase (PK) were added to convert ADP to ATP. To 4 of those wells, 36 U/mL of adenylate kinase was added to determine AMP levels. The plate was incubated for 30 minutes then 100 µL of the CellTiter-Glo® luminescent assay reagent (Promega) was added and incubated for an additional 15 minutes. Luminescence was measured using a Tecan Safire2 multimode microplate spectrophotometer. Relative ADP levels were determined by subtracting the wells with PEP/PK from those without. Relative AMP levels were determined by subtracting the wells with PEP/PK/AK from those with PEP/PK.

Lactic Acid Assay: Levels of lactic acid were measured by a coupled enzymatic assay. Cells were washed twice with 1x PBS and then scraped into 20 mM HEPES with 3 mM $MgCl_2$ pH 7.75. An equal volume of 10% TCA was added, lysate was incubated 3

minutes and then spun at $5000xg$ for 5 minutes Supernatant was transferred to a new tube and neutralized by diluting 1:5 with 1 M Tris pH 7.5. 40 µL of each sample was added to triplicate wells in a 96-well plate. 50 µl of 600 mM Hydrazine buffer with 1 M Glycine and 5.6 mM EDTA pH 9.5 was added to each well. 3 µL of 50 mM β-Nicotinamide Adenine Dinucleotide (β-NAD) was added to each well. Absorbance at 340 nm was measured using a Tecan Safire2 multimode microplate spectrophotometer. 10 Units of L-lactate dehydrogenase were added to each well. Absorbance was read every minute until assay reached completion, approximately 90 minutes. Relative lactic acid levels were determined by subtracting the wells without enzyme from those with it.

Brightfield Imaging: All images were obtained using a conventional wide-field microscope fitted with a 60x Nikon PlanApo objective.

Oil Red O Staining: Cells were washed twice in 1x PBS and fixed in 4% formaldehyde for one hour. Cells were washed in dH_2O three times before being stained with 5 mg/mL Oil Red O in 60% triethyl-phosphate for 30 minutes. Cells were washed in dH_2O six times before proceeding with analysis. All images were obtained using a conventional wide-field microscope fitted with a 60x Nikon PlanApo objective.

Fluorescent Imaging: Cells were seeded on glass coverslips. Cells were fixed in 4% formaldehyde for 15 minutes at room temperature, permeabilized with 0.5% Triton X-100 and 1% FBS in 1x PBS, and stained with primary antibodies overnight at 4°C. Alexa

Fluor® 488 or 594 donkey anti-mouse or rabbit secondary antibodies were used to detect bound primary antibody. For MitoTracker® staining, cells were treated for 30 minutes with 100 nM MitoTracker® Red prior to fixation. For staining of nuclei, cells were incubated with 1 µg/mL Hoechst 33258 pentahydrate (bis-benzimide) for 10 minutes. All images were obtained using a conventional wide-field microscope fitted with a 100x Nikon PlanApo objective.

2-Deoxyglucose Uptake Assay: Cells were plated in a 24-well dish. Cells were starved for 2 hours in Krebs-Ringer HEPES (KRH) buffer (130 mM NaCl, 5 mM KCl, 1.3 mM CaCl$_2$, 1.3 mM MgSO$_4$, and 25 mM HEPES, pH 7.4) with 2 mM sodium pyruvate and 1% BSA prior to a 30 minute stimulation with either 1 or 100 nm insulin. Uptake was initiated by the addition of [^{3}H]2-deoxy-D-glucose to a final assay concentration of 100 µM for 5 minutes at 37°C. Assays were terminated by three washes with ice-cold 1x PBS, and the cells were solubilized with 0.4 mL of 1% Triton X-100, and ^{3}H content was determined by scintillation counting. Nonspecific deoxyglucose uptake was measured in the presence of 20 µM cytochalasin B and subtracted from each sample to obtain specific uptake.

Oxygen Consumption: Cells were trypsinized and resuspended in KRH buffer supplemented with 1% fatty acid free BSA. Approximately 7.5x10^4 of 3T3-L1 cells, 2x10^5 BCl1 cells, or 1x10^5 primary myotubes in 150 µL of KRH buffer were added per well in a BD Oxygen Biosensor System plate (BD Biosciences) in triplicate. Plates were

sealed and fluorescence intensity recorded for 120 minutes (2 minute intervals) at an excitation wavelength of 485 nm and emission wavelength of 630 nm on a Tecan Safire2 multimode microplate spectrophotometer maintained at 37°C.

CHAPTER IV

DISCUSSION

Summary and Critique

On a cellular level, the unfolded protein response has been shown to be necessary for the function of secretory cells such as pancreatic β cells and antibody secreting plasma cells. UPR activity, specifically XBP1 splicing, is increased and important during the differentiation of plasma cells, but also during the development of secretory organs, hepatogenesis, cardiac myogenesis, and bone development (36-38,193,194). Similar to previous studies, we also find increased UPR activity during 3T3-L1 adipogenesis identifying another cell type where the UPR plays an important developmental role (127,195). In this study, we find that the UPR is necessary for the secretory function of 3T3-L1 adipocytes; upon XBP1 knockdown, adiponectin secretion is impaired. However, unlike previous studies which found adipogenesis was prevented by either treatment with chemical chaperones (127) or by siRNA mediated depletion of XBP1 (195), we do not see a block in differentiation. We transfected XBP1 siRNA at day 2 of differentiation resulting in only a partial knockdown and functional adipogenesis. This indicates that the adipocyte is able to function with either partial XBP1 expression or can compensate for its depletion. In addition, in XBP1$^{-/-}$ mice rescued with XBP1 expression in the liver, adipose depots are small but present indicating that adipogenesis can occur *in vivo* without XBP1 activity (36). Important to note, functional activity of the adipocytes upon

XBP1 deletion was not examined, so there could still be affects on this organ. Therefore, the regulation of the UPR, especially the IRE1 pathway, is important for proper adipocyte function but may not be necessary for adipogenesis.

From the initial discovery that UPR components respond to glucose deprivation, it has been proposed that the UPR can monitor nutrient levels and act accordingly. Since approximately 15-20% of the total cellular ATP is used for protein synthesis and folding (160,161), energetic regulation of the UPR is important to ensure that its activity will not put further stress on the cell. Adenine nucleotides, mainly ATP, have been suggested as key components in UPR activity. UPR signaling can be regulated by adenine nucleotide levels through the activation of IRE1 (25,28). ATP is also required for the function of ER chaperones during protein folding (162). Consequently, dysregulation of adenine nucleotide levels could affect ER function and protein folding on several levels. Signaling between the ER and mitochondria during calcium regulation and apoptosis has been previously demonstrated (131,132,189). Adenine nucleotides may act as another mechanism for inter-organelle communication. IRE1 may potentially function as a checkpoint for cellular energy status, attenuating or promoting UPR signaling in response to cellular energy conditions. In addition, several mouse models of UPR components demonstrate that the UPR plays a role in regulating the metabolic needs of an organism. Therefore, we sought to determine whether the metabolic status of the cell would regulate the UPR.

To address the metabolic regulation of UPR induction we looked at two methods of ATP production in the 3T3-L1 adipocyte: 1) mitochondrial oxidative phosphorylation

and 2) regeneration of ATP by adenylate kinase (AK). We first examined the effects of ATP synthesis by mitochondrial oxidative phosphorylation on the UPR. Tfam depletion reduces mtDNA and components of the electron transport chain resulting in impaired ATP production. However, this decrease in ATP does not appear to affect basal expression of UPR markers or tunicamycin induced UPR activity. However, under our conditions there may be a mechanism compensating for the chronic state of diminished ATP that resulted in the unaltered UPR activation we observed. We then used chemical inhibitors to generate an acute depletion of ATP. They were able to induce a small increase in the basal UPR signaling as determined by sXBP1 levels, similar to previous reports (128). It has also been shown that oligomycin induced mitochondrial dysfunction can activate an ER stress response due to impaired calcium regulation (196). The authors find that oligomycin treatment results in altered mitochondrial membrane potential and increased cytosolic calcium levels. This could explain the increase we show in sXBP1 mRNA levels upon FCCP and oligomycin treatment. However, when the cells were put under stress through tunicamycin treatment, those with diminished ATP levels were unable to further activate the UPR. This inhibition of oxidative phosphorylation appears to be either too severe or occurs too quickly for compensation resulting in the striking effects on UPR induction. In addition, Tfam depletion, which also results in altered mitochondrial membrane potential (145), shows a trend for increased ER stress that could indicate that calcium regulation is slightly altered. Surprisingly, treatment with 2-deoxyglucose does not have the same affect as FCCP and oligyomycin on sXBP1 levels induced by tunicamycin (Figure 2.9A). This difference could be due to the ability of cells

to use alternate carbon sources during aerobic conditions (197). In addition, 2-deoxyglucose has been shown to alter protein glycosylation and induce the UPR (198), which could explain why we see a trend for increased sXBP1 mRNA levels. However, further analysis on the metabolic alterations caused by these different inhibitors could help determine why this difference occurs though energy levels should be depleted under all conditions. This analysis could include the measurement of adenine nucleotide levels, rates of flux of various metabolic pathways including glycolysis and oxidative phosphorylation, and levels of small molecules including ROS and electron donors, NADH and FADH$_2$. Therefore, while there is mitochondrial regulation of UPR function, it does not appear to simply be the cell's total ATP levels and other compensatory metabolic pathways may be involved.

Another mechanism to generate ATP is by the enzymatic activity of the adenylate kinases, a conserved protein family involved in the interconversion of adenine nucleotides through the reversible reaction ATP+AMP⇔2ADP (120,177,178). AK1 may function to maximize ATP utilization by distributing newly generated ATP to areas of ATP deficiency through a phosphotransfer cascade (111,114,115). Though AK2 has been proposed to be involved in apoptosis (181-184), other roles have not been explored. We find that depleting either AK1 in myotubes or AK2 in adipocytes and B cells results in metabolic alterations. While AK1 depletion appears to increase fuel metabolism and oxygen consumption, AK2 depletion results in decreased oxygen consumption and altered glucose metabolism. These differences could be due to their different subcellular localization. Knockdown of both enzymes results in a small (15%) decrease in ATP

levels with a concurrent trend towards increased AMP levels. AK1 may promote efficient energy usage in the cytosol and upon knockdown the decreased ATP levels activate AMPK resulting in increased catabolic pathways, as indicated by increased fuel usage and oxidative metabolism. On the other hand, AK2 may promote the availability of ADP to the ATP synthase, which upon AK2 depletion might become a rate-limiting step. If ADP were unavailable, oxidative phosphorylation would decrease resulting in lower oxygen consumption. During impaired oxidative phosphorylation, protons cannot pass back into the matrix. As a result, the gradient becomes too strong and the protein complexes of the electron transport chain are unable to operate. This prevents NADH, which is made during the transfer of electrons, from being oxidized. Since NAD+ is required for the function of both glycolysis and the Krebs cycle, these pathways may also be inhibited, which could explain the effects we see on glucose metabolism (199,200). Therefore, the activity of both of these adenylate kinase enzymes is critical for metabolic regulation in several cell types.

We then examined how these alterations in metabolic status would affect UPR activity. AK1 depletion did not alter the levels of key UPR markers, either under basal conditions or upon tunicamycin induced ER stress. We and others (127) have shown that adipogenesis is accompanied by an increase in proteins involved in the UPR. AK2 depletion resulted in a dramatic reduction in this expression of UPR markers at both the mRNA and protein level. Of note, the mRNA levels of several key adipogenic markers show a non-significant decrease of about 30% (Figure 3.2D). This presents the question of whether the affect on the UPR by AK2 depletion is in fact actually a block in

differentiation that causes the UPR effect. We believe this is not the case for several reasons. First, we find that lipid accumulation is unchanged indicating that some aspects of adipogenesis are occurring normally. Second, we find mitochondrial biogenesis, which is also induced by adipocyte differentiation, is unchanged based upon mRNA levels (Figure 3.3C), protein levels (data not shown), and morphology shown by immunostaining (Figure 3.3D). Finally, we find that the mRNA levels of the UPR are reduced by 50-80%, much greater than any changes we see in adipocyte or mitochondrial markers, which would indicate that if the UPR effect was due to impaired adipogenesis, it would have to be more tightly regulated than even lipid accumulation. Though this is possible, it is highly unlikely, therefore we feel that the decreased levels of UPR markers at day 5 of differentiation is due to the depletion of AK2 early in adipogenesis. Also, we feel that the decrease in mRNAs of the UPR as well as the trend in decreased adipogenic mRNAs does not illustrate a general inhibition of transcription since the levels of other mRNAs are shown to be either unchanged or increased by quantitative RT-PCR. In addition, microarray analysis showed 1.9% of mRNAs were decreased and 1.5% were increased, indicating that general transcription was unaffected (data not shown). Therefore, we conclude that AK2 depletion specifically impairs the expression of UPR proteins during 3T3-L1 differentiation. Additional support for this conclusion comes from our finding that UPR induction during the differentiation of BCL1 cells is also specifically impaired by AK2 depletion while plasma cell differentiation as well as mitochondrial structure and gene expression is unaffected.

In addition to the inhibition of UPR activation during differentiation, AK2 depletion also resulted in diminished UPR activation under increased protein load due to impaired protein folding by tunicamycin treatment. We used tunicamycin because we believe that it is the most specific inhibitor of protein folding, due to its precise impairment of protein folding through impaired protein glycosylation (201). Other commonly used inhibitors include thapsigargin, Dithiothreitol (DTT), and Brefeldin A, but were not used due to the off target effects that can occur. Thapsigargin impairs the storage of calcium in the ER and by doing so raises cytosolic calcium levels (202), which can affect mitochondrial structure and function (203-205). DTT is a reducing agent that prevents proper protein folding, however it will reduce any available disulfide bond, which would affect the function of numerous cellular proteins (206). Brefeldin A blocks transport from the ER to the Golgi apparatus increasing the protein load in the ER thereby initiating the UPR (207). Disruption of the Golgi apparatus can have secondary effects on both lipid regulation (208,209) and lysosomes (210,211). For these reasons, we only assessed the role of AK2 in tunicamycin induced UPR activation. In this experiment, the cell had been allowed to differentiate normally and fully develop ER functionality. In addition, the induction of UPR proteins was allowed to progress normally. Therefore, we feel that this inhibition of AK2 is on the acute induction of the UPR in response to tunicamycin, rather than a global impairment of ER function. This again illustrates the specificity of AK2 depletion on UPR activity.

In addition, we show that the functionality of the ER was affected by AK2 depletion, as secretion was impaired in both the 3T3-L1 and BCL1 cell lines. This was

demonstrated by decreased levels of adiponectin and IgM in the culture media. However, there are other possible mechanisms for this result. We believe that this is a post-transcriptional event since both adiponectin and IgM mRNA levels are unchanged by decreased AK2 levels. To clearly demonstrate that AK2 depletion affects secretion, the rate of translation and protein turnover needs to be examined.

To begin with, in the 3T3-L1 cells, we see normal levels of adiponectin in the lysate but decreased levels in the media. We would expect that if adiponectin synthesis is normal and secretion is decreased, there would be increased levels in the lysate. There are two obvious reasons for this effect, either there is increased degradation or decreased synthesis. UPR activation includes induction of the ER degradation system, ERAD, so it would not be surprising that if adiponectin were not efficiently folded, it would be degraded. Another possibility is decreased translation of adiponectin, which would result in less expression. If the rate of secretion also decreased, the lysate levels would appear unchanged or lower. To conclusively determine the mechanism, we could analyze the incorporation of [^{35}S]-methionine into newly synthesized adiponectin with or without incubation with cycloheximide, which blocks translation. Thus we can measure the rate of protein expression and turnover to conclusively determine the cause of decreased adiponectin levels in the media.

Separately, we find that AK2 depletion affects both the expression and secretion of IgM based upon decreased levels in the lysate and media. It has been shown before that XBP1 splicing is required for both the synthesis and secretion of IgM (154). However, a more thorough analysis using [^{35}S]-methionine should provide a convincing

result about whether those same effects are occurring under our conditions. Therefore, we find that AK2, a protein that may stabilize mitochondrial and cellular energetics, appears essential for an adequate cellular response to ER stress and efficient regulation of major secretory proteins.

The different locations of AK1 and AK2 could explain the difference in the functional results upon the UPR. AKs have a unique ability to buffer changes in adenine nucleotide levels and allow the cell to quickly adapt to decreased energy levels. If AK1 is unable to efficiently transfer ATP through the cytosol to sites of usage, the cell may try to compensate via the altered metabolism that we observe. In the mitochondrial intermembrane space, AK2 may generate ATP when impaired mitochondrial activity results in increased ADP levels. Simultaneously, the AMP produced can activate AMPK to increase mitochondrial generated ATP (185-187). However, AK2 activity also can work in the opposite direction. Therefore, under conditions of sufficient ATP production, AK2 can convert AMP for the production of ADP, which would promote the generation of ATP through oxidative phosphorylation.

Changes in nucleotides can signal to IRE1 so the UPR can respond accordingly without compromising other important cellular functions. The ATP necessary for the UPR may come directly from the mitochondria or from specific pools of concentrated ATP in regions where the ER and mitochondria are closely located, similar to calcium regulation (131,132). Therefore, because of its location, AK2 may specifically regulate the nucleotides required for the ER. AK2 may act as a buffer for impaired mitochondrial function and provide nucleotides to the ER for proper protein folding and UPR signaling

(Figure 4.1). AK2 may have compensated for the impaired Tfam depletion, which is why there was no alteration in UPR activity. However, the effect of the mitochondrial inhibitors coupled with treatment with tunicamycin may have been too severe of a stress for AK2 to adequately compensate for resulting in impaired UPR activation.
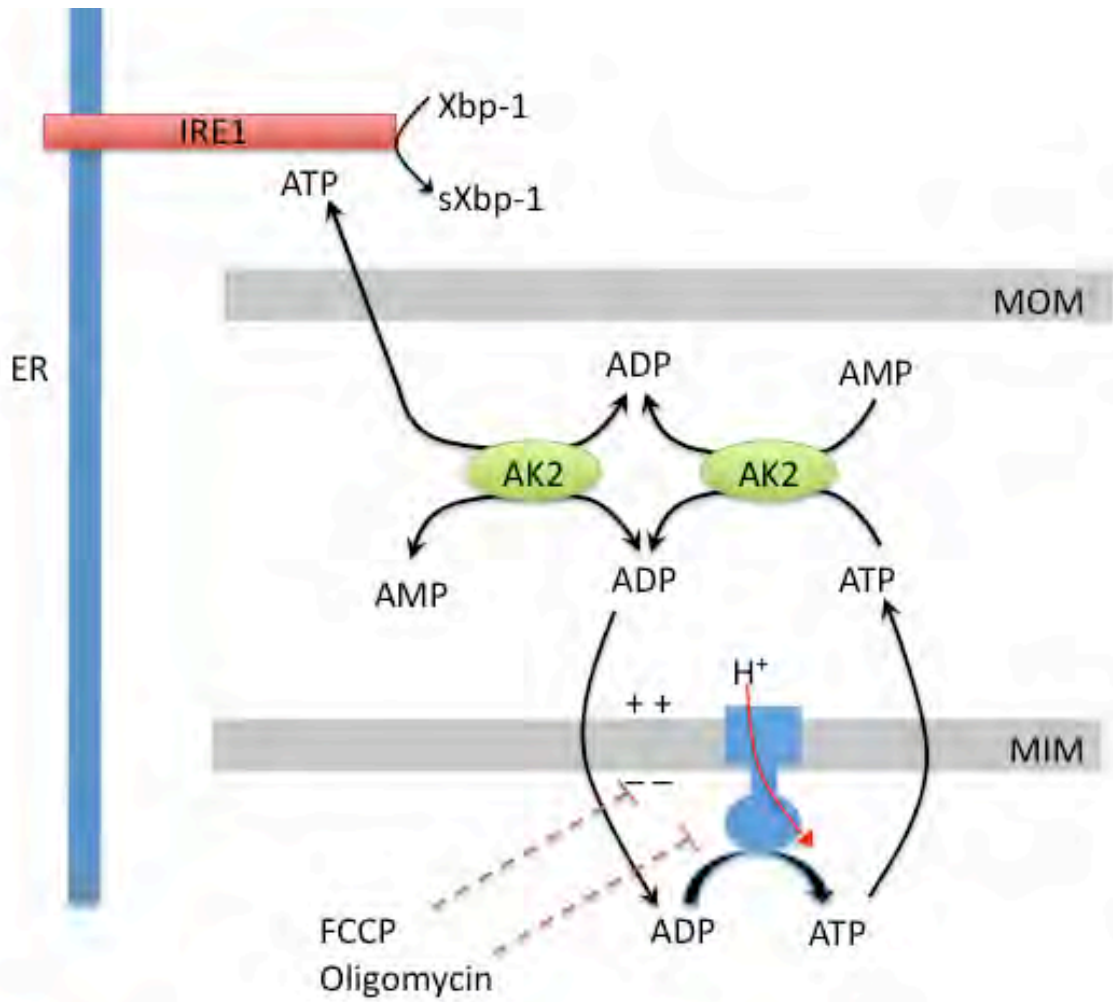
Figure 4.1: Model for the interactions between AK2 and IRE1.

AK2, localized to the mitochondrial intermembrane space, catalyzes the reversible interconversion of adenine nucleotides. In this location, AK2 can draw AMP into the high-energy nucleotide pool under conditions of high ATP production and ADP limitation. Conversely, under conditions of ADP accumulation, such as after FCCP-mediated uncoupling or oligomycin-mediated ATP synthase inhibition, AK2 can catalyze the synthesis of ATP from ADP to support IRE1 activity and other essential functions. In addition, AK2 may be necessary for channeling ATP from its site of synthesis to sites of contact with the ER, facilitating an energy flux to IRE1. MOM: mitochondrial outer membrane; MIM: mitochondrial inner membrane; ER: endoplasmic reticulum.

The model we have detailed is based upon our findings and the current knowledge concerning regulation of energy and the requirement of ATP by ER resident proteins. However, the existing tools available to us limit our conclusions. While we propose that AK2 may be promoting the generation of maintenance of a pool of ATP specifically for use by the ER, our data only suggests its possibility rather than conclusively show that it is in fact the mechanism. A detailed analysis of the subcellular localization of ATP pools, and how their levels change upon AK2 depletion would help support this theory. As mentioned before, BiP requires ATP for success in its protein folding capacity within the ER lumen (162). However, some studies indicate that it is only the binding, rather than the hydrolysis, of ATP that promotes BiP's activity (212,213). The nucleotide binding domain of IRE1 is located in its cytosolic region (25). Therefore there are two distinct subcellular regions that require adenine nucleotides, the ER lumen and the cytosolic side of the ER membrane.

Theoretically, this subcellular requirement for ATP would result in four possible scenarios for ER stress and UPR activation. 1) Adequate levels of ATP in ER and cytosol would lead to normal protein folding, no ER stress, and therefore no activation of the UPR. 2) Decreased ATP in the ER with normal levels in the cytosol would cause impaired protein folding leading to ER stress and activation of the UPR, which should respond normally. 3) Normal ATP levels in the ER and decreased cytosolic levels should allow for normal protein folding so even though there could be impaired UPR activation, this is not a problem since there is no ER stress. 4) Decreased ER and cytosolic ATP levels would result in impaired protein folding leading to ER stress, however the UPR

may not be able to fully respond due to impaired IRE1 activation. Therefore, based on our studies, the effect on the UPR by AK2 depletion would most likely be due to conditions such as is found in scenario 4, although scenario 3 could also be occurring if there is some other mechanism of increased ER stress under these conditions.

Notably, binding of ADP to this domain of IRE1 has been shown to promote greater activity than ATP binding (25). The normal levels of ATP and ADP in the cell are approximately 10mM and 1mM, respectively, but vary depending on cell type (214). Based on these concentrations, while ATP would most likely be the active molecule, ADP would also activate IRE1, especially under conditions of increased ADP to ATP ratios. Therefore, the result we see upon AK2 depletion could be a combination of decreased ATP and ADP levels. We observe decreases in total cellular ATP levels, however ADP levels appear to be unaffected. This could be due to our assay not being sensitive enough to measure any changes, or there could be changes in the subcellular location of these molecules rather than the global amount.

While we believe that the decrease in adiponectin and IgM secretion is due to impaired protein folding, there could be other possibilities for this result. Trafficking from ER to the Golgi Apparatus requires ATP (215), therefore, the decreased ATP could be preventing the exit of these proteins from the ER. In addition, motors required for exocytosis need to hydrolyze ATP to function (216,217). We disagree with these mechanisms since we would expect that retention of the proteins due to impaired trafficking at either stage would result in increased intracellular levels, which we do not observe.

It has been shown that adenylate kinase 2 mutations lead to increased levels of reactive oxygen species (ROS) in isolated fibroblasts (126). In addition, oligomycin and low levels of FCCP can increase ROS production (218,219). However, oxidative stress due to increased levels of ROS has been shown to induce ER stress and the UPR (220,221), therefore the small increase we see in sXBP1 mRNA levels upon FCCP and oligomycin treatment could be due to ROS, however the dramatic impairment by these molecules on tunicamycin induced UPR is most likely due to another mechanism. In addition, although AK2 mutations result in increased levels of ROS, we saw no change in basal levels of ROS upon AK2 depletion (data not shown), and increases in ROS would not explain the impaired UPR activation.

Based upon the previous data, we propose the model that depletion of AK2 leads to a decreased in ATP levels (Figure 4.2). Decreased ATP impairs both protein folding and induction of the UPR (which also adds to the impaired protein folding) leading to the decrease in protein secretion we observe. However, there are still other potential models that could explain our results. These would need to be addressed in order to confirm or dispute our conclusions.
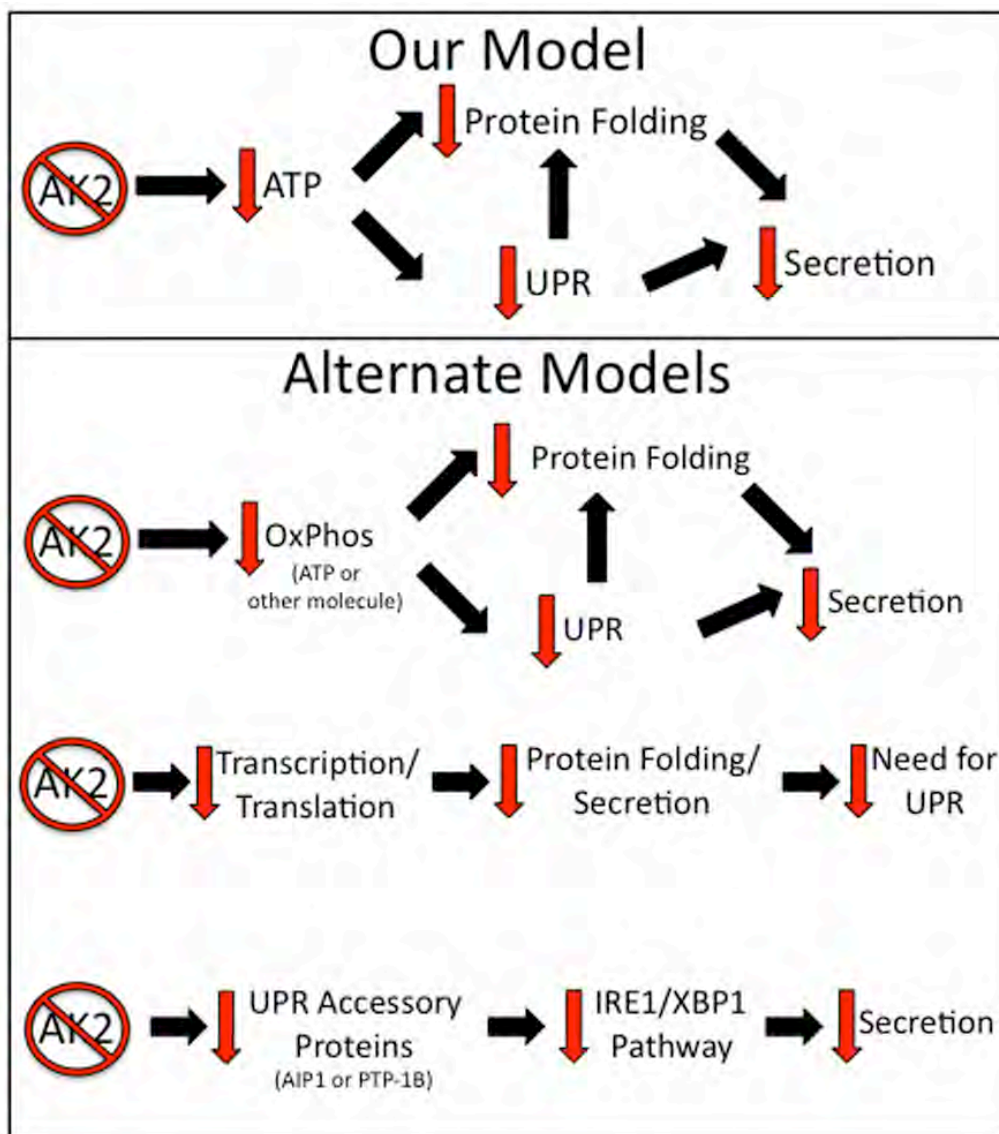
Figure 4.2: Alternate models for AK2 effect on the UPR.

Our model shows that the depletion of AK2 leads to decreased ATP, which impairs protein folding and the UPR resulting in decreased secretion. We acknowledge that there are at least three additional models that could explain our findings. First, AK2 depletion could result in altered products of oxidative phosphorylation (ATP or another factor) that could lead to the impaired protein folding, UPR, and secretion. Second, AK2 depletion may decrease either transcription or translation leading to decreased proteins in the ER, decreased secretion, and a lack of UPR activation. Finally, AK2 depletion may impair UPR accessory proteins, such as AIP1 or PTP-1B, leading to impaired IRE1/XBP1 pathway and decreased secretion.

We acknowledge that there are at least three additional models that could explain our findings. First, oxidative phosphorylation appears to be affected by AK2 depletion in our studies. Changes in the levels of ATP or another product from this mitochondrial pathway could lead to the impaired protein folding, UPR induction, and protein secretion that we observe. The similar effects we see on impairment of the UPR by FCCP and oligomycin treatment support this model. However, Tfam depletion also impairs oxidative phosphorylation and yet does not affect the UPR, thereby refuting this idea. To test this model, careful analysis would have to be performed to quantify products of oxidative phosphorylation and then determine their effects on UPR activation.

Second, AK2 depletion resulted in decreased levels of several mRNAs and proteins. If AK2 depletion led to a direct impairment of either transcription or translation in these cells, the result would be a decrease in the load on the ER due to a decreased requirement for protein folding and secretion. As a result, the need for the UPR to promote protein folding would be decreased, as demonstrated by the decreased levels of UPR markers. This model is supported by the finding that cycloheximide, an inhibitor of protein translation, can reduce UPR activation (222,223). Our gene chip data shows no global change in transcription, however careful analysis of total protein synthesis would also need to be conducted to disprove this hypothesis.

Finally, AK2 depletion may impair UPR accessory proteins, such as AIP1 or PTP-1B, leading to an impaired IRE1/XBP1 pathway and decreased secretion. Besides via the direct inhibition of classic UPR proteins, very few studies have demonstrated decreased UPR activation. Recent papers, however, have shown that two proteins

promote the UPR and decreasing their levels leads to impaired UPR activation. Apoptosis signal-regulating kinase 1 (ASK1) has been shown to be involved in JNK mediated induction of apoptosis by IRE1 activation (224-226). Another protein, ASK1-interacting protein 1 (AIP1), however, has been shown to be important for a more global transduction of UPR signaling (227). In AIP1 knockout cells, IRE1 activation and XBP1 splicing are impaired, as is ER stress mediated JNK activation. This regulation is potentially through the binding of AIP1 to IRE1, rather than an interaction through ASK1. Protein-tyrosine phosphatase 1B (PTP-1B) also has been shown to promote the IRE1 signaling cascade (228). PTP-1B knockout mouse embryonic fibroblasts (MEFs) show impaired XBP1 splicing, EDEM expression, JNK activation, and ER stress induced apoptosis. Therefore, either AIP1 or PTP-1B may be mediating the decreased UPR activation, though it is unlikely that AK2 can directly affect either of these proteins their levels should be measured. The lack of data on cellular alterations that impair the UPR supports the need to further understand the regulation by AK2 and its effect on cellular and whole body function.

Clinical Implications

White adipose tissue was traditionally thought to only function as a lipid storage depot. It is now known that it regulates whole body metabolism by monitoring nutrient levels and responding through the secretion of adipokines that act on the central nervous system and peripheral tissues to control caloric intake and utilization (6,7). Because

adipokines regulate whole body metabolism, defects in adipokine secretion due to impaired UPR function could result in similar disease states. The importance of AK2 has been shown through its requirement for lymphoid cell development in Zebrafish and the survival of bacteria, yeast, and *Drosophila* (108-110,124,126). However, since it is also necessary for UPR function and secretion, the consequences of AK2 depletion may affect health of an organism.

While the role of the UPR is to promote the proper function of the ER, it has been shown to play a key role in human health and disease. Several conditions, including neurodegeneration, tumor growth, the immune response, and metabolic disease have been linked to improper or impaired UPR activation. A major focus had been on the pro-apoptotic feature of the UPR and its relationship to disease. Recently, more direct links between UPR signaling and function/dysfunction has been shown to play a role in these maladies. The PERK/eIF2α branch has been shown to be important for glucose metabolism (54,229) and the UPR in adipose tissue seems to play a similar role since treatment of *ob/ob* mice with chemical chaperones relieves ER stress in adipose tissue and restores glucose homeostasis and insulin sensitivity (99). Therefore, the regulation of UPR activity by AK2 activity and manipulation of energetic levels could serve as important therapeutic targets.

Mutations in AK2 result in reticular dysgenesis, a rare form of human severe combined immunodeficiency (SCID) (126). These patients do not produce a functional immune system and are deficient in hematopoietic cells from both the myeloid and lymphoid lineages. Mitochondriopathy, based upon increased apoptosis and reactive

oxygen species as well as an altered mitochondrial membrane potential, was observed in fibroblasts from these patients. This has been proposed as the cause of the absence in hematopoietic cells, however it was not fully examined. The UPR has also been implicated in hematopoiesis, however only late stage B cell maturation appears to be affected by impaired IRE1/XBP1 signaling (30,230). The exact mechanism of AK2 impairment in development of reticular dysgenesis has not been clearly identified and we show that AK2 depletion affects UPR activity; therefore, the role of the UPR in early hematopoiesis, especially in relation to this disease, should be investigated.

Future Directions

The UPR has been linked to many diseases including defects in hematopoiesis and impaired immune function. Although the UPR has been well characterized in the differentiation of mature lymphoid cells, such as B cells and T cells (38,190), its potential role in the maturation of progenitor immune cells is not known. Since AK2 mutations have been shown to block hematopoiesis, a mouse model for AK2 function during development would aid in determining the root cause of the disease pathology seen in the SCID patients. Characterization of this mouse would help in determining whether the role of AK2 in UPR function is responsible for the human condition.

If the AK2 mouse model is viable and shows a similar phenotype to patients with reticular dysgenesis, it would be extremely useful for experiments involving reconstitution of immune cell lineages. The Rag2 mouse, often used for immune studies,

lacks lymphoid cells due to impaired VDJ rearrangement (231). On the other hand, the AK2 mouse would lack granulocytes and all cells from the lymphoid lineage resulting in no innate or adaptive immunity. This would allow it to be a more efficient model for the numerous research studies that require reconstitution of various aspects of the immune system.

In addition, further understanding of the regulation of the UPR by ATP and mitochondrial function as well as any mechanism by which the cell compensates for impaired mitochondrial function may be beneficial in treating several diseases linked to UPR function. Since ATP is the only adenine nucleotide that is consistently altered upon AK2 depletion, our results suggest that ATP levels are critical for UPR function. In addition, AK2 depletion results in a trend of the other adenine nucleotides towards increased levels, which may also be able to regulate the UPR. Our studies were only able to quantify total cellular levels of these molecules; however, measuring changes in the concentrations of local nucleotide pools may be a more accurate method. As of now, I know of no quantitative procedure to perform these experiments, but new *in vivo* fluorescent monitors for ATP may be useful as their specificity and responsiveness improves (232,233). The importance of AK2 expression during ER stress is supported by our preliminary data demonstrating its resistance to the block of translation induced by the UPR (Appendix I). Understanding the regulatory mechanisms for AK2 expression could help in determining how the cell adapts to cellular stress as well as offer greater insight into how to alter its expression and perhaps its activity.

The post-transcriptional regulation of AK2 that has been observed by several laboratories including our own could be a key mechanism by which to alter AK2 expression. Further analysis of the 5' and 3'UTR of AK2 as well as examination of the sequence for alternative ribosome binding sites, including an IRES, could help in determining the method of regulation. In addition, analysis of the rate of translation could show that while the level of transcript is unchanged, the number of polyribosomes actively translating the mRNA might be altered. These studies could provide useful insight into how the cell regulates AK2 expression and therefore, how its expression could be modulated.

Decreasing AK2 activity seems to specifically alter ER function while general metabolism and other cellular functions appear to be largely unaffected by the resulting decrease in ATP levels. Therefore, AK2 may be an important target for disease therapeutics. Since inhibition of AK2 blocks UPR function, compounds targeting this enzyme would be useful as a treatment for infections by viral strains that increase the UPR to promote their replication.

Conversely, by increasing AK2 activity, the hypothesis would be that UPR function would improve. However, AK2 has been associated with increased apoptosis upon release from the mitochondria (182,184). In addition, we found that constitutive overexpression of AK2 resulted in cell death (data not shown). Therefore, experiments examining increased AK2 activity would require careful regulation of AK2 levels to ensure cell survival. If the activity of the UPR can be increased, such as in the studies involving prolonged IRE1 signaling (75), the cell may be given enough time to recover

preventing a cellular cascade into a disease state. While increasing AK2 may not be a practical method for improving UPR function, the data presented here demonstrate the importance of energetic regulation on UPR activity. Therefore, other means of increasing the availability of ATP for ER function should be examined, including improving mitochondrial function in pathologies such as diabetes and Alzheimer's disease. This may improve protein folding and thereby slow or prevent the development of these diseases.

Though AK1 depletion did not affect UPR function, it did alter the metabolic status of the myotubes. Previous studies on the knockout mice have shown that they are relatively healthy with normal muscle contractility (114,115). They do display enhanced ATP synthesis indicating impaired energy efficiency. Preliminary studies in our lab demonstrate a resistance to high fat feeding indicating that the mice may burn more fuel for normal activity (Appendix II). Further studies are needed to characterize this phenotype and determine the mechanism for action. If inhibiting AK1 activity does decrease energy efficiency, drugs targeting this enzyme may be useful for weight loss and the treatment of obesity and diabetes. Of note, AK1 mutations have been associated with hemolytic anemia in a Japanese patient (234). Surprisingly, a sibling with the same genetic mutation did not show symptoms of the disease indicating compensation is possible. The possibility of a severe reaction to the lack of AK1 activity in the erythrocyte would need to be accounted for during any targeting of AK1 for therapeutic purposes.

The data presented in this thesis supports the function of the UPR during normal cellular secretion. It expands on the role ATP plays in promoting UPR activation that has been suggested in other studies. We focused on the regulation of the UPR by energy levels and determined the specificity of catabolic systems in ER function. Here we find that while ATP from mitochondrial oxidative phosphorylation can affect UPR function and secretion, AK2 activity appears to play a more specialized role in this regulation. Further studies of the energetic crosstalk between the ER and mitochondria and the role of AK2 would improve the understanding of protein synthesis and secretion and could also promote the development of new drugs to treat the numerous diseases associated with abnormal UPR and/or mitochondrial function.

REFERENCES

1. Cornier, M. A., Dabelea, D., Hernandez, T. L., Lindstrom, R. C., Steig, A. J., Stob, N. R., Van Pelt, R. E., Wang, H., and Eckel, R. H. (2008) *Endocr Rev* **29**, 777-822
2. Virtue, S., and Vidal-Puig, A. *Biochim Biophys Acta* **1801**, 338-349
3. Buchanan, T. A., Xiang, A., Kjos, S. L., and Watanabe, R. (2007) *Diabetes Care* **30 Suppl 2**, S105-111
4. Gale, E. A. (2001) *Diabetes* **50**, 217-226
5. Freeman, H., and Cox, R. D. (2006) *Hum Mol Genet* **15 Spec No 2**, R202-209
6. Havel, P. J. (2002) *Curr Opin Lipidol* **13**, 51-59
7. Rajala, M. W., and Scherer, P. E. (2003) *Endocrinology* **144**, 3765-3773
8. Berg, A. H., Combs, T. P., and Scherer, P. E. (2002) *Trends Endocrinol Metab* **13**, 84-89
9. Scherer, P. E., Williams, S., Fogliano, M., Baldini, G., and Lodish, H. F. (1995) *J Biol Chem* **270**, 26746-26749
10. Yamauchi, T., Kamon, J., Ito, Y., Tsuchida, A., Yokomizo, T., Kita, S., Sugiyama, T., Miyagishi, M., Hara, K., Tsunoda, M., Murakami, K., Ohteki, T., Uchida, S., Takekawa, S., Waki, H., Tsuno, N. H., Shibata, Y., Terauchi, Y., Froguel, P., Tobe, K., Koyasu, S., Taira, K., Kitamura, T., Shimizu, T., Nagai, R., and Kadowaki, T. (2003) *Nature* **423**, 762-769
11. Hebert, D. N., and Molinari, M. (2007) *Physiol Rev* **87**, 1377-1408
12. Ellgaard, L., and Helenius, A. (2003) *Nat Rev Mol Cell Biol* **4**, 181-191
13. Patel, S. D., Rajala, M. W., Rossetti, L., Scherer, P. E., and Shapiro, L. (2004) *Science* **304**, 1154-1158
14. Ron, D., and Walter, P. (2007) *Nat Rev Mol Cell Biol* **8**, 519-529
15. Shiu, R. P., Pouyssegur, J., and Pastan, I. (1977) *Proc Natl Acad Sci U S A* **74**, 3840-3844
16. Pouyssegur, J., Shiu, R. P., and Pastan, I. (1977) *Cell* **11**, 941-947
17. Harding, H. P., and Ron, D. (2002) *Diabetes* **51 Suppl 3**, S455-461
18. Lin, J. H., Walter, P., and Yen, T. S. (2008) *Annu Rev Pathol* **3**, 399-425
19. Zhao, L., and Ackerman, S. L. (2006) *Curr Opin Cell Biol* **18**, 444-452
20. Bertolotti, A., Zhang, Y., Hendershot, L. M., Harding, H. P., and Ron, D. (2000) *Nat Cell Biol* **2**, 326-332
21. Shen, J., Chen, X., Hendershot, L., and Prywes, R. (2002) *Dev Cell* **3**, 99-111
22. Wang, X. Z., Harding, H. P., Zhang, Y., Jolicoeur, E. M., Kuroda, M., and Ron, D. (1998) *EMBO J* **17**, 5708-5717
23. Tirasophon, W., Welihinda, A. A., and Kaufman, R. J. (1998) *Genes Dev* **12**, 1812-1824
24. Pincus, D., Chevalier, M. W., Arag√≥n, T. s., van Anken, E., Vidal, S. E., El-Samad, H., and Walter, P. *PLoS Biol* **8**, e1000415
25. Sidrauski, C., and Walter, P. (1997) *Cell* **90**, 1031-1039

26. Welihinda, A. A., and Kaufman, R. J. (1996) *J Biol Chem* **271**, 18181-18187
27. Shamu, C. E., and Walter, P. (1996) *EMBO J* **15**, 3028-3039
28. Papa, F. R., Zhang, C., Shokat, K., and Walter, P. (2003) *Science* **302**, 1533-1537
29. Kaufman, R. J., Scheuner, D., Schroder, M., Shen, X., Lee, K., Liu, C. Y., and Arnold, S. M. (2002) *Nat Rev Mol Cell Biol* **3**, 411-421
30. Zhang, K., Wong, H. N., Song, B., Miller, C. N., Scheuner, D., and Kaufman, R. J. (2005) *J Clin Invest* **115**, 268-281
31. Iwawaki, T., Akai, R., Yamanaka, S., and Kohno, K. (2009) *Proc Natl Acad Sci U S A* **106**, 16657-16662
32. Clauss, I. M., Chu, M., Zhao, J. L., and Glimcher, L. H. (1996) *Nucleic Acids Res* **24**, 1855-1864
33. Liou, H. C., Boothby, M. R., Finn, P. W., Davidon, R., Nabavi, N., Zeleznik-Le, N. J., Ting, J. P., and Glimcher, L. H. (1990) *Science* **247**, 1581-1584
34. Lee, A. H., Iwakoshi, N. N., and Glimcher, L. H. (2003) *Mol Cell Biol* **23**, 7448-7459
35. Acosta-Alvear, D., Zhou, Y., Blais, A., Tsikitis, M., Lents, N. H., Arias, C., Lennon, C. J., Kluger, Y., and Dynlacht, B. D. (2007) *Mol Cell* **27**, 53-66
36. Lee, A. H., Chu, G. C., Iwakoshi, N. N., and Glimcher, L. H. (2005) *EMBO J* **24**, 4368-4380
37. Reimold, A. M., Etkin, A., Clauss, I., Perkins, A., Friend, D. S., Zhang, J., Horton, H. F., Scott, A., Orkin, S. H., Byrne, M. C., Grusby, M. J., and Glimcher, L. H. (2000) *Genes Dev* **14**, 152-157
38. Reimold, A. M., Iwakoshi, N. N., Manis, J., Vallabhajosyula, P., Szomolanyi-Tsuda, E., Gravallese, E. M., Friend, D., Grusby, M. J., Alt, F., and Glimcher, L. H. (2001) *Nature* **412**, 300-307
39. Yoshida, H., Okada, T., Haze, K., Yanagi, H., Yura, T., Negishi, M., and Mori, K. (2000) *Mol Cell Biol* **20**, 6755-6767
40. Chen, X., Shen, J., and Prywes, R. (2002) *J Biol Chem* **277**, 13045-13052
41. Ye, J., Rawson, R. B., Komuro, R., Chen, X., Dave, U. P., Prywes, R., Brown, M. S., and Goldstein, J. L. (2000) *Mol Cell* **6**, 1355-1364
42. Okada, T., Yoshida, H., Akazawa, R., Negishi, M., and Mori, K. (2002) *Biochem J* **366**, 585-594
43. Yoshida, H., Matsui, T., Yamamoto, A., Okada, T., and Mori, K. (2001) *Cell* **107**, 881-891
44. Wu, J., Rutkowski, D. T., Dubois, M., Swathirajan, J., Saunders, T., Wang, J., Song, B., Yau, G. D., and Kaufman, R. J. (2007) *Dev Cell* **13**, 351-364
45. Harding, H. P., Zhang, Y., and Ron, D. (1999) *Nature* **397**, 271-274
46. Liu, C. Y., Schroder, M., and Kaufman, R. J. (2000) *J Biol Chem* **275**, 24881-24885
47. Owen, C. R., Kumar, R., Zhang, P., McGrath, B. C., Cavener, D. R., and Krause, G. S. (2005) *J Neurochem* **94**, 1235-1242
48. Shi, Y., Vattem, K. M., Sood, R., An, J., Liang, J., Stramm, L., and Wek, R. C. (1998) *Mol Cell Biol* **18**, 7499-7509

49.   Prostko, C. R., Brostrom, M. A., and Brostrom, C. O. (1993) *Mol Cell Biochem* **127-128**, 255-265

50.   Zhang, P., McGrath, B., Li, S., Frank, A., Zambito, F., Reinert, J., Gannon, M., Ma, K., McNaughton, K., and Cavener, D. R. (2002) *Mol Cell Biol* **22**, 3864-3874

51.   Hinnebusch, A. G. (1994) *Semin Cell Biol* **5**, 417-426

52.   Pain, V. M. (1996) *Eur J Biochem* **236**, 747-771

53.   Ito, T., Warnken, S. P., and May, W. S. (1999) *Biochem Biophys Res Commun* **265**, 589-594

54.   Scheuner, D., Song, B., McEwen, E., Liu, C., Laybutt, R., Gillespie, P., Saunders, T., Bonner-Weir, S., and Kaufman, R. J. (2001) *Mol Cell* **7**, 1165-1176

55.   Harding, H. P., Novoa, I., Zhang, Y., Zeng, H., Wek, R., Schapira, M., and Ron, D. (2000) *Mol Cell* **6**, 1099-1108

56.   Fernandez, J., Bode, B., Koromilas, A., Diehl, J. A., Krukovets, I., Snider, M. D., and Hatzoglou, M. (2002) *J Biol Chem* **277**, 11780-11787

57.   Hinnebusch, A. G. (1997) *J Biol Chem* **272**, 21661-21664

58.   Lu, P. D., Harding, H. P., and Ron, D. (2004) *J Cell Biol* **167**, 27-33

59.   Ma, Y., Brewer, J. W., Diehl, J. A., and Hendershot, L. M. (2002) *J Mol Biol* **318**, 1351-1365

60.   Ma, Y., and Hendershot, L. M. (2003) *J Biol Chem* **278**, 34864-34873

61.   Harding, H. P., Zhang, Y., Zeng, H., Novoa, I., Lu, P. D., Calfon, M., Sadri, N., Yun, C., Popko, B., Paules, R., Stojdl, D. F., Bell, J. C., Hettmann, T., Leiden, J. M., and Ron, D. (2003) *Mol Cell* **11**, 619-633

62.   Vashist, S., and Ng, D. T. (2004) *J Cell Biol* **165**, 41-52

63.   Molinari, M., Calanca, V., Galli, C., Lucca, P., and Paganetti, P. (2003) *Science* **299**, 1397-1400

64.   Hiller, M. M., Finger, A., Schweiger, M., and Wolf, D. H. (1996) *Science* **273**, 1725-1728

65.   Hosokawa, N., Wada, I., Hasegawa, K., Yorihuzi, T., Tremblay, L. O., Herscovics, A., and Nagata, K. (2001) *EMBO Rep* **2**, 415-422

66.   Yoneda, T., Imaizumi, K., Oono, K., Yui, D., Gomi, F., Katayama, T., and Tohyama, M. (2001) *J Biol Chem* **276**, 13935-13940

67.   Ron, D., and Habener, J. F. (1992) *Genes Dev* **6**, 439-453

68.   Batchvarova, N., Wang, X. Z., and Ron, D. (1995) *Embo J* **14**, 4654-4661

69.   Maytin, E. V., and Habener, J. F. (1998) *J Invest Dermatol* **110**, 238-246

70.   Matsumoto, M., Minami, M., Takeda, K., Sakao, Y., and Akira, S. (1996) *FEBS Lett* **395**, 143-147

71.   Maytin, E. V., Ubeda, M., Lin, J. C., and Habener, J. F. (2001) *Exp Cell Res* **267**, 193-204

72.   Ferri, K. F., and Kroemer, G. (2001) *Nat Cell Biol* **3**, E255-263

73.   Biagioli, M., Pifferi, S., Ragghianti, M., Bucci, S., Rizzuto, R., and Pinton, P. (2008) *Cell Calcium* **43**, 184-195

74.   Nakamura, K., Bossy-Wetzel, E., Burns, K., Fadel, M. P., Lozyk, M., Goping, I. S., Opas, M., Bleackley, R. C., Green, D. R., and Michalak, M. (2000) *J Cell Biol* **150**, 731-740

75. Lin, J. H., Li, H., Yasumura, D., Cohen, H. R., Zhang, C., Panning, B., Shokat, K. M., Lavail, M. M., and Walter, P. (2007) *Science* **318**, 944-949
76. Trojanowski, J. Q. (2002) *Ann Neurol* **52**, 263-265
77. Hoozemans, J. J., van Haastert, E. S., Nijholt, D. A., Rozemuller, A. J., Eikelenboom, P., and Scheper, W. (2009) *Am J Pathol* **174**, 1241-1251
78. Chafekar, S. M., Zwart, R., Veerhuis, R., Vanderstichele, H., Baas, F., and Scheper, W. (2008) *Curr Alzheimer Res* **5**, 469-474
79. Katayama, T., Imaizumi, K., Sato, N., Miyoshi, K., Kudo, T., Hitomi, J., Morihara, T., Yoneda, T., Gomi, F., Mori, Y., Nakano, Y., Takeda, J., Tsuda, T., Itoyama, Y., Murayama, O., Takashima, A., St George-Hyslop, P., Takeda, M., and Tohyama, M. (1999) *Nat Cell Biol* **1**, 479-485
80. Yang, Y., Turner, R. S., and Gaut, J. R. (1998) *J Biol Chem* **273**, 25552-25555
81. Hoozemans, J. J., van Haastert, E. S., Eikelenboom, P., de Vos, R. A., Rozemuller, J. M., and Scheper, W. (2007) *Biochem Biophys Res Commun* **354**, 707-711
82. Sado, M., Yamasaki, Y., Iwanaga, T., Onaka, Y., Ibuki, T., Nishihara, S., Mizuguchi, H., Momota, H., Kishibuchi, R., Hashimoto, T., Wada, D., Kitagawa, H., and Watanabe, T. K. (2009) *Brain Res* **1257**, 16-24
83. Koumenis, C., and Wouters, B. G. (2006) *Mol Cancer Res* **4**, 423-436
84. Koumenis, C., Naczki, C., Koritzinsky, M., Rastani, S., Diehl, A., Sonenberg, N., Koromilas, A., and Wouters, B. G. (2002) *Mol Cell Biol* **22**, 7405-7416
85. Bi, M., Naczki, C., Koritzinsky, M., Fels, D., Blais, J., Hu, N., Harding, H., Novoa, I., Varia, M., Raleigh, J., Scheuner, D., Kaufman, R. J., Bell, J., Ron, D., Wouters, B. G., and Koumenis, C. (2005) *EMBO J* **24**, 3470-3481
86. Romero-Ramirez, L., Cao, H., Nelson, D., Hammond, E., Lee, A. H., Yoshida, H., Mori, K., Glimcher, L. H., Denko, N. C., Giaccia, A. J., Le, Q. T., and Koong, A. C. (2004) *Cancer Res* **64**, 5943-5947
87. Huang, Z. M., Tan, T., Yoshida, H., Mori, K., Ma, Y., and Yen, T. S. (2005) *Mol Cell Biol* **25**, 7522-7533
88. Tirosh, B., Iwakoshi, N. N., Lilley, B. N., Lee, A. H., Glimcher, L. H., and Ploegh, H. L. (2005) *J Virol* **79**, 2768-2779
89. Baltzis, D., Qu, L. K., Papadopoulou, S., Blais, J. D., Bell, J. C., Sonenberg, N., and Koromilas, A. E. (2004) *J Virol* **78**, 12747-12761
90. Perkins, D. J., and Barber, G. N. (2004) *Mol Cell Biol* **24**, 2025-2040
91. Delepine, M., Nicolino, M., Barrett, T., Golamaully, M., Lathrop, G. M., and Julier, C. (2000) *Nat Genet* **25**, 406-409
92. Inoue, H., Tanizawa, Y., Wasson, J., Behn, P., Kalidas, K., Bernal-Mizrachi, E., Mueckler, M., Marshall, H., Donis-Keller, H., Crock, P., Rogers, D., Mikuni, M., Kumashiro, H., Higashi, K., Sobue, G., Oka, Y., and Permutt, M. A. (1998) *Nat Genet* **20**, 143-148
93. Fonseca, S. G., Fukuma, M., Lipson, K. L., Nguyen, L. X., Allen, J. R., Oka, Y., and Urano, F. (2005) *J Biol Chem* **280**, 39609-39615
94. Leroux, L., Desbois, P., Lamotte, L., Duvillie, B., Cordonnier, N., Jackerott, M., Jami, J., Bucchini, D., and Joshi, R. L. (2001) *Diabetes* **50 Suppl 1**, S150-153

95. Oyadomari, S., Koizumi, A., Takeda, K., Gotoh, T., Akira, S., Araki, E., and Mori, M. (2002) *J Clin Invest* **109**, 525-532

96. Ozcan, U., Cao, Q., Yilmaz, E., Lee, A. H., Iwakoshi, N. N., Ozdelen, E., Tuncman, G., Gorgun, C., Glimcher, L. H., and Hotamisligil, G. S. (2004) *Science* **306**, 457-461

97. Laybutt, D. R., Preston, A. M., Akerfeldt, M. C., Kench, J. G., Busch, A. K., Biankin, A. V., and Biden, T. J. (2007) *Diabetologia* **50**, 752-763

98. Kaufman, R. J. (2002) *J Clin Invest* **110**, 1389-1398

99. Ozcan, U., Yilmaz, E., Ozcan, L., Furuhashi, M., Vaillancourt, E., Smith, R. O., Gorgun, C. Z., and Hotamisligil, G. S. (2006) *Science* **313**, 1137-1140

100. Forner, F., Kumar, C., Luber, C. A., Fromme, T., Klingenspor, M., and Mann, M. (2009) *Cell Metab* **10**, 324-335

101. Pagliarini, D. J., Calvo, S. E., Chang, B., Sheth, S. A., Vafai, S. B., Ong, S. E., Walford, G. A., Sugiana, C., Boneh, A., Chen, W. K., Hill, D. E., Vidal, M., Evans, J. G., Thorburn, D. R., Carr, S. A., and Mootha, V. K. (2008) *Cell* **134**, 112-123

102. Wilson-Fritch, L., Burkart, A., Bell, G., Mendelson, K., Leszyk, J., Nicoloro, S., Czech, M., and Corvera, S. (2003) *Mol Cell Biol* **23**, 1085-1094

103. McBride, H. M., Neuspiel, M., and Wasiak, S. (2006) *Curr Biol* **16**, R551-560

104. Ernster, L., and Schatz, G. (1981) *J Cell Biol* **91**, 227s-255s

105. Shadel, G. S., and Clayton, D. A. (1997) *Annu Rev Biochem* **66**, 409-435

106. Larsson, N. G., and Clayton, D. A. (1995) *Annu Rev Genet* **29**, 151-178

107. Winder, W. W., and Hardie, D. G. (1999) *Am J Physiol* **277**, E1-10

108. Counago, R., and Shamoo, Y. (2005) *Extremophiles* **9**, 135-144

109. Konrad, M. (1993) *J Biol Chem* **268**, 11326-11334

110. Miron, S., Munier-Lehmann, H., and Craescu, C. T. (2004) *Biochemistry* **43**, 67-77

111. Dzeja, P. P., and Terzic, A. (2003) *J Exp Biol* **206**, 2039-2047

112. Khoo, J. C., and Russell, P. J. (1972) *Biochim Biophys Acta* **268**, 98-101

113. Tanabe, T., Yamada, M., Noma, T., Kajii, T., and Nakazawa, A. (1993) *J Biochem* **113**, 200-207

114. Janssen, E., de Groof, A., Wijers, M., Fransen, J., Dzeja, P. P., Terzic, A., and Wieringa, B. (2003) *J Biol Chem* **278**, 12937-12945

115. Janssen, E., Dzeja, P. P., Oerlemans, F., Simonetti, A. W., Heerschap, A., de Haan, A., Rush, P. S., Terjung, R. R., Wieringa, B., and Terzic, A. (2000) *EMBO J* **19**, 6371-6381

116. Dzeja, P. P., Vitkevicius, K. T., Redfield, M. M., Burnett, J. C., and Terzic, A. (1999) *Circ Res* **84**, 1137-1143

117. Hancock, C. R., Janssen, E., and Terjung, R. L. (2005) *Am J Physiol Cell Physiol* **288**, C1287-1297

118. Hittel, D. S., Hathout, Y., Hoffman, E. P., and Houmard, J. A. (2005) *Diabetes* **54**, 1283-1288

119. Kishi, F., Tanizawa, Y., and Nakazawa, A. (1987) *J Biol Chem* **262**, 11785-11789

120. Noma, T., Song, S., Yoon, Y. S., Tanaka, S., and Nakazawa, A. (1998) *Biochim Biophys Acta* **1395**, 34-39

121. Liu, R., Strom, A. L., Zhai, J., Gal, J., Bao, S., Gong, W., and Zhu, H. (2009) *Int J Biochem Cell Biol* **41**, 1371-1380

122. Tomasselli, A. G., Schirmer, R. H., and Noda, L. H. (1979) *Eur J Biochem* **93**, 257-262

123. Gellerich, F. N. (1992) *FEBS Lett* **297**, 55-58

124. Fujisawa, K., Murakami, R., Horiguchi, T., and Noma, T. (2009) *Comp Biochem Physiol B Biochem Mol Biol*

125. Lagresle-Peyrou, C., Six, E. M., Picard, C., Rieux-Laucat, F., Michel, V., Ditadi, A., Demerens-de Chappedelaine, C., Morillon, E., Valensi, F., Simon-Stoos, K. L., Mullikin, J. C., Noroski, L. M., Besse, C., Wulffraat, N. M., Ferster, A., Abecasis, M. M., Calvo, F., Petit, C., Candotti, F., Abel, L., Fischer, A., and Cavazzana-Calvo, M. (2009) *Nat Genet* **41**, 106-111

126. Pannicke, U., Honig, M., Hess, I., Friesen, C., Holzmann, K., Rump, E. M., Barth, T. F., Rojewski, M. T., Schulz, A., Boehm, T., Friedrich, W., and Schwarz, K. (2009) *Nat Genet* **41**, 101-105

127. Basseri, S., Lhotak, S., Sharma, A. M., and Austin, R. C. (2009) *J Lipid Res* **50**, 2486-2501

128. Koh, E. H., Park, J. Y., Park, H. S., Jeon, M. J., Ryu, J. W., Kim, M., Kim, S. Y., Kim, M. S., Kim, S. W., Park, I. S., Youn, J. H., and Lee, K. U. (2007) *Diabetes* **56**, 2973-2981

129. Vance, J. E. (1990) *J Biol Chem* **265**, 7248-7256

130. Rusinol, A. E., Cui, Z., Chen, M. H., and Vance, J. E. (1994) *J Biol Chem* **269**, 27494-27502

131. Rizzuto, R., Duchen, M. R., and Pozzan, T. (2004) *Sci STKE* **2004**, re1

132. Csordas, G., Renken, C., Varnai, P., Walter, L., Weaver, D., Buttle, K. F., Balla, T., Mannella, C. A., and Hajnoczky, G. (2006) *J Cell Biol* **174**, 915-921

133. Clairmont, C. A., De Maio, A., and Hirschberg, C. B. (1992) *J Biol Chem* **267**, 3983-3990

134. Arita, Y., Kihara, S., Ouchi, N., Takahashi, M., Maeda, K., Miyagawa, J., Hotta, K., Shimomura, I., Nakamura, T., Miyaoka, K., Kuriyama, H., Nishida, M., Yamashita, S., Okubo, K., Matsubara, K., Muraguchi, M., Ohmoto, Y., Funahashi, T., and Matsuzawa, Y. (1999) *Biochem Biophys Res Commun* **257**, 79-83

135. Pajvani, U. B., Hawkins, M., Combs, T. P., Rajala, M. W., Doebber, T., Berger, J. P., Wagner, J. A., Wu, M., Knopps, A., Xiang, A. H., Utzschneider, K. M., Kahn, S. E., Olefsky, J. M., Buchanan, T. A., and Scherer, P. E. (2004) *J Biol Chem* **279**, 12152-12162

136. Combs, T. P., Wagner, J. A., Berger, J., Doebber, T., Wang, W. J., Zhang, B. B., Tanen, M., Berg, A. H., O'Rahilly, S., Savage, D. B., Chatterjee, K., Weiss, S., Larson, P. J., Gottesdiener, K. M., Gertz, B. J., Charron, M. J., Scherer, P. E., and Moller, D. E. (2002) *Endocrinology* **143**, 998-1007

137. Tu, B. P., Ho-Schleyer, S. C., Travers, K. J., and Weissman, J. S. (2000) *Science* **290**, 1571-1574

138. Harding, H. P., Calfon, M., Urano, F., Novoa, I., and Ron, D. (2002) *Annu Rev Cell Dev Biol* **18**, 575-599

139. Patil, C., and Walter, P. (2001) *Curr Opin Cell Biol* **13**, 349-355

140. Schroder, M., and Kaufman, R. J. (2005) *Annu Rev Biochem* **74**, 739-789

141. Allen, J. R., Nguyen, L. X., Sargent, K. E., Lipson, K. L., Hackett, A., and Urano, F. (2004) *Biochem Biophys Res Commun* **324**, 166-170

142. Scheuner, D., Vander Mierde, D., Song, B., Flamez, D., Creemers, J. W., Tsukamoto, K., Ribick, M., Schuit, F. C., and Kaufman, R. J. (2005) *Nat Med* **11**, 757-764

143. Gass, J. N., Gifford, N. M., and Brewer, J. W. (2002) *J Biol Chem* **277**, 49047-49054

144. Scarpulla, R. C. (2008) *Physiol Rev* **88**, 611-638

145. Shi, X., Burkart, A., Nicoloro, S. M., Czech, M. P., Straubhaar, J., and Corvera, S. (2008) *J Biol Chem* **283**, 30658-30667

146. Miner, J. L. (2004) *J Anim Sci* **82**, 935-941

147. Kim, S., and Moustaid-Moussa, N. (2000) *J Nutr* **130**, 3110S-3115S

148. Hoffstedt, J., Arvidsson, E., Sjolin, E., Wahlen, K., and Arner, P. (2004) *J Clin Endocrinol Metab* **89**, 1391-1396

149. Powelka, A. M., Seth, A., Virbasius, J. V., Kiskinis, E., Nicoloro, S. M., Guilherme, A., Tang, X., Straubhaar, J., Cherniack, A. D., Parker, M. G., and Czech, M. P. (2006) *J Clin Invest* **116**, 125-136

150. Calfon, M., Zeng, H., Urano, F., Till, J. H., Hubbard, S. R., Harding, H. P., Clark, S. G., and Ron, D. (2002) *Nature* **415**, 92-96

151. Wang, X. Z., Lawson, B., Brewer, J. W., Zinszner, H., Sanjay, A., Mi, L. J., Boorstein, R., Kreibich, G., Hendershot, L. M., and Ron, D. (1996) *Mol Cell Biol* **16**, 4273-4280

152. Carlson, S. G., Fawcett, T. W., Bartlett, J. D., Bernier, M., and Holbrook, N. J. (1993) *Mol Cell Biol* **13**, 4736-4744

153. Habinowski, S. A., and Witters, L. A. (2001) *Biochem Biophys Res Commun* **286**, 852-856

154. Tirosh, B., Iwakoshi, N. N., Glimcher, L. H., and Ploegh, H. L. (2005) *J Exp Med* **202**, 505-516

155. Mora, S., and Pessin, J. E. (2002) *Diabetes Metab Res Rev* **18**, 345-356

156. Sevier, C. S., and Kaiser, C. A. (2008) *Biochim Biophys Acta* **1783**, 549-556

157. Gess, B., Hofbauer, K. H., Wenger, R. H., Lohaus, C., Meyer, H. E., and Kurtz, A. (2003) *Eur J Biochem* **270**, 2228-2235

158. Kwong, J. Q., Henning, M. S., Starkov, A. A., and Manfredi, G. (2007) *J Cell Biol* **179**, 1163-1177

159. Harding, H. P., Zeng, H., Zhang, Y., Jungries, R., Chung, P., Plesken, H., Sabatini, D. D., and Ron, D. (2001) *Mol Cell* **7**, 1153-1163

160. Wieser, W., and Krumschnabel, G. (2001) *Biochem J* **355**, 389-395

161. Buttgereit, F., and Brand, M. D. (1995) *Biochem J* **312 (Pt 1)**, 163-167

162. Dorner, A. J., and Kaufman, R. J. (1994) *Biologicals* **22**, 103-112
163. Livak, K. J., and Schmittgen, T. D. (2001) *Methods* **25**, 402-408
164. Gentleman, R. C., Carey, V. J., Bates, D. M., Bolstad, B., Dettling, M., Dudoit, S., Ellis, B., Gautier, L., Ge, Y., Gentry, J., Hornik, K., Hothorn, T., Huber, W., Iacus, S., Irizarry, R., Leisch, F., Li, C., Maechler, M., Rossini, A. J., Sawitzki, G., Smith, C., Smyth, G., Tierney, L., Yang, J. Y., and Zhang, J. (2004) *Genome Biol* **5**, R80
165. Bolstad, B. M., Irizarry, R. A., Astrand, M., and Speed, T. P. (2003) *Bioinformatics* **19**, 185-193
166. Lelliott, C., and Vidal-Puig, A. J. (2004) *Int J Obes Relat Metab Disord* **28 Suppl 4**, S22-28
167. Sharma, S., Adrogue, J. V., Golfman, L., Uray, I., Lemm, J., Youker, K., Noon, G. P., Frazier, O. H., and Taegtmeyer, H. (2004) *Faseb J* **18**, 1692-1700
168. Stumvoll, M., Goldstein, B. J., and van Haeften, T. W. (2005) *Lancet* **365**, 1333-1346
169. Unger, R. H. (2002) *Annu Rev Med* **53**, 319-336
170. Brand, M. D., and Curtis, R. K. (2002) *Biochem Soc Trans* **30**, 25-30
171. Hardie, D. G., and Carling, D. (1997) *Eur J Biochem* **246**, 259-273
172. Hardie, D. G. (2004) *J Cell Sci* **117**, 5479-5487
173. Jessen, N., and Goodyear, L. J. (2005) *J Appl Physiol* **99**, 330-337
174. Musi, N., Yu, H., and Goodyear, L. J. (2003) *Biochem Soc Trans* **31**, 191-195
175. Kahn, B. B., Alquier, T., Carling, D., and Hardie, D. G. (2005) *Cell Metab* **1**, 15-25
176. LaFramboise, W. A., Guthrie, R. D., Scalise, D., Elborne, V., Bombach, K. L., Armanious, C. S., and Magovern, J. A. (2003) *J Mol Cell Cardiol* **35**, 1307-1318
177. Fukami-Kobayashi, K., Nosaka, M., Nakazawa, A., and Go, M. (1996) *FEBS Lett* **385**, 214-220
178. Noma, T. (2005) *J Med Invest* **52**, 127-136
179. Van Rompay, A. R., Johansson, M., and Karlsson, A. (1999) *Eur J Biochem* **261**, 509-517
180. Nobumoto, M., Yamada, M., Song, S., Inouye, S., and Nakazawa, A. (1998) *J Biochem* **123**, 128-135
181. Single, B., Leist, M., and Nicotera, P. (1998) *Cell Death Differ* **5**, 1001-1003
182. Kohler, C., Gahm, A., Noma, T., Nakazawa, A., Orrenius, S., and Zhivotovsky, B. (1999) *FEBS Lett* **447**, 10-12
183. Samali, A., Cai, J., Zhivotovsky, B., Jones, D. P., and Orrenius, S. (1999) *EMBO J* **18**, 2040-2048
184. Lee, H. J., Pyo, J. O., Oh, Y., Kim, H. J., Hong, S. H., Jeon, Y. J., Kim, H., Cho, D. H., Woo, H. N., Song, S., Nam, J. H., Kim, K. S., and Jung, Y. K. (2007) *Nat Cell Biol* **9**, 1303-1310
185. Koh, H. J., Brandauer, J., and Goodyear, L. J. (2008) *Curr Opin Clin Nutr Metab Care* **11**, 227-232
186. Towler, M. C., and Hardie, D. G. (2007) *Circ Res* **100**, 328-341
187. Osler, M. E., and Zierath, J. R. (2008) *Endocrinology* **149**, 935-941

188. McLeod, L. E., and Proud, C. G. (2002) *FEBS Lett* **531**, 448-452
189. Pizzo, P., and Pozzan, T. (2007) *Trends Cell Biol* **17**, 511-517
190. Kamimura, D., and Bevan, M. J. (2008) *J Immunol* **181**, 5433-5441
191. Sabourin, L. A., Girgis-Gabardo, A., Seale, P., Asakura, A., and Rudnicki, M. A. (1999) *J Cell Biol* **144**, 631-643
192. Detimary, P., Jonas, J. C., and Henquin, J. C. (1995) *J Clin Invest* **96**, 1738-1745
193. Zambelli, A., Mongiardini, E., Villegas, S. N., Carri, N. G., Boot-Handford, R. P., and Wallis, G. A. (2005) *Cell Biol Int* **29**, 647-653
194. Masaki, T., Yoshida, M., and Noguchi, S. (1999) *Biochem Biophys Res Commun* **261**, 350-356
195. Sha, H., He, Y., Chen, H., Wang, C., Zenno, A., Shi, H., Yang, X., Zhang, X., and Qi, L. (2009) *Cell Metab* **9**, 556-564
196. Lim, J. H., Lee, H. J., Ho Jung, M., and Song, J. (2009) *Cell Signal* **21**, 169-177
197. Maher, J. C., Krishan, A., and Lampidis, T. J. (2004) *Cancer Chemother Pharmacol* **53**, 116-122
198. Kang, H. T., and Hwang, E. S. (2006) *Life Sci* **78**, 1392-1399
199. Kerbey, A. L., Randle, P. J., Cooper, R. H., Whitehouse, S., Pask, H. T., and Denton, R. M. (1976) *Biochem J* **154**, 327-348
200. Joshi, S., and Huang, Y. G. (1991) *Biochim Biophys Acta* **1067**, 255-258
201. Heifetz, A., Keenan, R. W., and Elbein, A. D. (1979) *Biochemistry* **18**, 2186-2192
202. Thastrup, O., Cullen, P. J., Drobak, B. K., Hanley, M. R., and Dawson, A. P. (1990) *Proc Natl Acad Sci U S A* **87**, 2466-2470
203. Beaver, J. P., and Waring, P. (1996) *Cell Death Differ* **3**, 415-424
204. Vercesi, A. E., Moreno, S. N., Bernardes, C. F., Meinicke, A. R., Fernandes, E. C., and Docampo, R. (1993) *J Biol Chem* **268**, 8564-8568
205. Hom, J. R., Gewandter, J. S., Michael, L., Sheu, S. S., and Yoon, Y. (2007) *J Cell Physiol* **212**, 498-508
206. Cleland, W. W. (1964) *Biochemistry* **3**, 480-482
207. Fujiwara, T., Oda, K., Yokota, S., Takatsuki, A., and Ikehara, Y. (1988) *J Biol Chem* **263**, 18545-18552
208. Beller, M., Sztalryd, C., Southall, N., Bell, M., Jackle, H., Auld, D. S., and Oliver, B. (2008) *PLoS Biol* **6**, e292
209. Kallen, K. J., Quinn, P., and Allan, D. (1993) *Biochem J* **289 (Pt 1)**, 307-312
210. Wood, S. A., and Brown, W. J. (1992) *J Cell Biol* **119**, 273-285
211. Lippincott-Schwartz, J., Yuan, L., Tipper, C., Amherdt, M., Orci, L., and Klausner, R. D. (1991) *Cell* **67**, 601-616
212. Wei, J., Gaut, J. R., and Hendershot, L. M. (1995) *J Biol Chem* **270**, 26677-26682
213. Vidal, V., Qiu, N. H., Redfield, B., Carlino, A., Brot, N., and Weissbach, H. (1996) *Arch Biochem Biophys* **330**, 314-318
214. Ataullakhanov, F. I., and Vitvitsky, V. M. (2002) *Biosci Rep* **22**, 501-511
215. Fukasawa, M., Nishijima, M., and Hanada, K. (1999) *J Cell Biol* **144**, 673-685
216. Schnapp, B. J. (2003) *J Cell Sci* **116**, 2125-2135
217. Johnson, K. A. (1985) *Annu Rev Biophys Biophys Chem* **14**, 161-188
218. Kirkland, R. A., and Franklin, J. L. (2007) *Exp Neurol* **204**, 458-461

219. Brennan, J. P., Southworth, R., Medina, R. A., Davidson, S. M., Duchen, M. R., and Shattock, M. J. (2006) *Cardiovasc Res* **72**, 313-321

220. He, S., Yaung, J., Kim, Y. H., Barron, E., Ryan, S. J., and Hinton, D. R. (2008) *Graefes Arch Clin Exp Ophthalmol* **246**, 677-683

221. Xue, X., Piao, J. H., Nakajima, A., Sakon-Komazawa, S., Kojima, Y., Mori, K., Yagita, H., Okumura, K., Harding, H., and Nakano, H. (2005) *J Biol Chem* **280**, 33917-33925

222. Fels, D. R., Ye, J., Segan, A. T., Kridel, S. J., Spiotto, M., Olson, M., Koong, A. C., and Koumenis, C. (2008) *Cancer Res* **68**, 9323-9330

223. Elouil, H., Bensellam, M., Guiot, Y., Vander Mierde, D., Pascal, S. M., Schuit, F. C., and Jonas, J. C. (2007) *Diabetologia* **50**, 1442-1452

224. Urano, F., Wang, X., Bertolotti, A., Zhang, Y., Chung, P., Harding, H. P., and Ron, D. (2000) *Science* **287**, 664-666

225. Nishitoh, H., Saitoh, M., Mochida, Y., Takeda, K., Nakano, H., Rothe, M., Miyazono, K., and Ichijo, H. (1998) *Mol Cell* **2**, 389-395

226. Nishitoh, H., Matsuzawa, A., Tobiume, K., Saegusa, K., Takeda, K., Inoue, K., Hori, S., Kakizuka, A., and Ichijo, H. (2002) *Genes Dev* **16**, 1345-1355

227. Luo, D., He, Y., Zhang, H., Yu, L., Chen, H., Xu, Z., Tang, S., Urano, F., and Min, W. (2008) *J Biol Chem* **283**, 11905-11912

228. Gu, F., Nguyen, D. T., Stuible, M., Dube, N., Tremblay, M. L., and Chevet, E. (2004) *J Biol Chem* **279**, 49689-49693

229. Zhang, P., McGrath, B. C., Reinert, J., Olsen, D. S., Lei, L., Gill, S., Wek, S. A., Vattem, K. M., Wek, R. C., Kimball, S. R., Jefferson, L. S., and Cavener, D. R. (2002) *Mol Cell Biol* **22**, 6681-6688

230. Iwakoshi, N. N., Lee, A. H., and Glimcher, L. H. (2003) *Immunol Rev* **194**, 29-38

231. Shinkai, Y., Rathbun, G., Lam, K. P., Oltz, E. M., Stewart, V., Mendelsohn, M., Charron, J., Datta, M., Young, F., Stall, A. M., and et al. (1992) *Cell* **68**, 855-867

232. Imamura, H., Nhat, K. P., Togawa, H., Saito, K., Iino, R., Kato-Yamada, Y., Nagai, T., and Noji, H. (2009) *Proc Natl Acad Sci U S A* **106**, 15651-15656

233. Berg, J., Hung, Y. P., and Yellen, G. (2009) *Nat Methods* **6**, 161-166

234. Matsuura, S., Igarashi, M., Tanizawa, Y., Yamada, M., Kishi, F., Kajii, T., Fujii, H., Miwa, S., Sakurai, M., and Nakazawa, A. (1989) *J Biol Chem* **264**, 10148-10155

235. Zhou, J., Liu, C. Y., Back, S. H., Clark, R. L., Peisach, D., Xu, Z., and Kaufman, R. J. (2006) *Proc Natl Acad Sci U S A* **103**, 14343-14348

236. Rutkowski, D. T., Arnold, S. M., Miller, C. N., Wu, J., Li, J., Gunnison, K. M., Mori, K., Sadighi Akha, A. A., Raden, D., and Kaufman, R. J. (2006) *PLoS Biol* **4**, e374

237. Glembotski, C. C. (2007) *Circ Res* **101**, 975-984

238. Hosogai, N., Fukuhara, A., Oshima, K., Miyata, Y., Tanaka, S., Segawa, K., Furukawa, S., Tochino, Y., Komuro, R., Matsuda, M., and Shimomura, I. (2007) *Diabetes* **56**, 901-911

239. Hori, O., Ichinoda, F., Tamatani, T., Yamaguchi, A., Sato, N., Ozawa, K., Kitao, Y., Miyazaki, M., Harding, H. P., Ron, D., Tohyama, M., D, M. S., and Ogawa, S. (2002) *J Cell Biol* **157**, 1151-1160

240. Klier, H., Magdolen, V., Schricker, R., Strobel, G., Lottspeich, F., and Bandlow, W. (1996) *Biochim Biophys Acta* **1280**, 251-256

241. Oishi, K., Okano, H., and Sawa, H. (2007) *J Cell Biol* **179**, 1149-1162

242. Brand, M. D. (2005) *Biochem Soc Trans* **33**, 897-904

243. Tanabe, T., Yamada, M., Noma, T., Kajii, T., and Nakazawa, A. (1993) *J Biochem (Tokyo)* **113**, 200-207

244. Barnes, B. R., Glund, S., Long, Y. C., Hjalm, G., Andersson, L., and Zierath, J. R. (2005) *Faseb J* **19**, 773-779

245. Barnes, B. R., Marklund, S., Steiler, T. L., Walter, M., Hjalm, G., Amarger, V., Mahlapuu, M., Leng, Y., Johansson, C., Galuska, D., Lindgren, K., Abrink, M., Stapleton, D., Zierath, J. R., and Andersson, L. (2004) *J Biol Chem* **279**, 38441-38447

246. Lee, W. J., Kim, M., Park, H. S., Kim, H. S., Jeon, M. J., Oh, K. S., Koh, E. H., Won, J. C., Kim, M. S., Oh, G. T., Yoon, M., Lee, K. U., and Park, J. Y. (2006) *Biochem Biophys Res Commun* **340**, 291-295

247. Hardie, D. G., Scott, J. W., Pan, D. A., and Hudson, E. R. (2003) *FEBS Lett* **546**, 113-120

248. Kemp, B. E., Mitchelhill, K. I., Stapleton, D., Michell, B. J., Chen, Z. P., and Witters, L. A. (1999) *Trends Biochem Sci* **24**, 22-25

249. Kanehisa, M., Goto, S., Kawashima, S., and Nakaya, A. (2002) *Nucleic Acids Res* **30**, 42-46

250. Yu, H., Hirshman, M. F., Fujii, N., Pomerleau, J. M., Peter, L. E., and Goodyear, L. J. (2006) *Am J Physiol Endocrinol Metab* **291**, E557-565

251. Nilsson, E. C., Long, Y. C., Martinsson, S., Glund, S., Garcia-Roves, P., Svensson, L. T., Andersson, L., Zierath, J. R., and Mahlapuu, M. (2006) *J Biol Chem* **281**, 7244-7252

252. Mahlapuu, M., Johansson, C., Lindgren, K., Hjalm, G., Barnes, B. R., Krook, A., Zierath, J. R., Andersson, L., and Marklund, S. (2004) *Am J Physiol Endocrinol Metab* **286**, E194-200

253. Nilsson, E. C., Long, Y. C., Martinsson, S., Glund, S., Garcia-Roves, P., Svensson, L. T., Andersson, L., Zierath, J. R., and Mahlapuu, M. (2006) *J Biol Chem* **281**, 7244-7252

254. Carrasco, A. J., Dzeja, P. P., Alekseev, A. E., Pucar, D., Zingman, L. V., Abraham, M. R., Hodgson, D., Bienengraeber, M., Puceat, M., Janssen, E., Wieringa, B., and Terzic, A. (2001) *Proc Natl Acad Sci U S A* **98**, 7623-7628

255. Janssen, E., Terzic, A., Wieringa, B., and Dzeja, P. P. (2003) *J Biol Chem* **278**, 30441-30449

256. Hancock, C. R., Janssen, E., and Terjung, R. L. (2005) *J Appl Physiol*

257. Vergun, O., and Reynolds, I. J. (2004) *Biophys J* **87**, 3585-3593

258. Rudra, D., and Warner, J. R. (2004) *Genes Dev* **18**, 2431-2436

259. Reiling, J. H., and Sabatini, D. M. (2006) *Oncogene* **25**, 6373-6383

260. Sarbassov, D. D., Ali, S. M., and Sabatini, D. M. (2005) *Curr Opin Cell Biol* **17**, 596-603

261. Bergeron, R., Ren, J. M., Cadman, K. S., Moore, I. K., Perret, P., Pypaert, M., Young, L. H., Semenkovich, C. F., and Shulman, G. I. (2001) *Am J Physiol Endocrinol Metab* **281**, E1340-1346

262. Zong, H., Ren, J. M., Young, L. H., Pypaert, M., Mu, J., Birnbaum, M. J., and Shulman, G. I. (2002) *Proc Natl Acad Sci U S A* **99**, 15983-15987

263. Bouchard, C., and Tremblay, A. (1997) *J Nutr* **127**, 943S-947S

264. Inouye, S., Yamada, Y., Miura, K., Suzuki, H., Kawata, K., Shinoda, K., and Nakazawa, A. (1999) *Biochem Biophys Res Commun* **254**, 618-622

APPENDIX I

A MITOCHONDRIAL RESPONSE TO THE UPR VIA TRANSLATIONAL CONTROL MECHANISMS

The following data includes unpublished results.

2-D PAGE analysis was performed by the Proteomic Fractionation Core Facility. John Leszyk performed the mass spectrometry analysis. I performed the remaining experiments contained within this appendix.

Summary

When the protein folding capacity of the ER is exceeded, it triggers signaling pathways that increase chaperone levels and diminish protein secretory load. Here we find that ER stress brings about remodeling of mitochondria through differential effects on translation of mitochondria specific proteins. While translation of most cellular proteins is attenuated, translation of a set of soluble mitochondrial proteins is either unaffected or increased in response to ER stress. One of these proteins is adenylate kinase 2 (AK2), an enzyme localized to the mitochondrial intermembrane space that catalyzes the reversible reaction AMP+ATP⇔2ADP. An active cross-communication between ER function and mitochondrial energy homeostatic pathways could explain the link between ER stress and immune, neurodegenerative, endocrine and cardiovascular pathologies which are also associated with mitochondrial dysfunction.

Background

As discussed previously, the ER must adapt to acute and chronic changes in secretory protein load. Three known signaling pathways are triggered by ER stress, the PERK, ATF6, and IRE1 pathways (138,140,235). Together they initiate an adaptive response that decreases protein secretory load and enhances chaperone biosynthesis, known as the UPR (Unfolded Protein Response). PERK is a transmembrane kinase that phosphorylates eIF2α, resulting in the suppression of general protein translation. ATF6 is proteolytically processed into an active transcription factor that induces genes involved in endoplasmic reticulum folding. IRE1 is an ER membrane-spanning, bi-functional

kinase/site-specific endoribonuclease that catalyzes XBP1 mRNA splicing, generating a stable mRNA product (sXBP1) from which the transcription factor XBP1 is translated. ER stress simultaneously induces pro-apoptotic signals such as JNK activation (224), and the ultimate fate of cells undergoing ER stress appears to depend on their ability to sustain adaptive UPR signaling while mitigating pro-apoptotic signaling (14,75,236). The strength of UPR signaling, particularly that of IRE1, influences cell fate in response to ER stress (75), but the mechanisms that determine the duration and magnitude of the UPR are not known. These mechanisms are important as, in a physiological context, unresolved ER stress is linked to multiple human pathologies (19,75).

An essential feature of the UPR is the increased synthesis of ER chaperones. ER chaperones bind and release folding intermediates in a manner coupled to ATP hydrolysis. Thus, adequate ER function must involve both a sufficient number of chaperones and an ATP supply that maximizes chaperone function. Consistent with the notion that adequate energy metabolism is important for normal ER function are observations that ischemia, which is associated with reduced nutrient delivery and decreased ATP production, affects several features of the ER stress response both in brain and in myocardium (237). In obesity, adipose tissue displays evidence of enhanced PERK activity (96), which may represent altered ER stress resulting from obesity related hypoxia (238). While these results are suggestive, the precise molecular links between ER physiological function and cellular energy metabolic status are unknown.

In order to better define the relationship between energy homeostasis and ER stress, we conducted experiments in 3T3-L1 adipocytes, which recapitulate many

characteristics of primary adipose cells, including triglyceride storage, glucose transport and insulin sensitivity. A specific, major function of adipocytes is to secrete adiponectin, a 247 amino acid polypetide that undergoes extensive folding to form a trimer stabilized through disulfide bonds (8,9). High molecular weight complexes of trimeric adiponectin are formed and secreted into the circulation, reaching concentrations of 10-20 ug/ml, suggesting that adiponectin secretion comprises a substantial load on the adipocyte ER. Interestingly, a robust increase in mitochondrial biogenesis occurs within this period (Figure 2-1B and (102)), making the differentiating adipocyte an excellent model system to study the potential interplay between energy homeostatic mechanisms and ER function.

Results

As previously shown, adiponectin secretion by 3T3-L1 adipocytes begins at day 4 of differentiation (Figure 2.1C), and the levels of key proteins of the UPR, including BiP ERO1α, increase in parallel (Figure 2.2B). Thus, differentiation is accompanied by a robust induction of the ER folding pathways, probably reflective of compensating UPR induction, and of mitochondrial biogenesis (Figure 2.1B and (102)).

In order to understand the UPR in 3T3-L1 adipocytes, we used tunicamycin, thapsigargin, and brefeldin A, all previously shown to induce ER stress in other cell types. One of the immediate responses to ER stress is the phosphorylation of the protein translation initiation factor eIF2α by PERK. Exposure of cells to all three of the chemicals resulted in global inhibition of translation, reflected as a decrease in [^{35}S]-

methionine labeling of proteins in whole cell extracts (Figure I.1A). However, in response to tunicamycin, which is a much more specific activator of ER stress, we noted a pronounced and consistent increase in $[^{35}S]$-methionine labeling of a band of the apparent molecular weight of ~25 kDa as well as smaller increases in several other bands (Figure I.1A, arrows) seen over the background of the globally decreased $[^{35}S]$-methionine labeling. Increased labeling of this ~25 kDa band was detected within 30 minutes of addition of tunicamycin, and was evident at very low levels of the inhibitor (Figure I.1B and C). Further fractionation of the crude extract revealed that this band co-purified with mitochondria (Figure I.1D).
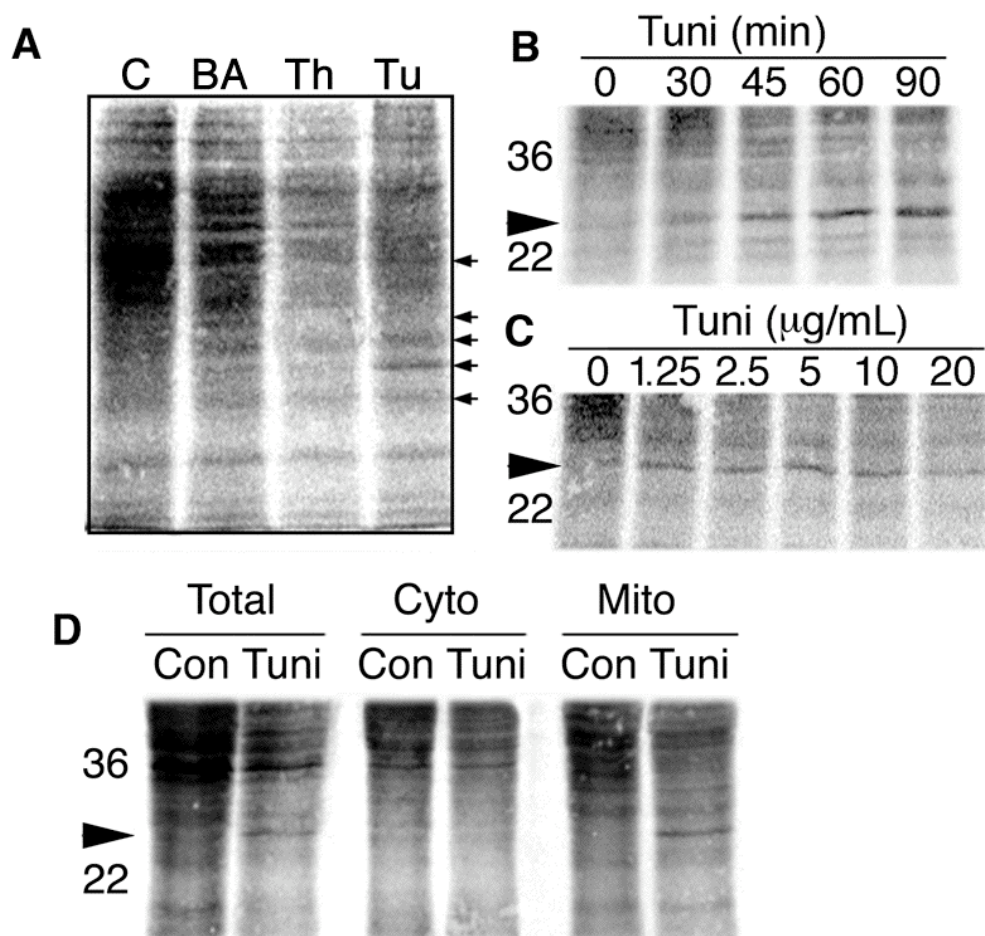
Figure I.1: Paradoxical enhancement of a (^{35}S)-methionine band during the UPR.

A. Duplicate wells of 3T3-L1 adipocytes were exposed to brefeldin A (BA), thapsigargin (Th) or tunicamycin (Tu) and pulsed with [^{35}S]-methionine for 30 minutes. Cell lysates were analyzed by SDS-PAGE gels and phosphoimaging. Arrows indicate the enhanced incorporation of radioactivity into protein bands. B. Time course of the ~25 kDa band expression with tunicamycin (Tuni) treatment. C. Dose dependency of the ~25 kDa band expression with tunicamycin (Tuni) treatment. D. Co-purification of ~25 kDa band with the crude mitochondrial (Mito) fraction and not with the cytosolic (Cyto) fraction from control (Con) and tunicamycin (Tuni) treated cells. Results are from one representative experiment, which was confirmed 3 times.

This finding prompted us to analyze the effects of tunicamycin on turnover of mitochondrial proteins in more detail. To ensure that the effects seen were due to changes in translation, and not transcriptional responses to ER stress that could alter mitochondrial composition (239), cells were treated for 60 minutes with actinomycin D to inhibit transcription prior to exposure to tunicamycin for 2 hours. Cells were then pulsed for 30 minutes with [^{35}S]-methionine, and soluble proteins from purified mitochondria were analyzed by 2D gel electrophoresis. Gels were transferred to nitrocellulose filters, which were exposed to phosphorimager screen to estimate [^{35}S]-methionine incorporation (Figure I.2A and B, green color). The blots were then stained to visualize total protein amounts in specific spots (Figure I.2A and B, red color). The overlap of the two signals reflects the extent of [^{35}S]-methionine incorporation relative to total protein, where yellow to green reflects higher and red to yellow lower incorporation rates. Three results are evident from this experiment; first, that the basal turnover rate of soluble mitochondrial proteins is very variable, with some high abundance proteins displaying very little [^{35}S]-methionine incorporation (Figure I.2A, red spots), and proteins of low abundance displaying the largest incorporation of [^{35}S]-methionine (Figure I.2A, green spots), revealing very rapid turnover. Second, that the predominant effect of tunicamycin is to decrease translation, reflected by decrease in [^{35}S]-methionine incorporation into proteins of high turnover. And third, that several proteins escape translational repression in response to tunicamycin, reflected by increased [^{35}S]-methionine incorporation (green spots in Figure I.2B).

Figure I.2: Tunicamycin affects translation of soluble mitochondrial proteins.

3T3-L1 adipocytes were treated with actinomycin D and then without (A) or with (B) tunicamycin (+Tuni) and labeled with [^{35}S]-methionine. Mitochondria were purified, soluble proteins extracted with sodium carbonate, and separated on pH 4 to 7 isoelectric focusing strips followed by PAGE. Gels were transferred to nitrocellulose filters, which were exposed to reveal [^{35}S]-methionine incorporation (^{35}S, green signal) and stained to reveal total protein levels (Sypro, red signal. Results are from one representative experiment, which was confirmed 3 times.

To better identify those proteins that escape translational repression, we compared the patterns of [^{35}S]-methionine incorporation in control cells (Figure I.3A, blue) with those seen in tunicamycin-treated cells (Figure I.3A, red). Visual inspection of the overlapped filters reveals those proteins that are highly sensitive to translational inhibition (blue spots), and also those that escape inhibition (purple spots) or are enhanced in response to tunicamycin (red spots). A quantitative analysis of this experiment, in which the relative volume of each spot from the control or tunicamycin treated samples are compared (Figure I.3B and C), reveals that translation of approximately ~6 % of the spots detected is stimulated (increased by more than 2-fold) in response to the drug. To explore the functional relevance of this subset of proteins, we proceeded to identify by mass spectrometry a prominent series of spots with isoelectric points around pH 7, in the region between 25-30 kDa, which were stimulated in their [^{35}S]-methionine incorporation in response to tunicamycin (Figure 1.3C, rectangle).
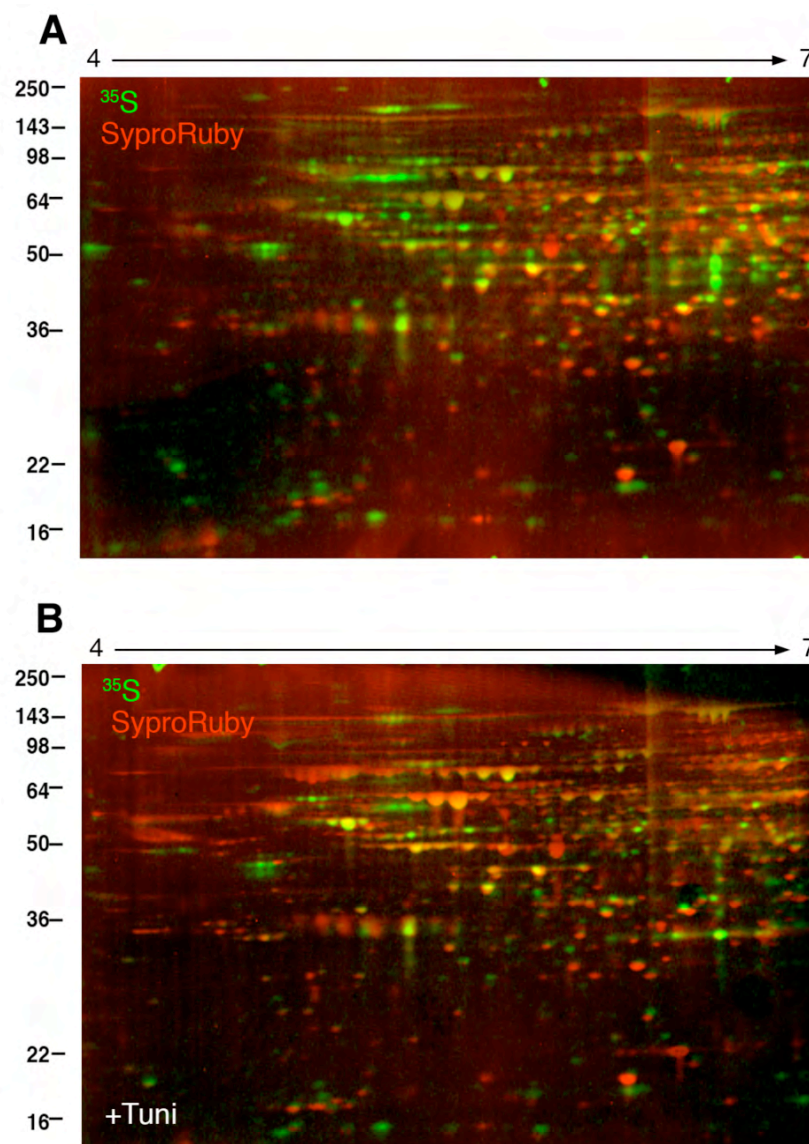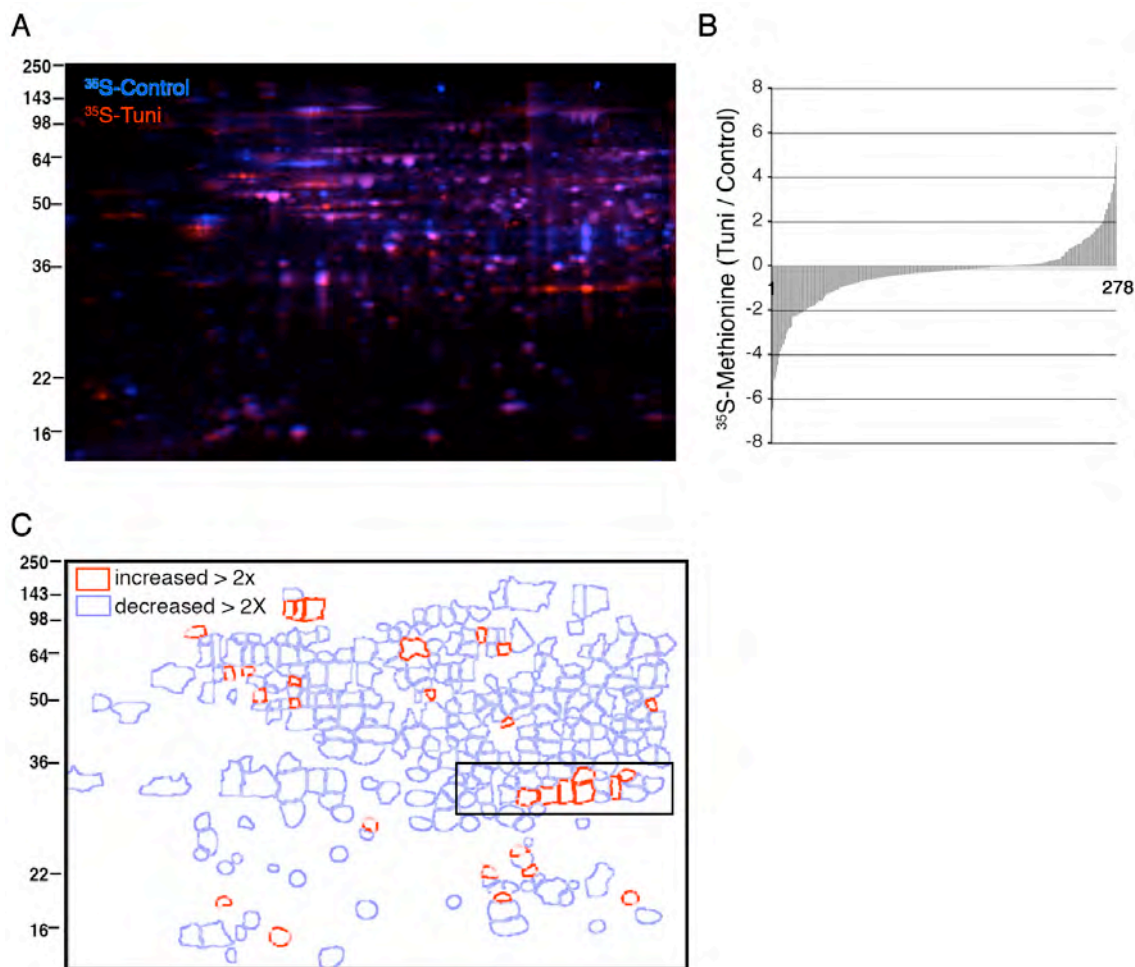
Figure I.3: Effects of tunicamycin of translation of soluble mitochondrial proteins.

3T3-L1 adipocytes were treated with actinomycin D and then without or with tunicamycin and labeled with [^{35}S]-methionine. Mitochondria were purified, soluble proteins extracted with sodium carbonate, and separated on pH 4 to 7 isoelectric focusing strips followed by PAGE. Gels were transferred to nitrocellulose filters, which were exposed to reveal [^{35}S]-methionine incorporation A. Overlapped images of [^{35}S]-methionine incorporation from untreated (^{35}S-control, blue signal) and tunicamycin treated (^{35}S-Tuni, red signal) samples. B. Ratio of [^{35}S]-methionine incorporation into 278 spots identified in samples from tunicamycin-treated cells relative to controls. C. Outlines of identified spots, where blue outlines represent decreased and red outlines increased [^{35}S]-methionine incorporation in response to tunicamycin. Rectangle indicates region subjected to further analysis by mass spectrometry. Results are from one representative experiment, which was confirmed 3 times.

These results suggest that the translation of mRNAs encoding for at least some mitochondrial proteins is controlled in response to ER stress in ways that prevent translational inhibition, and/or enhances translation. Furthermore, this response may be relevant for the overall cellular response to such stress. To further explore this hypothesis, we proceeded to identify those proteins that fail to respond to tunicamycin with decreased [^{35}S]-methionine incorporation, and characterize their function in relation to ER stress. These proteins were identified by comparison of the ratio of SyproRuby staining and [^{35}S]-methionine incorporation under control (Figure I.4A, top panel) and tunicamycin-treated (Figure I.4A, bottom panel) conditions. Amongst the most salient of these (more yellow or red in Figure I-4 bottom panel compared to top panel) were a series of protein spots with isoelectric points around pH 7, in the region between 25-30 kDa. These were excised from gels run in parallel, and analyzed by Mass spectrometry (Figure I.4A). From these, peptides corresponding to two proteins, adenylate kinase 2 (gi: 34328230) and a hypothetical protein of unknown function (gi: 31560255) that corresponds to a mitochondrial protein (101) were reproducibly detected.
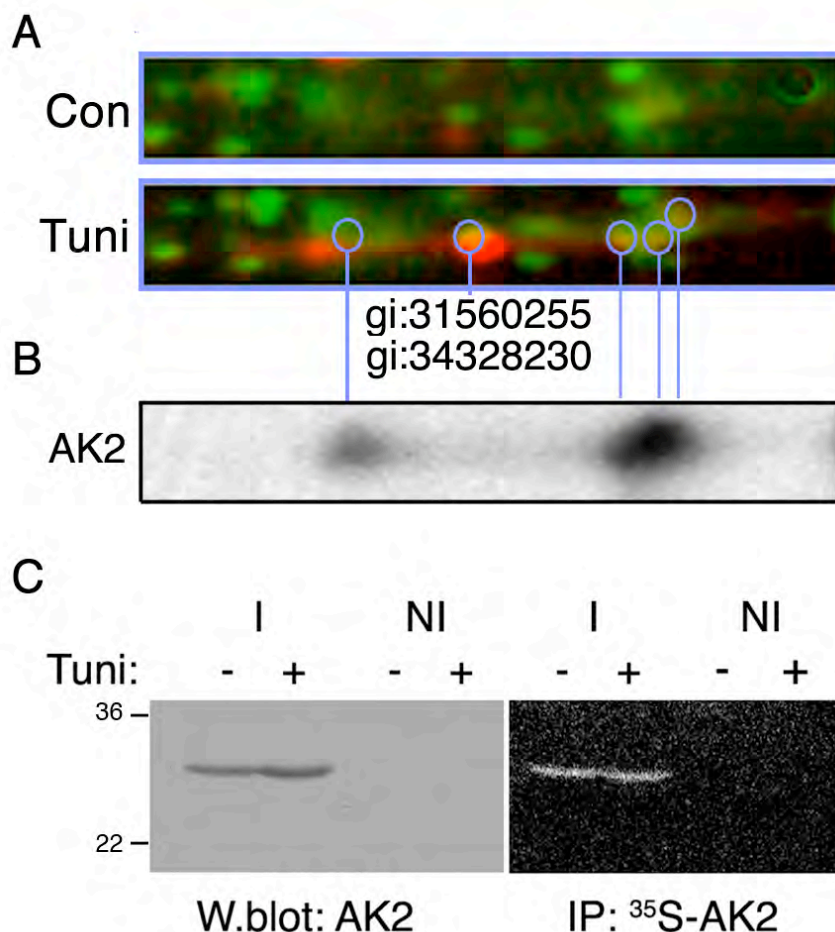
Figure I.4: Identification of proteins that escape translational suppression.

A. 3T3-L1 adipocytes were treated with actinomycin D and then tunicamycin followed by labeling with [^{35}S]-methionine. Soluble mitochondrial proteins were separated in parallel 2D gels, one was stained (green signal) and one transferred to nitrocellulose for subsequent exposure to reveal [^{35}S]-methionine incorporation (red signal). The overlapped images were used to identify spots corresponding to proteins displaying unchanged or enhanced [^{35}S]-methionine incorporation in response to tunicamycin (red or yellow spots). Blue circles indicate the regions subjected to excision and mass spectrometry, and the corresponding gene identifier numbers of the proteins identified. B. Western blot of AK2 performed on the nitrocellulose filter, demonstrating correspondence with the identified protein. C. Immunoprecipitation with AK2 specific (I) or non-immune (NI) rabbit antibodies from cells treated as above without (-) or with (+) tunicamycin and labeled with [^{35}S]-methionine, followed by western blot analysis and exposure to phosphorimager screens.

Western blot analysis confirmed that AK2 indeed corresponded to several of the spots of interest (Figure I.4B), and immunoprecipitation experiments with antibodies to AK2 confirmed that AK2 escapes translational attenuation during ER stress (Figure 1.4C). The heterogeneous mobility of yeast adenylate kinase on isoelectric focusing gels has been previously noted (240), but the biochemical basis for this altered mobility is unclear.

The other protein identified, gi: 31560255, is a hypothetical mammalian protein identified in a mitochondrial proteomic screen (101). It is a homolog to the *C. elegans* protein RMD-1, which has been shown to associate with microtubules (241). Depletion of this protein impairs mitotic chromosome segregation. Western blot analysis with an antibody generated against this protein showed co-localization with one of the identified spots (Figure I.5). Further analysis is required to determine whether this protein escapes the translational block induced by tunicamycin. In addition, further confirmation of its mitochondrial localization as well as the function of this protein may provide insight into why it is alternatively regulated.
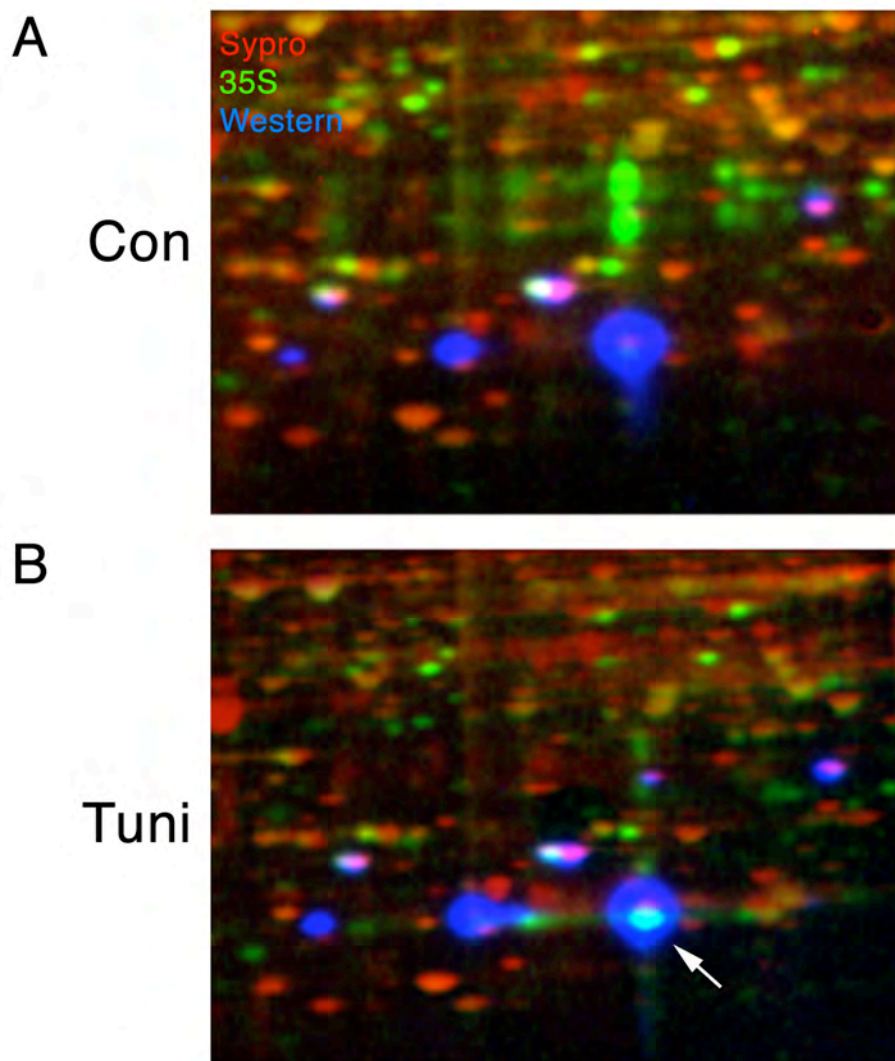
Figure I.5: Co-localization of gi: 31560255 with translationally upregulated spot.

3T3-L1 adipocytes were treated with actinomycin D and then without (A) or with (B) tunicamycin followed by labeling with [^{35}S]-methionine. Soluble mitochondrial proteins were separated in parallel 2D gels, one was stained (red signal) and one transferred to nitrocellulose for subsequent exposure to reveal [^{35}S]-methionine incorporation (green signal). The overlapped images were used to identify spots corresponding to proteins displaying unchanged or enhanced [^{35}S]-methionine incorporation in response to tunicamycin (green or yellow spots). Western blot analysis of gi: 31560255 was performed on the nitrocellulose filter, demonstrating co-localization of the identified protein (blue spots) with the spot subjected to excision (arrow).

Conclusions

AK2 is a member of an ancient family of proteins (EC. 2.7.4.3), present from bacteria to humans, that catalyze the reversible reaction ATP+AMP⇔2ADP. The function of AK is classically described to be the maintenance of a constant concentration and fixed ratio of adenine nucleotides, and the single isoform of adenylate kinase present in bacteria and lower eukaryotes is essential for life, underscoring the crucial biological relevance of adenine nucleotide interconversion (108-110). The findings reported here demonstrate that AK2 protein levels can be acutely regulated by posttranscriptional control mechanisms, revealing a new level of regulation for these essential kinases. While these results are consistent with previous findings that show that the levels of AK2 protein are not predictable from mRNA levels (120), they are first to directly demonstrate translational control in an acute setting. More work is needed to determine which if any of the many known molecular mechanisms that control translation operate on AKs. In addition more work is required to determine whether the regulation of AKs is a universal feature of cells that undergo chronic ER stress, and to determine whether it plays a role in cellular adaptation. In addition, several proteins that separated with a soluble mitochondrial fraction were shown to escape the translational attenuation elicited by tunicamycin. The identity and function of these proteins may provide insight into the cellular response to ER stress. The results shown here suggest that this translational regulation and the affected proteins will be important new targets of investigation.

Experimental Procedures

Reagents: Chicken IgY against AK2 was generated by immunization with full-length purified mouse AK2. Rabbit IgG against the protein encoded by gi: 31560255 was generated by immunization with a C-terminal peptide.

Cell Culture: All cells were obtained from American Type Culture Collection and grown under 10% CO_2 and cultured in Dulbecco modified Eagle medium (DMEM) supplemented with 10% fetal bovine serum (FBS), 100 U of penicillin/ml, and 100 µg of streptomycin/ml which was replaced every 48 hours unless otherwise stated. 3T3-L1 cells were grown on 150-mm dishes. Three days after reaching confluence (day 0), media was replaced with culture media containing a differentiation cocktail consisting of 0.5 mM 3-isobutyl-1-methylxanthine (Sigma), 0.25 µM dexamethasone (Sigma), and 1 µM insulin (Sigma). 72 hours later (day 3) media was replaced with culture media, which was replaced every 48 hours. Experiments were performed with day 7 cells. Other treatments were as follows: 17 µM brefeldin A for 2 hours, 2 µM Thapsigargin, 6 µM tunicamycin for 2 hours or as indicated, and 2 µg/mL actinomycin D for 1 hour prior to tunicamycin treatment.

[^{35}S]-Methionine Incorporation: Cells were fed 24 hours prior to the experiment, and were treated as described in each figure legend. Cells were then pulsed with 50 µCi/mL ^{35}S Methionine/Cysteine for 30 minutes, rinsed twice in phosphate-buffered saline and once in isolation buffer (250 mM sucrose, 0.5 mM EGTA, 5 mM HEPES; pH 7.4), and

homogenized by 7 passages through a 27-gauge needle. Homogenates were centrifuged at 500xg for 10 minutes. The postnuclear supernatant was centrifuged at 18,000xg for 25 minutes. An aliquot of the supernatant (cytosolic fraction) was taken for analysis. The pellet was resuspended in 20% sucrose in isolation buffer and centrifuged at 18,000xg for 30 minutes. The pellet was resuspended in 60% sucrose (in 10 mM Tris with 0.05 mM EDTA) for further processing. The suspension was overlaid with a 53% sucrose layer (in 10 mM Tris with 0.05 mM EDTA) and a 44% sucrose layer (in 10 mM Tris with 0.05 mM EDTA). The sucrose step gradient was centrifuged at 141,000xg for 2 hours. The purified mitochondria settled at the 44-53% sucrose interface. The mitochondrial layer was removed, diluted in isolation buffer, and centrifuged at 18,000xg for 30 minutes. The mitochondrial pellet was suspended in 200 µl of 100 mM sodium carbonate pH 11, vortexed and centrifuged at 288,000xg for 10 minutes. The solubilized proteins were prepared for 2D analysis.

2D Gel Analysis: Samples were acetone-precipitated and solubilized in 40 mM Tris, 7 M urea, 2 M thiourea, and 2% CHAPS, reduced with tributylphosphine, and alkylated with 10 mM acrylamide for 90 minutes at room temperature. After a second round of acetone precipitation, the pellet was solubilized in 7 M urea, 2 M thiourea, and 2% CHAPS (resuspension buffer), and the buffer was run through a 10 kDa cutoff Amicon Ultra device with at least 2 volumes of the resuspension buffer to reduce the conductivity of the sample. Seventy-five micrograms of protein were subjected to isoelectric focusing (IEF) on 11 cm pH 4 to 7 immobilized pH gradient strips (Proteome Systems, Sydney, NSW,

Australia). After IEF, immobilized pH gradient strips were equilibrated in 6 M urea, 2% sodium dodecyl sulfate (SDS), 50 mM Tris-acetate buffer, pH 7.0, and 0.01% bromphenol blue and subjected to SDS-PAGE on 6 to 15% Gel Chips (Proteome Systems). Gels were electroblotted onto nitrocellulose, or fixed and stained in SYPRO Ruby (Invitrogen). Blots were exposed to phosphorimager screens followed by SYPRO Ruby staining. Spot detection, matching, background subtraction, and normalization analysis of all images was performed using Progenesis Discovery software (Nonlinear Dynamics Inc., Newcastle upon Tyne, UK).

Mass Spectrometry: Spots excised from polyacrylamide gels were digested in-gel with trypsin. Analysis was performed on a Kratos Axima QIT (Shimadzu Instruments) matrix-assisted-laser desorption/ionization time-of-flight (MALDI-TOF) mass spectrometer. Peptides were analyzed in positive ion mode in mid-mass range (700-3000 Da). The instrument was externally calibrated with Angiotensin II (MH+ of 1046.54), P14R (MH+ of 1533.86) and ACTH clip 18-39 (MH+ of 2465.20). Precursors were selected based on signal intensity at a mass resolution width of 250 for CID fragmentation (MS/MS) using Argon as the collision gas. All spectra were peak processed with Mascot Distiller (Matrix Sciences, Ltd.) prior to database searching. Database searches were performed in house with the Mascot search engine (Matrix Sciences, Ltd.). For MS searches the Peptide Mass Fingerprint program was used with a peptide mass tolerance of 50 ppm. For MS/MS searches (CID spectra) the MS/MS Ion Search program was used with a Precursor tolerance of 50 ppm and a fragment tolerance of 0.5 Da.

Immunoblot Analysis: The membranes were blocked with 5% nonfat-milk in Tris-buffered saline (TBS) with 0.1% Tween and incubated with primary antibodies overnight. They were then incubated with anti-chicken IgY or anti-rabbit IgG horseradish peroxidase conjugated antibodies (Sigma) and detected using enhanced chemiluminescence (Perkin Elmer Life Sciences, Inc.).

APPENDIX II

ENHANCED OXIDATIVE METABOLISM AND RESISTANCE TO OBESITY IN RESPONSE TO ADENYLATE KINASE 1 DEPLETION

The following data includes unpublished results and Affymetrix gene chip data taken from:

Nilsson EC, Long YC, Martinsson S, Glund S, Garcia-Roves P, Svensson LT, Andersson L, Zierath JR & Mahlapuu M (2006) Opposite transcriptional regulation in skeletal muscle of AMP-activated protein kinase gamma3 R225Q transgenic versus knock-out mice. *J Biol Chem* 281, 7244–7252.

Femke Streijger fed the animals and aided in the dissections. I performed microarray analysis experiments on wild type and AK1$^{-/-}$ muscle. The core facility performed the genechip hybridization and Juerg Straubhaar performed the statistical analysis on the resulting data. I performed the remaining experiments contained within this appendix.

Summary

Energy expenditure in live organisms is determined by the amount of work performed and by the efficiencies with which ATP is produced and used for such work. Imbalances in nutrient availability and energy expenditure lead to obesity and associated co-morbidities. Thus, understanding the molecular mechanisms that control energy expenditure is important. The enzyme adenylate kinase 1 (AK1) has been found to influence the efficiency of ATP utilization during muscle contraction. In Chapter 3, we found that deletion of AK1 in primary myotubes results in enhanced glucose transport and oxygen consumption, suggesting that increased oxidative metabolism is elicited as a compensatory response to inefficient ATP utilization resulting from AK1 depletion. Here we find this effect is relevant *in vivo*, as AK1$^{-/-}$ mice are resistant to fat accumulation induced by a high fat diet. Moreover, expression of genes of oxidative metabolism and ATP synthesis is increased in muscles from AK1$^{-/-}$ mice, and genes involved in ribosome synthesis are decreased. Similarities with other perturbations that enhance oxidative metabolism, such as a mutation in the muscle-specific γ3 subunit of AMP-activated protein kinase, are seen throughout the expressed genome of AK1$^{-/-}$ mouse muscle. These results indicate that AK1 can play an important role in controlling muscle and whole body energy homeostasis, and point to the AK family of enzymes as novel potential sites of both dysfunction and therapeutic intervention in metabolic disease.

Background

Obesity and its many associated co-morbidities are caused by an imbalance between food intake and energy expenditure (166-169). Addressing this problem requires an understanding of the mechanisms by which fuel consumption, energy production, and energy utilization are coordinated. In single cells energy production in the form of adenine nucleotides ATP and ADP is tightly coupled with energy utilization for motility or anabolic processes (242). Even in cells that have acute high-energy requirements, such as skeletal and cardiac myocytes and neurons, ATP synthesis is highly coordinated with ATP utilization, such that the steady state levels of ATP remain constant over a wide range of workloads. In these cells, carbohydrate or lipid fuels are channeled to mitochondria for oxidative phosphorylation, where ATP is primarily synthesized, and this process is enhanced dramatically in response to increased ATP utilization.

Among the important molecular mechanisms by which energy flux is regulated in single cells are enzymatic activities that utilize, are regulated by, or alter the levels of adenine nucleotides. For example, an increase in the AMP/ATP ratio ensuing from enhanced ATP utilization is sensed by AMP-activated protein kinase (AMPK), which then triggers an increase in fuel consumption that facilitates the restoration of ATP levels (171-175). In addition, AMPK activation results in decreased energy expenditure by minimizing the activity of anabolic pathways.

An enzyme that influences adenine nucleotide levels is adenylate kinase (AK), which catalyzes the reversible phosphoryl transfer reaction AMP + ATP $\Leftrightarrow$ 2ADP. AK is present in organisms from bacteria to humans, and its single isoform in lower eukayotes

is essential for survival. The human genome encodes for 9 genes bearing similarity to AK that differ in cellular and subcellular distribution. AK1 is responsible for over 95% of AK activity in skeletal muscle (243). AK has been thought to provide the principal homeostatic mechanism to maintain proper levels of adenine nucleotide under various metabolic states. It has also been proposed that via phosphotransfer networks, AK channels ATP from sites of ATP production to sites of utilization (111).

Given the importance of AK activity, and the fact that AK1 is by far the predominant AK activity in muscle, it was rather surprising that mice lacking AK1 are seemingly normal (114,115,117). They are able to maintain normal levels of ATP and show similar muscular capability as wild type mice. They do display enhanced ATP synthesis during muscle contraction, indicating more ATP was generated to maintain normal contractility (114,115). These results suggest that compensatory mechanisms are elicited in these mice to adapt to the lack of this enzyme. These results are consistent with a proposed role of adenylate kinase to of improve the efficiency of ATP utilization in cells through the operation of phosphotransfer networks (111), or other yet unknown mechanisms.

To better define the compensatory mechanisms by which AK1 deficiency leads to increased ATP production, and whether the effects of AK1 depletion in muscle are sufficient to impact whole body metabolism, we have analyzed the phenotype of $AK1^{-/-}$ mice on a high fat diet. Here, we find that $AK1^{-/-}$ mice are protected from fat accumulation. This protection is likely to be due to enhanced oxidative metabolism *in vivo*, as genes in the pathways of oxidative metabolism are increased in muscles from

these mice. Interestingly, changes throughout the expressed genome of muscles from AK1$^{-/-}$ mice are highly concordant with those induced by a dominant mutation in the γ3 subunit of AMP kinase (Prkag3^{R225Q} mice), a condition in which fuel utilization and work performance are maximized (244,245), and discordant with mice lacking the γ3 gene. Thus, alterations in AK1 have a highly significant rapid effect on energy metabolism, and the compensatory changes elicited by changes in AK1 levels resemble those produced by changes in AMPK, a central regulator of energy balance (171-175). This work points to the adenylate kinases as novel potential sites of dysfunction and/or intervention in obesity and other metabolic diseases.

Results

We have shown that AK1 depletion rapidly enhances basal glucose uptake and oxygen consumption in differentiated primary myotubes, suggesting that AK1 depletion enhances oxidative metabolism to increase ATP production (Figure 3.11). To determine whether the metabolic changes elicited by AK1 depletion at the cellular level would translate into changes in whole body fuel metabolism, AK1$^{-/-}$ mice were fed either normal diet or high fat diet for 18 weeks. The average body weight of AK1$^{-/-}$ mice on a normal diet was higher than that of wild type controls (Figure II.1A, left panel), but the size of the epididymal fat pads were comparable (Figure II.1A, right panel). This tendency towards a more lean whole body mass was more apparent upon high fat feeding, where the total body weight of AK1$^{-/-}$ mice and their wild type littermates were not significantly

different (Figure II.1B, left panel), but the degree of adiposity in the AK1$^{-/-}$ mice was

significantly lower than that of the wild type littermates (Figure II.1B, right panel).
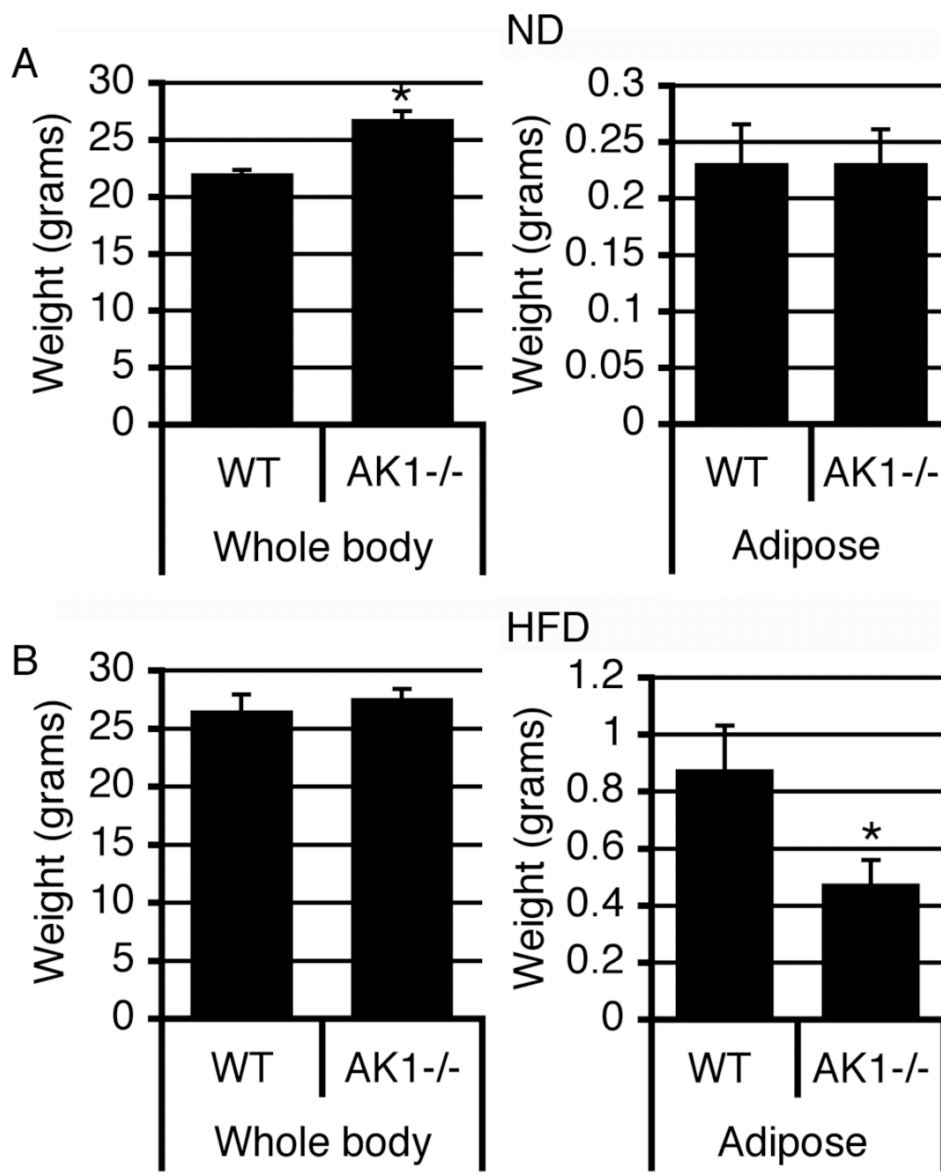
Figure II.1: Response of the AK1^{-/-} mice to high fat feeding.

A. Whole body weight (left) and isolated epididymal adipose tissue weight (right) in grams (n=9) of AK1$^{-/-}$ mice and wild type controls (WT) fed normal diet (ND). B. Whole body weight (left) and isolated epididymal adipose tissue weight (right) in grams (n=9) of WT and AK1$^{-/-}$ fed a high fat diet for 18 weeks (HFD).

Consistent with the observed differences in adiposity, the serum leptin levels of the wild type mice increased about 6-fold while those of the AK1$^{-/-}$ mice only increased around 3-fold in response to the high fat diet (Figure II.2A). The attenuation of fat depot expansion appears to be due to decreased lipid accumulation per cell, as the average lipid droplet size of isolated adipocytes from wild type mice was significantly larger than that from AK1$^{-/-}$ mice when animals were exposed to a high fat diet (Figure II.2B and C). While further phenotyping needs to be performed to determine the basis for the differences in lean body mass between the AK1$^{-/-}$ and wild type animals, our results are consistent with a protection from lipid accumulation in response to changes in muscle oxidative metabolism elicited by AK1 depletion.
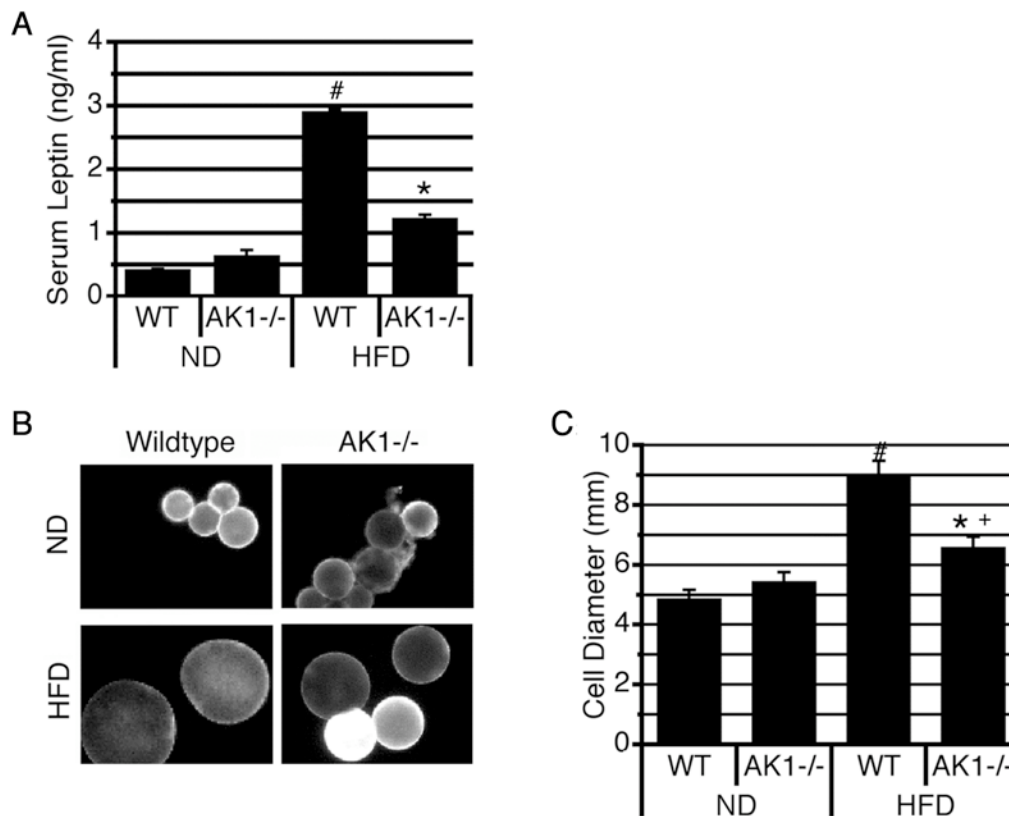
Figure II.2: Response of the AK1$^{-/-}$ mouse adipose to high fat feeding.

A. Leptin values in serum from WT and AK1$^{-/-}$ animals fed ND or HFD for 18 weeks (n=9). B. Isolated adipocytes from WT and AK1$^{-/-}$ stained with anti-perilipin antibody. C. Cell diameter in millimeters (n=14). * indicates $p<0.05$ between WT and AK1$^{-/-}$ by paired 2-tailed Student t-test. # indicates $p<0.05$ between WT ND and WT HFD by paired 2-tailed Student t-test. + indicates $p<0.050$ between AK1$^{-/-}$ ND and AK1$^{-/-}$ HFD by paired 2-tailed Student t-test.

To further test the hypothesis that AK1 depletion leads to enhanced muscle oxidative metabolism *in vivo*, we analyzed the global changes in gene expression that accompany AK1 deletion, and compared them with alterations induced by changes in AMP-sensitive protein kinase (AMPK), which is a central regulator of energy metabolism (107,171,172,246-248).

Of the 45037 probes present in the MOE430-2 Affymetrix GeneChip, 865 were significantly ($p<0.05$) upregulated by more than 10% in muscles from AK1^{-/-} mice compared to controls (range 1.1 – 7.8 fold). Of these, 245 probes had annotations in KEGG (Kyoto Encyclopedia of Genes and Genomes) (249), and were significantly annotated to 36 pathways, shown in Table II.1. The most significantly represented metabolic pathways were that of oxidative phosphorylation, ATP synthesis, and glycolysis/gluconeogenesis. These changes are consistent with an increase in steady-state fuel utilization in response to AK1 deficiency, and with the previously reported increase in glycolytic flux in muscles from AK1^{-/-} mice (114,115). Significant downregulation of 1619 probes also occurred in the AK1^{-/-} muscle. Of these, 276 probes were annotated to 44 KEGG pathways, the most salient being the ribosomal pathway (Table II.1).

TABLE 1			
INCREASED in AK1^{-/-}		DECREASED in AK1^{-/-}	
KEGG Pathway	P value	KEGG Pathway	P value
Oxidative phosphorylation	6.28E-16	Ribosome	< 2.22e-16
ECM-receptor interaction	6.17E-11	MAPK signaling pathway	3.62E-14
Focal adhesion	2.62E-10	Wnt signaling pathway	3.77E-14
ATP synthesis	6.25E-07	Cell cycle	1.43E-11
Glycolysis / Gluconeogenesis	1.82E-06	Phosphatidylinositol signaling system	1.81E-10
MAPK signaling pathway	3.65E-05	Huntington's disease	2.19E-10
Carbon fixation	0.00013477	Calcium signaling pathway	1.69E-08
Pentose phosphate pathway	0.00020791	Insulin signaling pathway	1.70E-08
Starch and sucrose metabolism	0.00021868	Basal transcription factors	6.67E-08
Valine, leucine and isoleucine degradation	0.00046573	Inositol phosphate metabolism	6.80E-08
Fatty acid metabolism	0.00049936	TGF-beta signaling pathway	3.25E-07
gamma-Hexachlorocyclohexane degradation	0.00062564	Benzoate degradation via CoA ligation	4.30E-06
TGF-beta signaling pathway	0.00080461	Neurodegenerative Disorders	8.41E-06
Cell adhesion molecules (CAMs)	0.00103084	Adipocytokine signaling pathway	1.17E-05
Adherens junction	0.00173257	Adherens junction	3.56E-05
Glutathione metabolism	0.00195161	Notch signaling pathway	8.59E-05
Butanoate metabolism	0.00410956	DNA polymerase	9.52E-05
Nitrogen metabolism	0.00566353	Nicotinate and nicotinamide metabolism	0.00033866
Tight junction	0.006045	Alzheimer's disease	0.00044752
Nucleotide sugars metabolism	0.00639769	Toll-like receptor signaling pathway	0.00053714
Pentose and glucuronate interconversions	0.00718602	Glutathione metabolism	0.00113208
Gap junction	0.00775716	Valine, leucine and isoleucine degradation	0.00141952
Cyanoamino acid metabolism	0.0105907	Jak-STAT signaling pathway	0.00156384
Hematopoietic cell lineage	0.01137075	Tryptophan metabolism	0.00169053
Adipocytokine signaling pathway	0.01256125	Aminoacyl-tRNA synthetases	0.00237739
Ubiquinone biosynthesis	0.01778983	Glycine, serine and threonine metabolism	0.00346765
Riboflavin metabolism	0.01963987	Gap junction	0.00347963
Glycine, serine and threonine metabolism	0.02820949	B cell receptor signaling pathway	0.0053048
Valine, leucine and isoleucine biosynthesis	0.02975211	Glycerophospholipid metabolism	0.00554265
Glycerophospholipid metabolism	0.03433134	Purine metabolism	0.00704883
Regulation of actin	0.0383473	Protein export	0.00857957

cytoskeleton			
Purine metabolism	0.03934515	Butanoate metabolism	0.01112014
Lysine degradation	0.03975178	Focal adhesion	0.01369923
Cytokine-cytokine receptor interaction	0.04076289	Parkinson's disease	0.0141911
Toll-like receptor signaling pathway	0.04263423	Regulation of actin cytoskeleton	0.01481001
Pyruvate metabolism	0.0474699	Urea cycle and metabolism of amino groups	0.01528664
		Apoptosis	0.01710462
		Porphyrin and chlorophyll metabolism	0.01761754
		Alkaloid biosynthesis II	0.01761754
		Circadian rhythm	0.02146565
		Valine, leucine and isoleucine biosynthesis	0.02370443
		Androgen and estrogen metabolism	0.02725566
		T cell receptor signaling pathway	0.03377148

Table II.1: Pathways analysis in response to AK1 knockout.

Affymetrix GeneChip databases were obtained as described in Materials and Methods. Analysis was performed using annotations in KEGG to determine significantly enriched pathways. Pathways listed are significantly populated by genes that increase or decrease in response to AK1 knockout.

Transgenic expression of a mutation in the muscle-specific, gamma regulatory subunit of AMPK (TgPrkag3^{225Q}) (244,245,250-252) elicits increased fat oxidation in muscle. Analysis of published Affymetrix databases of muscle from TgPrkag3^{225Q} mice (253) revealed 299 probes that were significantly ($p < 0.05$) upregulated by more than 10% compared to non-transgenic controls (range: 1.1 - 2.36 fold). Of these, 97 probes had annotations in KEGG, to 19 pathways, of which the most significantly represented were that of oxidative phosphorylation and starch metabolism (Table II.2), consistent with the reported alterations in glycogen deposition and fat oxidation in muscles from these mice (244,245). Significant downregulation of 348 probes also occurred in TgPrkag3^{225Q} muscle. These were annotated to 11 KEGG pathways, which, like in the AK1$^{-/-}$ muscle included the ribosomal and diverse signal transduction pathways (Table II.2).

TABLE 2			
INCREASED in TgPrkag3^{225Q}		*DECREASED in TgPrkag3^{225Q}*	
KEGG Pathway	*P value*	*KEGG Pathway*	*P value*
Oxidative phosphorylation	1.59E-07	Ribosome	< 2.22e-16
Starch and sucrose metabolism	1.08E-06	DNA polymerase	6.25E-05
Nucleotide sugars metabolism	3.83E-06	TGF-beta signaling pathway	0.00011669
Pentose and glucuronate interconversions	4.75E-06	Glutathione metabolism	0.0010422
Galactose metabolism	3.27E-05	Notch signaling pathway	0.00885056
Novobiocin biosynthesis	3.65E-05	MAPK signaling pathway	0.00994324
Carbon fixation	0.00015475	Arginine and proline metabolism	0.01484344
Alkaloid biosynthesis I	0.00016692	Wnt signaling pathway	0.01855903
ATP synthesis	0.00019103	Prion disease	0.02278944
Synthesis and degradation of ketone bodies	0.00036008	Urea cycle and metabolism of amino groups	0.03587762
Arginine and proline metabolism	0.00049755	Selenoamino acid metabolism	0.04327788
Phenylalanine metabolism	0.00136156		
Phenylalanine, tyrosine and tryptophan biosynthesis	0.00163826		
Cysteine metabolism	0.0020962		
Fructose and mannose metabolism	0.00531628		
Alanine and aspartate metabolism	0.00805732		
Tyrosine metabolism	0.01017063		
Glutamate metabolism	0.01484851		
Glutathione metabolism	0.02009483		

Table II.2: Pathways analysis in response to transgenic expression of Prkag3^{225Q}.

Affymetrix GeneChip databases were obtained as described in Materials and Methods. Analysis was performed using annotations in KEGG to determine significantly enriched pathways. Pathways listed are significantly populated by genes that increase or decrease in response to transgenic expression of Prkag3^{225Q}.

When the changes induced by TgPrkag3^{225Q} were compared to those induced by AK1 knockout, a highly significant correlation (Pearson correlation 0.36; P=2.963E-14) was observed throughout the 1963 probes that were significantly altered (increased or decreased) by either perturbation (Figure II.3A). A significant correlation was maintained (Pearson correlation 0.79; P= 0.005) even when only those 225 probes that were altered by both perturbations were compared (Figure II.3B). Of the 91 probes that were increased by both TgPrkag3^{225Q} and AK1$^{-/-}$, 42 were annotated to 8 KEGG pathways, the most significant of which were oxidative phosphorylation and ATP synthesis (Table II.3). 116 probes were decreased in both TgPrkag3^{225Q} and AK1$^{-/-}$, of which 39 were annotated to 2 KEGG pathways, the ribosomal and notch signaling pathways (Table II.3). Probes reciprocally regulated in TgPrkag3^{225Q} and AK1$^{-/-}$ were not annotated to any significant KEGG pathway. Thus, the overall genetic signature produced by TgPrkag3^{225Q} is highly similar to that produced by the lack of AK1, and includes increased expression of genes of oxidative metabolism, and decreased expression of ribosome synthesis genes.
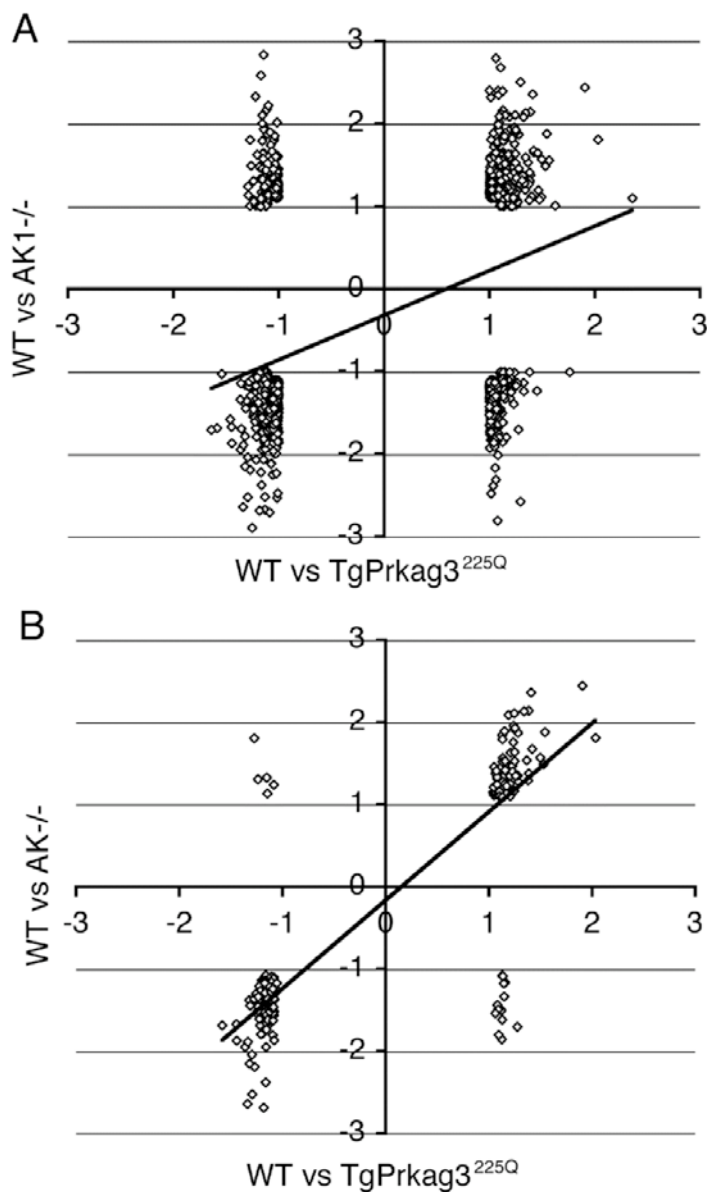
Figure II.3: Gene expression induced by AK1$^{-/-}$ or increased AMPK activation.

Gene expression analysis from mice with the AK1 deletion (AK1-/-), transgenic expression of Prkag3^{225Q} (TgPrkag3^{225Q}). Affymetrix GeneChip databases were obtained as described in Materials and Methods. A: Correlation between the 1963 genes that were significantly altered either in AK1$^{-/-}$ or in TgPrkag3^{225Q}. B: Correlation between the 255 genes significantly altered in both AK1$^{-/-}$ and TgPrkag3^{225Q}. The correlation values and statistical significance are described in the text.

TABLE 3			
INCREASED in TgPrkag3^{225Q} AND AK1$^{-/-}$		*DECREASED in TgPrkag3^{225Q} AND AK1$^{-/-}$*	
KEGG Pathway	*P value*	*KEGG Pathway*	*P value*
Oxidative phosphorylation	6.63E-07	Ribosome	2.47E-16
ATP synthesis	0.00024334	Notch signaling pathway	0.001192
Nucleotide sugars metabolism	0.00058089		
Pentose and glucuronate interconversions	0.00065688		
Starch and sucrose metabolism	0.0019398		
Galactose metabolism	0.00823947		
Pyruvate metabolism	0.02107063		
Carbon fixation	0.04715053		

Table II.3: Co-regulation by AK1 knockout and AMPK activation.

Affymetrix GeneChip databases were obtained as described in Materials and Methods. Analysis was performed using annotations in KEGG to determine significantly enriched pathways. Pathways listed are significantly populated by genes similarly regulated by both AK1 knockout and transgenic expression of Prkag3^{225Q}.

To further define the specificity of the changes induced by TgPrkag3^{225Q} and AK1$^{-/-}$, we also compared them with gene expression changes induced by the absence of the AMPK gamma 3 subunit (Prkag3$^{-/-}$), conditions in which oxidative metabolism would be expected to be impaired. Consistent with this notion, these mice displayed significant downregulation of 407 probes of which 109 were annotated to 21 KEGG pathways, the most significant of which were oxidative phosphorylation and the citric acid cycle (Table II.4). Significant upregulation of 579 probes was also seen, of which 158 were annotated to 14 pathways, which did not include major ATP-generating metabolic pathways (Table II.4).

TABLE 4			
INCREASED IN AMPKg3 -/-		*DECREASED IN AMPKg3 -/-*	
KEGG Pathway	*P value*	*KEGG Pathway*	*P value*
Ribosome	< 2.22e-16	Oxidative phosphorylation	3.76E-07
MAPK signaling pathway	0.0018499	Citrate cycle (TCA cycle)	6.90E-05
Neurodegenerative Disorders	0.0053206	Nucleotide sugars metabolism	0.00012584
Insulin signaling pathway	0.0079063	Pentose and glucuronate interconversions	0.00014855
Parkinson's disease	0.0082755	Galactose metabolism	0.00050073
Aminosugars metabolism	0.0083659	Arginine and proline metabolism	0.00067533
Valine, leucine and isoleucine degradation	0.0184083	Starch and sucrose metabolism	0.00156465
Phenylalanine, tyrosine and tryptophan biosynthesis	0.0290124	ATP synthesis	0.00206983
Glycerophospholipid metabolism	0.0311116	Carbon fixation	0.00219274
Ethylbenzene degradation	0.0364429	Novobiocin biosynthesis	0.00246121
N-Glycan degradation	0.0417588	Cyanoamino acid metabolism	0.00516133
Benzoate degradation via CoA ligation	0.0436785	Alkaloid biosynthesis I	0.00626312
Prion disease	0.0445194	Phenylalanine metabolism	0.01500918
Protein export	0.047346	Glyoxylate and dicarboxylate metabolism	0.02431501
		Phenylalanine, tyrosine and tryptophan biosynthesis	0.02644191
		Tryptophan metabolism	0.02981624
		Cysteine metabolism	0.03091156
		Methane metabolism	0.03565699
		Glycolysis / Gluconeogenesis	0.03739465
		Glycine, serine and threonine metabolism	0.04539238
		Cytokine-cytokine receptor interaction	0.04574703
		One carbon pool by folate	0.04591963

Table II.4: Pathways analysis in response to Prkag3 knockout.

Affymetrix GeneChip databases were obtained as described in Materials and Methods. Analysis was performed using annotations in KEGG to determine significantly enriched pathways. Pathways listed are significantly populated by genes that increase or decrease in response to Prkag3 knockout (Prkag3-/-).

When the changes induced in Prkag3$^{-/-}$ mice were compared to those induced in the TgPrkag3^{225Q}, a significant negative correlation (Pearson correlation -0.509; P=3.090E-09) was seen throughout the 2025 probes that were altered by either perturbation (Figure II.4A). Of the 356 probes that were both upregulated in TgPrkag3^{225Q} and downregulated in Prkag3$^{-/-}$, 110 were annotated to 24 KEGG pathways, the most significant of which was oxidative phosphorylation (Table II.5). A similar reciprocal correlation was seen in the comparison between Prkag3$^{-/-}$ and AK1$^{-/-}$ mice (Pearson correlation -0.398; P=3.553E-62) throughout 2049 probes (Figure II.4B). Of the 470 probes upregulated in the AK1$^{-/-}$ muscle and downregulated in the Prkag3$^{-/-}$ muscle, 163 were annotated to 25 KEGG pathways, of which the most significant was also oxidative phosphorylation (Table II.5). Together these results support the hypothesis that AK1 deficiency induces an increase in muscle fuel oxidation to compensate for inefficient ATP utilization.
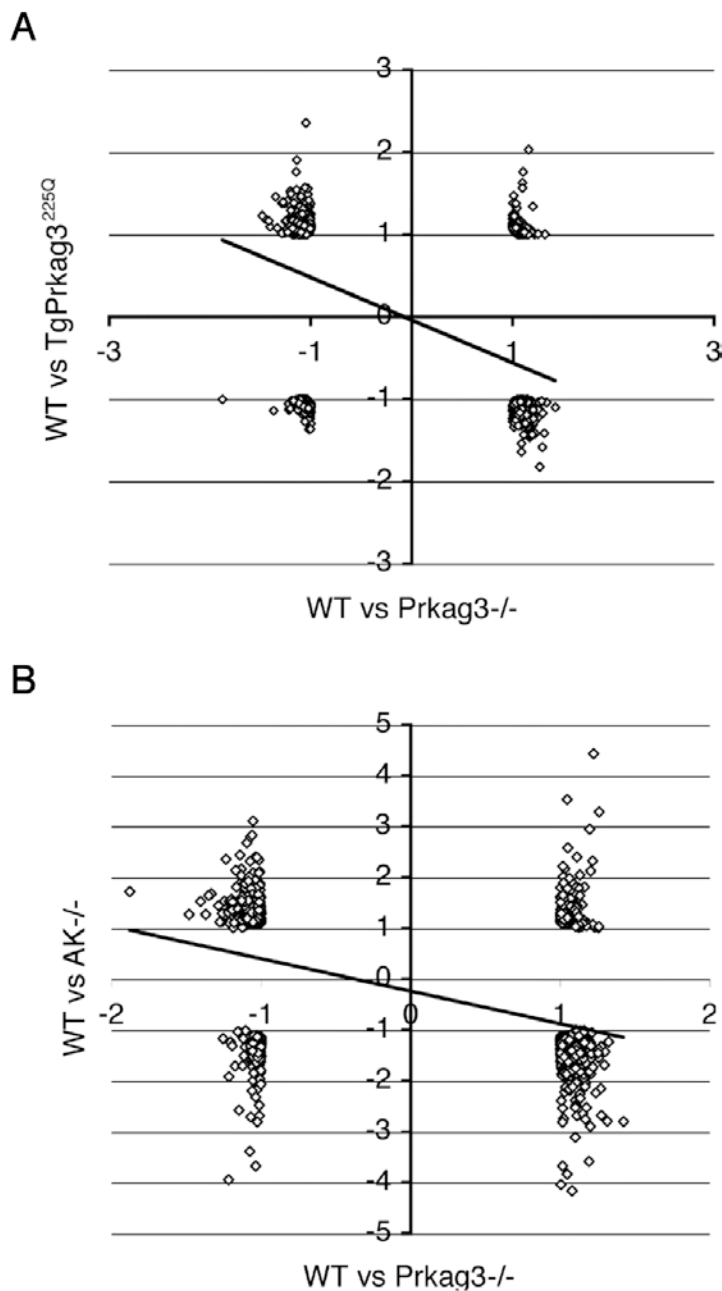
Figure II.4: Gene expression induced by AK1 deletion or altered AMPK activation.

Gene expression analysis from mice with the AK1 deletion (AK1-/-), transgenic expression of Prkag3^{225Q} (TgPrkag3^{225Q}) and Prkag3 deletion (Prkag3-/-). Affymetrix GeneChip databases were obtained as described in Materials and Methods. A. Correlation between the 2025 genes significantly altered either in TgPrkag3^{225Q} or Prkag3$^{-/-}$. B. Correlation between the 2049 genes significantly altered either in AK1$^{-/-}$ or Prkag3$^{-/-}$. The correlation values and statistical significance are described in the text.

TABLE 5			
INCREASED in TgPrkag3^{225Q} AND DECREASED in AMPKg3 -/-		INCREASED in AK1 -/- AND DECREASED in AMPKg3 -/-	
KEGG Pathway	P value	KEGG Pathway	P value
Oxidative phosphorylation	1.55E-08	Oxidative phosphorylation	1.51E-15
Starch and sucrose metabolism	2.66E-06	ECM-receptor interaction	2.66E-08
Nucleotide sugars metabolism	6.82E-06	ATP synthesis	1.63E-05
Pentose and glucuronate interconversions	8.44E-06	Carbon fixation	6.09E-05
ATP synthesis	4.26E-05	Starch and sucrose metabolism	8.93E-05
Novobiocin biosynthesis	5.17E-05	Glycolysis / Gluconeogenesis	0.0001746
Galactose metabolism	6.34E-05	Adipocytokine signaling pathway	0.00030173
Alkaloid biosynthesis I	0.00023585	Nucleotide sugars metabolism	0.00030445
Arginine and proline metabolism	0.00084883	Pentose and glucuronate interconversions	0.00035859
Phenylalanine metabolism	0.00209409	Fatty acid metabolism	0.00135669
Phenylalanine, tyrosine and tryptophan biosynthesis	0.00228838	Novobiocin biosynthesis	0.00385855
Carbon fixation	0.0026333	Focal adhesion	0.00480606
Cysteine metabolism	0.0029225	Cysteine metabolism	0.00483472
Cyanoamino acid metabolism	0.00569057	Pyruvate metabolism	0.00646492
Fructose and mannose metabolism	0.00865596	Glutathione metabolism	0.00749087
Alanine and aspartate metabolism	0.01107617	Galactose metabolism	0.00953447
Synthesis and degradation of ketone bodies	0.01116507	Alkaloid biosynthesis I	0.00974511
Tyrosine metabolism	0.01510871	Citrate cycle (TCA cycle)	0.01191082
Pyruvate metabolism	0.01703923	Arginine and proline metabolism	0.01191082
Glutamate metabolism	0.02022357	Hematopoietic cell lineage	0.01964042
Glutathione metabolism	0.02721871	Phenylalanine metabolism	0.02735982
Hematopoietic cell lineage	0.03266883	Valine, leucine and isoleucine degradation	0.03279888
Methane metabolism	0.03906596	Phenylalanine, tyrosine and tryptophan biosynthesis	0.04023578
Glycolysis / Gluconeogenesis	0.04367849	Nitrogen metabolism	0.04023578
		Purine metabolism	0.04468538

Table II.5: Reciprocal regulation upon AK1 deletion and altered AMPK activation.

Affymetrix GeneChip databases were obtained as described in Materials and Methods. Analysis was performed using annotations in KEGG to determine significantly enriched pathways. Pathways listed are significantly populated by genes reciprocally regulated by Prkag3 knockout, and either AK1 knockout or transgenic expression of Prkag3^{225Q}.

Conclusions

The adenylate kinase reaction, ATP + AMP$\Leftrightarrow$2ADP is a component of cellular phosphotransfer networks (111,254,255), and its absence has been shown to result in a decreased efficiency of ATP utilization in muscle (114,115). The results shown in this thesis reveal the importance of adenylate kinase in controlling the rate of oxidative metabolism in muscle, evidenced by the increase in glucose and oxygen consumption seen in isolated muscle cells depleted of AK1 (Figure 3.11), by the expression of genes involved in fuel oxidation in muscles from AK1$^{-/-}$ mice (Table II.1), and by the protection from fat accumulation seen in these mice (Figure II.1). This increase in metabolic pathways of fuel utilization and oxidative phosphorylation is likely to be required to compensate for the inefficiency of ATP utilization caused by the absence of AK1. This compensatory mechanism can explain the enhanced ability of AK1$^{-/-}$ muscles to sustain high ATP levels upon isometric contraction (117,256).

The mechanism by which AK1 depletion leads to the observed compensatory increase in fuel oxidation is not known. The only known role of AK is the reversible phosphoryl transfer reaction between ATP, AMP and ADP. If this is indeed the sole function of AK, alterations in cell function in response to changes in AK levels or activity are likely to result from chronic changes in adenine nucleotide ratios. These may in turn directly affect mitochondrial functions, for example by modulating the effects of calcium on mitochondrial membrane potential (257), or indirectly through the activities of enzymes sensitive to adenine nucleotide ratios. The only observed alteration in adenine nucleotide levels found in the AK1$^{-/-}$ muscle is a significant increase in total AMP, but

further work is required to define the source and metabolic significance of this elevation (117,256).

It is interesting that, in addition to a significant increase in genes of the oxidative phosphorylation pathway, muscles from $AK1^{-/-}$ mice also display decreases in more than 20 genes encoding for ribosomal proteins, in RNA polymerase 1 and in RNA polymerase 2 binding proteins. Ribosomal protein biosynthesis is suppressed under different cellular stress conditions, (258) possibly as an energy economizing response. These results suggest that adaptation to AK1 deficiency involves both enhanced ATP production from fuel oxidation, and suppressed ATP utilization. Ribosomal RNA synthesis in response to nutrient and energy conditions is controlled by the mammalian target of rapamycin (mTOR), suggesting that the changes in nucleotide levels elicited by AK1 deficiency are sensed by this kinase. Many signaling mechanisms could result in decreased mTOR activity and ribosome biogenesis, including changes in reactive oxygen species, thymoma viral proto-oncogene/protein kinase B (Akt/PKB) signaling, and AMPK signaling (259,260), and further work will be required to identify which of those mechanisms is sensitive to AK1 depletion.

The possibility that AMPK signaling might be involved in mediating some of the effects of AK1 deletion is suggested by the evidence for both enhancement of fuel oxidation and suppression of energy consumption in $AK1^{-/-}$ mice muscle, a response known to be coordinated by AMPK signaling. In addition, compensatory increases in mitochondrial density seen in mice lacking AK1 (114) are also consistent with activation of AMPK (261,262). The concordance between the gene expression patterns seen in

muscles from AK1$^{-/-}$ mice and TgPrkag3^{225Q} mice, as well as the discordance with Prkag3$^{-/-}$ mice are also consistent with this possibility. However, in previous reports, muscles from AK1$^{-/-}$ mice subjected to moderate isometric contraction contained less phospho-AMPK compared to controls (256). If this indeed reflects a chronic impairment in AMPK activation in muscles from AK1$^{-/-}$ mice, it will be very important to determine the nature of an AK1-regulated, non-AMPK dependent mechanisms that enhances energy production and conserves energy use.

The hypothesis that AK1 enhances the efficiency of ATP utilization, thereby decreasing the need for fuel oxidation raises the interesting possibility that differences in the level or activity of AK1 may contribute to determining individual basal metabolic rates and susceptibility to weight gain (263). Indeed, increased levels of AK1 have been reported in skeletal muscle from morbidly obese patients (118), although whether this correlation is causal cannot be established from these studies. Nevertheless the results shown here suggest that inhibition of AK1 could enhance fuel utilization and ameliorate obesity in these patients.

Our experiments in isolated muscle cells indicate that increased oxidative metabolism is an autonomous cellular response to AK1 deficiency, and support the concept that enhanced muscle metabolism is the basis for the resistance of AK1$^{-/-}$ mice to fat accumulation. However, because AK1 is also present in brain (264) and pancreatic beta cells, albeit at much lower levels that in skeletal muscle, we cannot rule out the possibility that an effect of AK1 knockout in these other tissues might also contribute to the phenotype of the AK1 null mouse. Further experiments involving more in-depth

metabolic phenotyping of a fully backcrossed AK1$^{-/-}$ mouse, as well as tissue-specific knockdown of AK1 will be necessary to determine the contribution of each tissue to the AK1$^{-/-}$ phenotype.

In summary, we demonstrate that alterations in energy efficiency due to AK1 disruption can enhance muscle oxidative metabolism and affect whole body fuel metabolism. The effects of AK1 depletion are comparable to those seen upon perturbation of AMPK, a master regulator of energy balance, underscoring the importance of the AK reaction. Further research on the adenylate kinases is necessary to evaluate their role on important aspects of human energy balance.

Experimental Procedures

Animals: All procedures were carried out following either the guidelines from the University of Massachusetts Medical School Institution Animal Care and Use Committee (UMMA-IACUC) or the guidelines for the Care and Use of Laboratory Animals of the Dutch Council and were approved by the Institutional Animal Care and Use Committee at the University of Nijmegen. A cohort of gene-targeted mice carrying a HygroBR replacement mutation in the exon 3–5 region of the AK1 gene was generated and maintained as previously described (114). Male homozygous AK1-deficient and wild type littermates (both with 50–50% C57BL/6 x 129/Ola mixed inbred background) were used throughout experiments. Mice were housed 3 per cage, and half of the mice were fed a standard mouse chow (Sniff) and the rest were fed a high fat diet (Hope Farms) *ad*

libitum. This diet regimen was used for eighteen weeks. Gastrocnemius muscle was isolated and snap frozen in liquid nitrogen.

Affymetrix GeneChip Expression Analysis: Analysis was performed as previously described (102,149). Briefly, total RNA was prepared from three sets each of gastrocnemius muscle from AK1$^{-/-}$ mice and AK1$^{+/+}$ littermates. Affymetrix protocols were followed for the preparation of cRNA from total RNA, which was hybridized according to Affymetrix instructions to a MOE430-2 Chips. The GeneChips were washed with a GeneChip Fluidics Station 400 and were scanned with an HP GeneArrayScanner (Affymetrix). Raw expression data, as well as the CEL files published by Nilsson et al. (251) were analyzed with the Bioconductor statistical environment (164) using RMA (165) and MAS5, a Bioconductor implementation of the MAS 5.0 algorithm (Affymetrix). The "fold change" for each gene was determined by dividing the mean of the average difference from three independent experiments. Correlations between gene expression sets were evaluated using the Pearson product moment correlation coefficient.

Serum Analysis: Leptin levels were determined using an ELISA kit following the protocol exactly (Linco Research Inc).

Primary Adipose Cell Isolation: Epididymal fat pads were weighed, minced into 0.3 cm^3 pieces, and incubated for 30-45 minutes at 37°C in an orbital shaker shaking at 100 rpm in 1 mg/mL collagenase in Krebs-Ringer HEPES (KRH) buffer (130 mM NaCl, 5 mM

KCl, 1.3 mM CaCl2, 1.3 mM MgSO4, and 25 mM HEPES) supplemented with 2 mM pyruvate and 2.5% BSA, pH 7.4. The digested samples were squeezed through chiffon material, and the isolated cells were washed three times in KRH buffer containing 2.5% BSA prior to immunofluorescence analysis using anti-perilipin antibodies.